



# THE UNIVERSITY *of* EDINBURGH

This thesis has been submitted in fulfilment of the requirements for a postgraduate degree (e.g. PhD, MPhil, DClinPsychol) at the University of Edinburgh. Please note the following terms and conditions of use:

- This work is protected by copyright and other intellectual property rights, which are retained by the thesis author, unless otherwise stated.
- A copy can be downloaded for personal non-commercial research or study, without prior permission or charge.
- This thesis cannot be reproduced or quoted extensively from without first obtaining permission in writing from the author.
- The content must not be changed in any way or sold commercially in any format or medium without the formal permission of the author.
- When referring to this work, full bibliographic details including the author, title, awarding institution and date of the thesis must be given.

**Prevention and reversal of thymus involution  
mediated by the transcription factor Foxn1**

Nicholas Bredenkamp


Thesis presented for the degree of the Doctor of Philosophy

The University of Edinburgh

2011

## Declaration

The work presented in this thesis is my own, except where otherwise stated.

A handwritten signature in black ink, appearing to read 'NB' followed by a stylized flourish.

Nicholas Bredekamp

## **Acknowledgements**

I am grateful to Clare Blackburn for allowing me the opportunity to undertake a PhD project in her lab, for the substantial support and guidance she provided, and for the intellectual flexibility that she allowed me throughout the project. I am also grateful to the Darwin Trust of Edinburgh for their financial support. I owe many thanks to all the members of the Blackburn laboratory, including Frances and Diana for their generous help in the lab, and Craig, Alison, Alistair, Michelle, Xin, Terri, Tanya and Christele for help and advice with experimental techniques and constructive discussions (scientific or otherwise). Thanks also to Andrew Smith for help with molecular cloning techniques, and to Nancy Manley for providing reagents. The experiments performed in this thesis would not have been possible were it not for Carol Manson and the Animal Unit staff that provided excellent animal care and performed the required experimental procedures expertly. Thanks also to the Tissue Culture Facility staff, Jan Ure and the Transgenic Service Facility for help with transgenic mouse generation, and Simon Monard and Jan Vrana for help with cell sorting.

I would also like to thank my family for their continued support throughout my studies. Lastly, I owe my deepest gratitude to Sarah Lea for her endless encouragement, patience and sense of perspective.

## Abstract

Central to the age-associated decrease in immune system function, characterised by the increase in the frequency and severity of infections and autoimmune diseases, is the decrease in production of naïve T cells by the thymus. This results from the targeted degeneration or involution of the thymus with age. One of the principal causes of involution is the loss of organisation and functionality of the thymic epithelium, which confers the primary function of the organ via interactive regulation of T cell development. Although the mechanisms that govern the deterioration of the thymic epithelium are poorly understood, a number of recent reports indicate that the transcription factor, Foxn1, is required to maintain this compartment in the postnatal thymus.

Thus, the first aim of this study was to precisely profile Foxn1 expression levels in aging postnatal thymic epithelial cells. The second aim was to investigate the effects of up-regulating Foxn1 in the aging thymus, which was achieved using a novel, regulatable Foxn1 mouse model generated during this study.

In this study I show that Foxn1 is expressed at different levels in different postnatal thymic epithelial cell (TEC) sub-populations suggesting a dosage-dependent mode of action for Foxn1. Additionally, using two experimental approaches, I show that Foxn1 expression decreases with age in TECs, supporting the current data that implicate the loss of Foxn1 as a potential cause of thymus involution. Next, I generated a tissue-specific, regulatable Foxn1 mouse model that allowed me to modulate Foxn1 expression in the postnatal thymus. Firstly, using this model, I show that thymus involution can be prevented by the up-regulation and maintenance of Foxn1 expression from the onset of involution. Thymi that up-regulated Foxn1 were overtly larger and exhibited greater cellularity in both the thymocyte and epithelial compartments compared to age matched controls. Additionally, the larger TEC compartment contained a higher proportion of functional and proliferating TECs that up-regulated a panel of genes involved in TEC development and function. Next, I show that Foxn1 up-regulation in aged, involuted thymi is sufficient to partially reverse involution, as shown by an increase in TEC organisation and intrathymic T cell numbers. While other strategies that promote thymic rebound or reversal have been reported, including cytokine treatment or sex steroid ablation, these approaches are complicated by side effects and toxicity. Hence, I propose a novel model for immune reconstitution through the regulation of Foxn1 expression in the postnatal thymus.

# Table of contents

<b>Declaration</b> .....	<b>1</b>
<b>Acknowledgements</b> .....	<b>2</b>
<b>Abstract</b> .....	<b>3</b>
<b>Table of contents</b> .....	<b>4</b>
<b>Abbreviations</b> .....	<b>7</b>
<b>Chapter 1: Introduction</b> .....	<b>9</b>
<b>1.1 The thymus</b> .....	<b>9</b>
1.1.1 Thymic epithelial cells.....	11
1.1.2 Non-epithelial components.....	12
<b>1.2 T cell development</b> .....	<b>13</b>
1.2.1 HPCs and seeding of the postnatal thymus.....	13
1.2.2 Intrathymic T cell development.....	14
<b>1.3 Thymus organogenesis</b> .....	<b>18</b>
1.3.1 Origin and regulation of early development .....	18
1.3.2 <i>Foxn1</i> and thymus organogenesis.....	20
<b>1.4 The postnatal thymus</b> .....	<b>23</b>
1.4.1 <i>Foxn1</i> in the postnatal thymus .....	23
1.4.2 Other genetic factors in the postnatal thymic epithelium.....	25
<b>1.5 Thymus involution</b> .....	<b>26</b>
1.5.1 Mechanisms of thymus involution.....	27
1.5.2 Consequences of thymus involution .....	28
1.5.3 Models of immune reconstitution .....	29
1.5.3.1 Sex steroid modulation.....	29
1.5.3.2 Keratinocyte growth factor .....	30
1.5.3.3 Interleukin-7.....	31
1.5.3.4 Growth Hormone .....	31
1.5.3.5 <i>In vitro</i> T cell development.....	32
1.5.3.6 Thymus transplantation.....	32
1.5.4 <i>Foxn1</i> and thymus involution .....	33
<b>1.6 Aims</b> .....	<b>35</b>
<b>Chapter 2: Materials and methods</b> .....	<b>36</b>
<b>2.1 Mice</b> .....	<b>36</b>
2.1.1 Mice strains.....	36
2.1.1.1 <i>Foxn1</i> <sup>Cre</sup> .....	36
2.1.1.2 Tg(CAG-FLPe).....	36
2.1.1.3 <i>Foxn1</i> <sup>GFP</sup> .....	36
2.1.1.4 ROSA26 <sup>CAG-STOP-Foxn1ERT2</sup> .....	37
2.1.2 Tamoxifen treatment.....	37
2.1.3 5-Bromo-2'-deoxyuridine (BrdU) treatment.....	37
<b>2.2 Molecular biology</b> .....	<b>37</b>
2.2.1 Isolation of nucleic acids .....	37
2.2.1.1 Plasmid DNA .....	37
2.2.1.2 Genomic DNA .....	37
2.2.1.3 RNA .....	38
2.2.2 Molecular cloning.....	38

2.2.2.1 Conventional cloning .....	38
2.2.2.1.1 Oligonucleotide sequences .....	38
2.2.2.2 PCR cloning .....	39
2.2.2.3 Transformation of chemically competent <i>E. coli</i> .....	39
2.2.3 PCR.....	39
2.2.3.1 PCR Primers .....	39
2.2.3.2 Conventional PCR .....	40
2.2.3.3 Genotyping PCR .....	40
2.2.3.4 Quantitative RT-PCR.....	40
2.2.4 DNA sequencing.....	41
2.2.5 Southern blotting .....	41
2.2.5.1 Generation of Southern blotting probes by PCR.....	42
2.2.5.2 Southern blot preparation.....	43
2.2.5.3 Southern blot hybridisation.....	43
2.2.6 Western blotting .....	43
2.2.7 Luciferase assay.....	44
<b>2.3 Immunohistochemistry .....</b>	<b>44</b>
2.3.1 Sample processing and staining.....	44
2.3.2 Cytospin preparation.....	45
2.3.3 Antibodies.....	45
<b>2.4 Flow cytometry .....</b>	<b>46</b>
2.4.1 Cell preparation .....	46
2.4.1.1 Postnatal TEC enrichment .....	46
2.4.2 Cell staining.....	47
2.4.3 Antibodies.....	47
2.4.4 Flow cytometry instruments .....	48
<b>2.5 Cell culture .....</b>	<b>48</b>
2.5.1 ES cell electroporation and isolation of targeted clones .....	48
2.5.2 Karyotyping and transgenic mouse generation.....	49
<b>2.6 Statistical analyses .....</b>	<b>49</b>
<b>Chapter 3: Transcriptional profile of Foxn1 in the thymic epithelium .....</b>	<b>50</b>
<b>3.1 Introduction .....</b>	<b>50</b>
<b>3.2 Results.....</b>	<b>50</b>
3.2.1 Isolation of defined TEC subpopulations .....	50
3.2.2 Foxn1 is differentially expressed in the major TEC compartments.....	53
3.2.3 Foxn1 expression decreases with age in the thymic epithelium .....	56
<b>3.3 Discussion .....</b>	<b>58</b>
<b>Chapter 4: Generation of a conditional, inducible Foxn1 mouse model.....</b>	<b>60</b>
<b>4.1 Introduction .....</b>	<b>60</b>
<b>4.2 Evaluation of experimental approach.....</b>	<b>61</b>
<b>4.3 Generation of R26-CAG-STOP-Foxn1<sup>ER</sup> transgenic mouse line.....</b>	<b>62</b>
4.3.1 Targeting vector construction .....	62
4.3.1.1 Foxn1 <sup>ER</sup> -IRES-GFP construction .....	62
4.3.1.2 CAG-floxed STOP construction .....	64
4.3.1.3 Final targeting vector assembly .....	64
4.3.2 ES cell targeting, selection and screening.....	67
4.3.3 Generation of R26-CAG-STOP-Foxn1 <sup>ER</sup> transgenic mice .....	69
<b>4.4 Preliminary characterisation of R26-CAG-STOP-Foxn1<sup>ER</sup> mice .....</b>	<b>69</b>
4.4.1 The Foxn1 <sup>ER</sup> fusion protein is transcriptionally active and Tamoxifen responsive <i>in vitro</i> .....	69

4.4.2 Foxn1ER-IRES-GFP is expressed after Cre mediated excision of the STOP cassette in CAG-STOP-Foxn1ER mice .....	72
4.4.3 Foxn1ER is regulatable by Tamoxifen treatment <i>in vivo</i> .....	74
<b>4.5 Concluding remarks .....</b>	<b>77</b>
<b>Chapter 5: Maintained expression of Foxn1 prevents thymus involution.....</b>	<b>78</b>
<b>5.1 Introduction .....</b>	<b>78</b>
<b>5.2. Experimental strategy and preliminary validation .....</b>	<b>79</b>
5.2.1 Experimental mice .....	79
5.2.2 Control mice .....	79
5.2.3 Foxn1 mRNA levels in experimental and control mice.....	79
5.2.4 Hair phenotype .....	79
<b>5.3 Results.....</b>	<b>81</b>
5.3.1 Thymus size.....	81
5.3.2 T cells numbers and composition .....	83
5.3.3 TEC numbers and phenotype.....	88
5.3.4 TEC gene expression and proliferation.....	92
<b>5.4 Discussion .....</b>	<b>95</b>
<b>Chapter 6: Reversal of involution after up-regulation of Foxn1 in the aged thymus.....</b>	<b>97</b>
<b>6.1 Introduction .....</b>	<b>97</b>
<b>6.2 Experimental strategy .....</b>	<b>97</b>
6.2.1 Experimental mice .....	97
6.2.2 Control mice .....	98
<b>6.3 Results.....</b>	<b>98</b>
6.3.1 Thymus size.....	98
6.3.2 T cell numbers and composition .....	100
6.3.2.1 CD4/CD8 T cell analysis .....	101
6.3.2.2 Triple negative cell analysis.....	103
6.3.3 Total nuclear Foxn1 expression in aged TECs .....	106
6.3.4 TEC architecture and phenotype.....	108
6.3.5 TEC gene expression .....	115
<b>6.4 Discussion .....</b>	<b>117</b>
<b>Chapter 7: Concluding remarks.....</b>	<b>119</b>
<b>7.1 Foxn1 in the postnatal thymus.....</b>	<b>119</b>
<b>7.2 Experimental considerations: present and future .....</b>	<b>121</b>
<b>References .....</b>	<b>124</b>



## Abbreviations

4-OHT	4-hydroxy-tamoxifen
BM	Bone marrow
BSA	Bovine serum albumin
CMJ	Cortico-medullary junction
cTEC	Cortical thymic epithelial cell
DC	Dendritic cell
DN	Double negative
DP	Double positive
EpCAM	Epithelial cell adhesion molecule
ETP	Early thymic progenitor
Fgf	Fibroblast growth factor
HC	Haematopoietic cell
HPC	Haematopoietic progenitor cell
HSCT	Haematopoietic stem cell transplant
IC	Isotype control
IL	Interleukin
IP	Intraperitoneal
IRES	Internal ribosome entry site
K	Keratin
KGF	Keratinocyte growth factor
LHRH	Luteinising hormone-releasing hormone
MHC	Major histocompatibility complex
MHCII	Major histocompatibility complex class II
mTEC	Medullary thymic epithelial cell
NC	Neural crest
NK	Natural killer
PBS	Phosphate buffered saline
qRT-PCR	Quantitative real-time polymerase chain reaction
R26	ROSA26 locus
RAG	Recombinase activating gene
SP	Single positive
Tam	Tamoxifen
TCR	T cell receptor

TEC	Thymic epithelial cell
TN	Triple negative
TREC	T cell receptor excision circle
U	Units
UEA	<i>Ulex europaeus</i> agglutinin

# Chapter 1: Introduction

---

## 1.1 The thymus

The thymus is an organ that is an essential component of the adaptive immune system in vertebrates (Bajoghli et al., 2009; Bajoghli et al., 2010); in humans and rodents the thymus is situated in superior mediastinum just above the heart. The primary function of the thymus is to regulate the development of self-restricted, self-tolerant naïve T (thymus) cells that are exported from the organ, and function as a fundamental component of the adaptive immune system (Miller, 1961). Athymia in a variety of human disorders or rodent experimental models results in severe or complete immunodeficiency (Flanagan, 1966; Kirkpatrick and DiGeorge, 1968).

The thymus is a complex structure composed of a highly organised epithelial network, developing thymocytes, non-epithelial stromal elements, non-T cell lineage hematopoietic cells (HCs) and a rich vasculature network (Boyd et al., 1993; Kendall, 1991).

Histologically, the thymus can be subdivided into three main areas, the medulla, the cortex and the subcapsular region (Figure 1.1a). The thymus is encapsulated by layers of connective tissue that penetrate the organ, as trabeculae, from the outer cortex to the cortico-medullary junction (CMJ), providing a structural link to the inner medulla (Boyd et al., 1993).

Importantly, these trabeculae are well vascularised and form the foundation of the extensive vascular network that is required for hematopoietic cell traffic to and from the thymus (Boyd et al., 1993). Immediately lining the subcapsule and trabeculae is the first layer of epithelium, thus creating the barrier between the external and internal thymic microenvironments (Boyd et al., 1993). The encapsulated stromal compartment constitutes a fraction of the total cellularity of the thymus but it is highly heterogeneous and contains numerous cell types including epithelial cells, fibroblasts, macrophages and dendritic cells (Boyd et al., 1993; Gray et al., 2002). This stromal complexity is reflective of the array of functions required to support proper thymocyte differentiation in the thymus (Figure 1.1b).

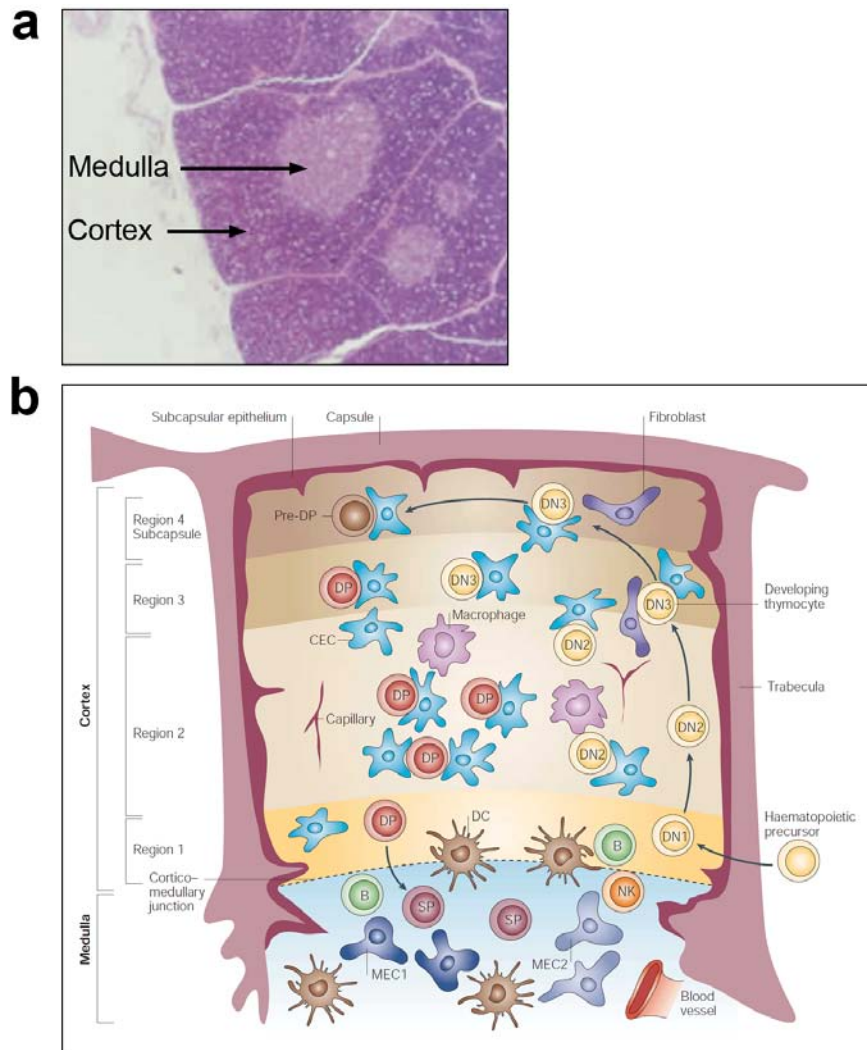


**Figure 1.1 Morphology of the postnatal thymus.**

**(a)** Hematoxylin staining reveals the general organisation of the paediatric human thymus, composed of the inner medulla and outer cortex regions (M. Ritter, Imperial College London). **(b)** Composition of the postnatal thymus, showing the relationship between the epithelium and developing thymocytes (Blackburn and Manley, 2004).

### 1.1.1 Thymic epithelial cells

The stroma constitutes a small fraction of total thymus cellularity, approximately 1-2%, of which the epithelium constitutes a further fraction (Gray et al, 2006 and see Chapter 3). It is the thymic epithelial cells (TECs) – broadly subdivided into medullary and cortical TECs (mTECs and cTECs) – that confer the primary function of the thymus via progressive, interactive mediation of thymocyte development (Boyd et al., 1993). The three-dimensional organisation of the thymic epithelium in a reticular network is distinct from other epithelia that are normally organised as layers on a basal membrane (van Ewijk et al., 1999).

Initial studies identified six major epithelial cell subtypes in the human thymus based on ultrastructural morphology and lucency (van de Wijngaert et al., 1984) (Table 1.1). Broadly, these different subtypes were located at the subcapsule/perivascular, cortical and medullary regions. Numerous studies further expanded on these findings through the use of monoclonal antibody panels and various cytokeratin proteins as a means of identifying various TEC subpopulations (Godfrey et al., 1990; Nicolas et al., 1985; Van Vliet et al., 1985). The studies were aggregated into a phenotypic classification system for TEC subtypes in humans and rodents, called clusters of thymic epithelial staining (CTES) (Kampinga et al., 1989) (Table 1.2). Together, these data establish that the thymus is composed of regionalised epithelial cell subtypes that are morphologically and phenotypically distinct, an essential arrangement that allows the progressive regulation of thymocyte development.

**Table 1.1 Morphological classifications of human epithelial subtypes**

Designation	Characteristic	Location
Type 1	Subcapsular-perivascular	Subcapsular, surrounding capillaries in cortex and CMJ
Type 2	Pale	Outer cortex
Type 3	Intermediate	Mid/deep cortex
Type 4	Dark	Deep cortex
Type 5	Undifferentiated	Medullary
Type 6	Large-medullary	Medullary, adjacent or part of Hassall's corpuscles*

\* Small clusters of keratinised mTECs; found commonly in human thymi and rarely in mouse thymi (Hassall, 1849)

**Table 1.2 Phenotypic classifications of human and rodent epithelial subtypes**

CTES group	Specificity
I	Pan epithelial
II	Subcapsule/perivascular
III	Cortex
IV	Medulla
V	Hassall's corpuscles
VI	Type 1 epithelium*
XX	Miscellaneous

\*Epithelial cells that layer the subcapsule and trabeculae

### 1.1.2 Non-epithelial components

A variety of non-epithelial cell types are important for thymus function and architecture, including cells derived from the neural crest (NC) and bone marrow (BM). Dendritic cells (DCs) constitute about 2.5% of total stromal cellularity and are scattered throughout the thymus although they are particularly concentrated at the CMJ and in the medulla (Ardavin, 1997; Boyd et al., 1993; Gray et al., 2002). All DCs express high levels of MHC class II and are classified into two populations based on their developmental pattern (Ardavin et al., 1993; Donskoy and Goldschneider, 2003). One population develops in phase with T cells, including gated arrival in the thymus, and other develops in a manner that is unrelated to T cell developmental kinetics (Donskoy and Goldschneider, 2003). DCs fulfil an important role, through their location in the thymus and their ability to present antigens, in the negative selection of thymocytes (Ardavin, 1997). A further hematopoietic cell population in the thymus is the myeloid-derived macrophages, which constitute less than 1% of the stroma (Gray et al., 2002). Thymic macrophages are morphologically and phenotypically heterogeneous and are most commonly found in the cortex (Boyd et al., 1993). These cortical macrophages are characterised by a large cytoplasmic volume and numerous lysosomes that contain the remnants of phagocytosed thymocytes, indicative of their role in the removal of apoptosed thymocytes from the thymic microenvironment (Duijvestijn and Hoefsmit, 1981). Lastly, the thymic stroma contains populations of fibroblasts that secrete extracellular matrix (ECM) complexes, including collagens and glycoproteins which are important for thymocyte differentiation and migration; although TECs also contribute to this microenvironment as they too secrete ECM complexes (Boyd et al., 1993; Savino et al., 1993).

Non-stromal elements also contribute to the architectural integrity and functionality of the thymus. The thymus contains an extensive vascular network: arteries enter the thymus through the capsule and trabeculae and then enter the stromal microenvironment at the CMJ, before branching into arterioles and capillaries that extend into the cortex towards the subcapsular region, and finally drain in post-capillary venules in the medulla and at the CMJ (Boyd et al., 1993; Kato and Schoefl, 1989). This vascular network is fundamental to thymus function as it provides the means for hematopoietic precursor cell (HPC) entrance into, and naïve T cell exit from the thymus. Another important component of the thymus is the NC-derived mesenchymal cells, which form the thymic capsule and invaginations within the lobe that surround blood vessels (Le Douarin and Jotereau, 1975). These cells are required for thymus development via epithelial-mesenchymal interactions (Auerbach, 1960; Suniara et al., 2000) and also persist in the adult thymus (Foster et al., 2008; Muller et al., 2008). During development these mesenchymal cells produce mitogenic, soluble growth factors required by the epithelium (Revest et al., 2001). These NCCs are also a source of precursors for pericytes in the thymus, which offer support to the thymic blood vessels (Foster et al., 2008). Thus, the thymus consists of an array of non-epithelial cellular components that fulfil a range of functions within the organ.

## **1.2 T cell development**

Hematopoietic precursor cells colonise at the thymus from the vasculature and undergo an ordered, developmental progression into naïve T cells that are eventually exported from the thymus to function in the adaptive immune system. Thymocyte development proceeds in a phenotypically progressive manner, mediated by the thymic stroma in spatially distinct microenvironments (Petrie and Zuniga-Pflucker, 2007; Takahama, 2006).

### **1.2.1 HPCs and seeding of the postnatal thymus**

There is no resident HSC population in the thymus, and thus the thymus is seeded with HPCs that originate in the bone marrow and enter via the vasculature at the cortico-medullary junction (Kyewski, 1987; Ushiki, 1986). The precise identity and functional characteristics of earliest intrathymic progenitor cells remains controversial, in particular the breadth of lymphoid and myeloid potential in these cells (Petrie and Kincade, 2005). This is perpetuated by differences in lineage potential results obtained from *in vitro* and *in vivo* approaches (Ehrlich et al., 2011). Various studies have established that the earliest intrathymic progenitors are multi-potent and are able to give rise to T cells, B cells, natural killer (NK) T cells, dendritic cells and myeloid lineage cells (Allman et al., 2003; Bell and Bhandoola,

2008; Porritt et al., 2004; Wada et al., 2008; Wu et al., 1991). It is also possible that the thymus is seeded by different progenitor populations with different phenotypic and functional properties.

The seeding of the postnatal thymus is a non-continuous process (Foss et al., 2001). Mice of various ages and, age-matched mice with synchronised intrathymic gating were intravenously injected with allogenic bone marrow cells and assayed for thymic chimerism. The contribution of the allogenic cells within the thymus allowed a model of the kinetics of thymocyte gating to be proposed. Thymocyte importation into the thymus was controlled by repeating cycles of temporally exclusive receptive (open gate), and longer refractive (closed gate) periods. It is proposed that saturation of the niches for the earliest intrathymic progenitor cells is the primary contributing factor for the importation gate closing (Foss et al., 2001).

### **1.2.2 Intrathymic T cell development**

Hematopoietic precursors homing to the thymus are not yet committed to the T cell lineage and do not express the CD4 or CD8 co-receptors which characterise most peripheral T cells, and hence are termed double negative (DN) cells (Godfrey et al., 1993; Porritt et al., 2004). Ordered intrathymic differentiation of these cells results in the simultaneous acquisition of CD4 and CD8, termed double positive (DP) cells and subsequently the loss of either CD4 or CD8 to generate single positive (SP) cells. Finally, SP cells undergo a process of functional maturation before emigration to the periphery (Fowlkes et al., 1985). This DN-DP-SP differentiation sequence is stringently regulated and occurs in distinct stromal microenvironments (Petrie and Zuniga-Pflucker, 2007). DN precursors can further be subdivided into four functionally distinct subsets based on their expression of CD44 and CD25 (Godfrey et al., 1993). A schematic representation of the intrathymic developmental progression of T cells in the thymus is shown in Figure 1.2.



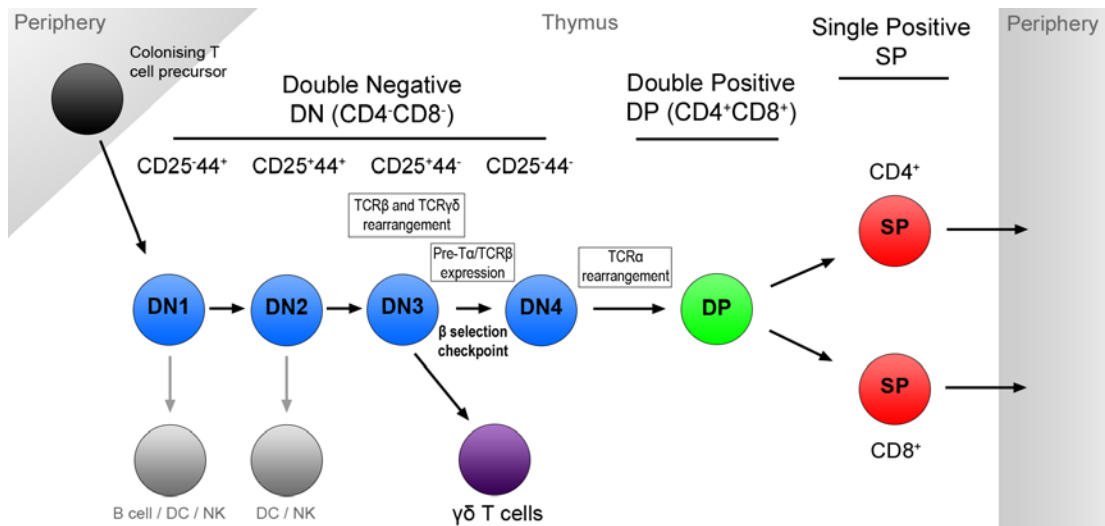


**Figure 1.2 Schematic representation of intrathymic T cell development.**

Hematopoietic precursor cells undergo a well-defined development process to MHC-restricted, self-tolerant naïve T cells. DC – dendritic cell, NK – natural killer T cell.

Once homed to the thymus, immature DN1 cells, characterised by CD44<sup>+</sup> and c-kit<sup>+</sup> expression, remain in the cortex immediately adjacent to medulla and proliferate extensively (Godfrey et al., 1993; Lind et al., 2001; Shortman et al., 1990). These cells are not yet committed to the T cell lineage and have the potential to differentiate into B cells, T cells, DCs, NK cells and myeloid cells (Allman et al., 2003; Bell and Bhandoola, 2008; Porritt et al., 2004; Wada et al., 2008). The factors that mediate precursor cell homing and colonisation are complex, and include stromal cell-produced integrin ligands (such as laminin and fibronectin), P-selectin (endothelium produced) and various chemokines (such as CXCL12, CCL19, CCL21 and CCL25); while proliferation is proposed to be mediated by kit ligand (stem cell factor, SCF) (Petrie and Zuniga-Pflucker, 2007).

DN1 cells then migrate to the inner cortex to become DN2 cells, which maintain CD44 and c-kit expression but also up-regulate CD25 (CD25<sup>+</sup>CD44<sup>+</sup>) (Godfrey et al., 1993). This marks the onset of lineage commitment as recombination activating gene (RAG) expression is up-regulated and the first T cell receptor (TCR) rearrangements occur (TCRγ and TCRδ) (Capone et al., 1998; Wilson et al., 1994). However, DN2 cells still exhibit some degree of non-T cell lineage potential, including NK cell and DC potential (Lucas et al., 1998; Schmitt et al., 2004a). Notch signalling is crucial for T cell commitment in the DN1-DN2 transition; abrogation of the Notch ligand, Delta-like 4 (Dll4) in the epithelium results in a complete

block in normal T cell development at the DN1 stage and a corresponding accumulation of intrathymic B cells (Koch et al., 2008; Schmitt et al., 2004a). Accordingly, Dll4 is expressed by the majority of cTECs (approximately 85%) (Koch et al., 2008). Additionally, interleukin-7 (IL-7) and SCF are required for DN2 thymocyte proliferation (Godfrey et al., 1992; Moore and Zlotnik, 1995).

Progression to DN3 is marked by down-regulation of CD44 and c-kit and up-regulation of CD24 and occurs as the cells migrate through the outer cortex towards the subcapsular zone (Godfrey et al., 1993; Petrie and Zuniga-Pflucker, 2007). At this stage, the commitment to the T cell lineage is complete as DN3 cells undergo widespread TCR $\beta$  and TCR $\gamma$  rearrangement (Godfrey et al., 1993); mice deficient for RAG-1 exhibit a severe block at the DN3 stage (Mombaerts et al., 1992b). At this stage, thymocytes can be selected into one of two developmental pathways: those that undergo successful  $\gamma\delta$  chain rearrangement become  $\gamma\delta$ T cells, whereas those that successfully rearrange the TCR $\beta$  chain are selected to develop into  $\alpha\beta$ T cells (Bluestone et al., 1987). Stromal produced factors that are important at this stage are CCL25, which may play a role in the polarised migration of thymocytes, and IL-7 which is required for thymocyte survival (Benz et al., 2004; Uehara et al., 2006).

The final transition in the DN population, to DN4, occurs in the subcapsular zone and is characterised by the loss of CD25 (CD44<sup>+</sup>CD25<sup>-</sup>) and the onset of TCR $\alpha$  gene rearrangement (Godfrey et al., 1993); the progression from DN3 to DN4 is termed the  $\beta$  selection checkpoint. Successful rearrangement of the TCR $\beta$  chain results in the formation of a pre-T $\alpha$ /TCR $\beta$  complex which is expressed by the precursors of  $\alpha\beta$ T cells (Mombaerts et al., 1992a). Pre-TCR signalling is important for the survival and differentiation of developing thymocytes, and also prevents the rearrangement of the second TCR $\beta$  allele (Aifantis et al., 1997). Survival of thymocytes here is mediated by Notch signalling as conditional inactivation of Notch1 results in a maturational arrest at the DN3 stage (Wolfer et al., 2002). Additionally, CXCR4 is important at this stage as it up-regulates Bcl-2A1, which inhibits Caspase 3-mediated apoptosis, to promote thymocyte survival (Janas and Turner, 2010). Thymocytes begin to up-regulate CD4 and CD8 marking the start of the transition to the DP stage (Petrie et al., 1990). The successful rearrangement of the TCR $\alpha$  gene and the formation of TCR $\alpha\beta$  heterodimers, through affinity competition, is crucial for subsequent thymocyte survival (Trop et al., 2000).

Thymocytes now migrate inwards from the capsule such that developing DP cells are found throughout the cortex (Petrie and Zuniga-Pflucker, 2007). During this period they undergo the process of positive selection, which removes clones carrying non-productively rearranged TCR $\alpha$  genes. Only DP thymocytes that have correctly rearranged their TCR chains and whose  $\alpha\beta$  TCRs have the ability to interact with sufficient affinity with self-MHC ligands, present on the surface of cortical stromal cells, survive. It is estimated that 95% of thymocytes die at this stage (Benoist and Mathis, 1989). Various intracellular signalling events are important for the survival of positively selected DP thymocytes, including the termination of RAG expression and the increase in Bcl-2, which protects the cells against apoptosis (Brandle et al., 1992; Linette et al., 1994). Next, thymocytes undergo the DP-SP transition; cells that bear MHC class I restricted  $\alpha\beta$ TCRs retain CD8 expression, while cells that bear MHC class II restricted  $\alpha\beta$ TCRs retain CD4 expression (Kaye et al., 1989; Teh et al., 1988). A number of models have been proposed to account for the divergence of the CD4/CD8 lineage, including stochastic, instructive and kinetic signalling models (Brugnera et al., 2000; Germain, 2002). In the stochastic and instructive models, CD4 or CD8 co-receptors are either randomly or instructively repressed, respectively. In the kinetic signalling model, CD8 expression is terminated by default through up-regulation of IL-7R; if loss of CD8 signalling does not disrupt TCR signalling then the CD4 lineage is produced, however in contrast, if this does disrupt TCR signalling then CD4 is silenced and CD8 expression is reinduced (Brugnera et al., 2000). At the molecular level, the zinc finger transcription factor, Th-POK, has been identified as necessary and sufficient for commitment to the CD4 lineage. A mutation in this gene caused a redirection of CD4 SP cells to the CD8 lineage (He et al., 2005; Keefe et al., 1999).

Next, SP thymocytes migrate into the medulla and undergo negative selection. Migration of positively selected thymocytes into the medulla is dependent on CCR7 (Ueno et al., 2004). Mice deficient for CCR7 or its stromal cell-produced ligands (CCL19 and CCL21) showed an accumulation of mature SP thymocytes in the cortex. The outer medulla and CMJ are rich in dendritic cells which play an important role in the induction of negative selection (Kyewski et al., 1986). Similar to positive selection, TCR and MHC molecular interactions are required to further develop the T cell repertoire. However, at this checkpoint SP clones whose TCR has a high affinity for self-MHC and peptide complexes in the thymus are deleted (Sprent et al., 1990). Representation of an immunological “self” is ensured by a mechanism in which DCs present a range of non-thymic, tissue-specific peptides to developing T cells, a process that is critical for the establishment of self tolerance (Kyewski

et al., 1986). These peripheral tissue-specific antigens are synthesised by a sub-population of medullary epithelial cells, partly under the control of the Autoimmune Regulator (Aire) transcription factor, and are supplied to DCs via cross-presentation (Anderson et al., 2002; Kyewski and Derbinski, 2004). Consequently, Aire deficient mice develop a defined profile of autoimmune disorders called polyendocrinopathy-candidiasis-ectodermal dystrophy (APECED) (Anderson et al., 2002). At this stage post-selection thymocytes are not yet functionally mature and undergo further processing events in the medulla, including crosstalk communication with the epithelium via the lymphotoxin- $\beta$  receptor signalling pathway, before export to the periphery (Boehm et al., 2003). This extended period in the medulla is also important for the development of regulatory T (Treg) cells which mostly differentiate from CD4<sup>+</sup> SP cells, and are defined by the expression of Foxp3 (Fontenot et al., 2005; Josefowicz and Rudensky, 2009). Thus, as described above, the self-MHC restricted, self-tolerant naïve T cell repertoire is established through progressive interactions with the thymic stromal in defined microenvironments.

### **1.3 Thymus organogenesis**

#### **1.3.1 Origin and regulation of early development**

The thymus develops from the endoderm of the third pharyngeal pouch, originating from a common primordium with the parathyroid gland (Gordon et al., 2001; Gordon et al., 2004). Correct early pouch formation, from E8 to E10.5, is dependent on *T-box protein 1 (Tbx1)*. Mutations in *Tbx1* result in thymic hypoplasia or athymia and a spectrum of cranio-facial abnormalities, which are caused by the failed development of the second, third and fourth pharyngeal pouches (Jerome and Papaioannou, 2001). *Fibroblast growth factor 8 (Fgf8)* is also important for pouch formation as this growth factor is down-regulated in *Tbx1* mutants and exhibits a mutant phenotype of disrupted pouch and thymus development (Abu-Issa et al., 2002).

The antero-posterior identity of the third pharyngeal pouch is proposed to be set-up by a *Hox-Pax-Eya-Six* network of transcription factors (Xu et al., 2002) (Figure 1.3). *Hoxa3* mutants exhibit a developmental block at the stage of the formation of the common primordium and show a specific down-regulation of *Paired box (Pax) 1* and *9* genes in third pharyngeal pouch (Manley and Capecchi, 1995). Furthermore, in *Eya1* null mutant embryos, *Hoxa3* and *Pax1/9* expression was shown to be normal but *Six1* expression was reduced in the third pouch endoderm (Xu et al., 2002). However, more recent data have shown that *Six1* and *Eya1* expression in the pouches does not require *Pax1* and *Pax9* function, suggesting that

they may function independently or upstream of Pax1/Pax9 (Zou et al., 2006). Furthermore, Pax1 expression was shown to require Six1 and Eya1, while Tbx1 and Fgf8 expression was reduced in *Eya1*<sup>-/-</sup> mutants, indicating that Eya1 may act upstream of early events in the initiation of thymus organogenesis (Zou et al., 2006). The difficulty in interpreting these data may be due to the possible compounding effects of Eya1, which is expressed in the pharyngeal endoderm, ectoderm and neural crest cells between E9.5 and E10.5 (Xu et al., 2002). Thus, while it is clear that these transcription factors all have roles in the determining the identity of the third pharyngeal pouch, a precise model for their interactions remains unclear.

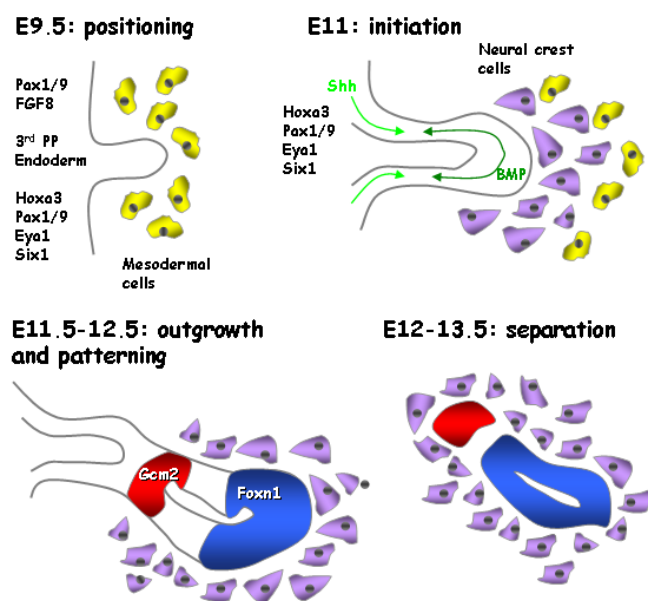


**Figure 1.3 Molecular control of thymus and parathyroid organogenesis.**

Pax 1 and 9 are expressed in the pharyngeal endoderm from E9.5 (Peters et al., 1998; Wallin et al., 1996). While their transcriptional relationships with *Eya* and *Six* are unclear, it is evident that both *Pax1* and *Pax9* are required for TEC development and normal thymic function. *Pax1* null thymi are hypoplastic, up to five-fold smaller than wildtype thymi, and exhibit altered distribution in the CD4/CD8 T cell populations (Wallin et al., 1996). The *Pax9* null phenotype is more severe as null thymi form as ectopic rudiments in the larynx, are severely hypoplastic from E14.5 onwards and cannot support  $\gamma\delta$  T cell development (Hetzer-Egger et al., 2002).

The patterning of the common primordium into thymus and parathyroid compartments is initially evidenced by the parathyroid specific marker, *Glial cells missing homologue 2* (*Gcm2*). *Gcm2* is expressed in the anterior domain of the third pouch endoderm at E10.5 and subsequently is restricted to dorsal and anterior domain of the common primordium, marking the parathyroid-fated cells (Gordon et al., 2001). At this stage, *Rhox4* marks the ventral region of the pouch opposing *Gcm2*, although the functional significance of this is unclear (Morris et al., 2006). Later, the Forkhead box transcription factor, *Foxn1* (discussed in detail below), which marks the prospective thymus domain, becomes expressed in the ventral region of the shared primordium at approximately E11.25 (Gordon et al., 2001). Additionally, opposing gradients of Sonic hedgehog (*Shh*) and Bone morphogenetic protein 4 (*BMP4*) may be important for specification of parathyroid and thymus identity (Moore-Scott and Manley, 2005) (Figure 1.3).

Subsequent to the endoderm patterning, the organ primordia begin to form. During this process, interactions between the neural crest cells (NCCs), which migrate into the pharyngeal arches from around E9, and the cells in the primordia, play a crucial role in thymus organogenesis (Auerbach, 1960). The NCCs, which will eventually give rise to the intrathymic mesenchyme and the mesenchymal capsule surrounding the thymus (Foster et al., 2008; Muller et al., 2008), influence organogenesis at least in part, via soluble growth factor signaling. The growth factor *Fgf10*, expressed in the mesenchymal cells and its receptor *Fgfr2IIIb*, expressed in the pharyngeal region and restricted to the thymic epithelium, have been shown to be required for thymus development after E12.5 (Revest et al., 2001). Concurrently, there is outgrowth of the primordium, detachment from the pharynx and surface ectoderm and separation of the thymic and parathyroid rudiments (Blackburn and Manley, 2004) (Figure 1.3).

### **1.3.2 *Foxn1* and thymus organogenesis**

*Foxn1* is a member of the Forkhead box (Fox) transcription factor family, named for the involuted head phenotype observed in *Drosophila melanogaster* fork head gene mutants (Weigel et al., 1989). The unifying characteristic of this family of transcription factors is the highly conserved, ~100-residue Forkhead DNA-binding domain, comprised of three  $\alpha$ -helices, three  $\beta$ -sheets and 2 wings or loops (Clark et al., 1993; Hannenhalli and Kaestner, 2009) (Figure 1.4a,b). There are over 40 Forkhead family members in mammals which have diverse biological functions including roles in organogenesis, cell cycle regulation, chromatin remodelling and tissue homeostasis.

*Foxn1* is the gene mutated in the classical mouse nude phenotype which is characterised by athymia and hairlessness (Flanagan, 1966; Nehls et al., 1994); a point mutation in *Foxn1* generates a similar phenotype in humans (Frank et al., 1999). *Foxn1* is expressed in the ventral posterior region of the third pharyngeal pouch from approximately E11.25, as shown by *in situ* hybridization (Gordon et al., 2001), although *Foxn1* transcripts can be detected by RT-PCR as early as E9-E10.5 (Balciunaite et al., 2002; Nehls et al., 1994). However, initiation of thymus organogenesis appears to proceed normally in *Foxn1* null mice until E11.5, indicating that *Foxn1* function is required only after this point (Nehls et al., 1996). Additionally, *Foxn1* is expressed in the epidermis and hair follicles of the skin from E15.5 (Lee et al., 1999).

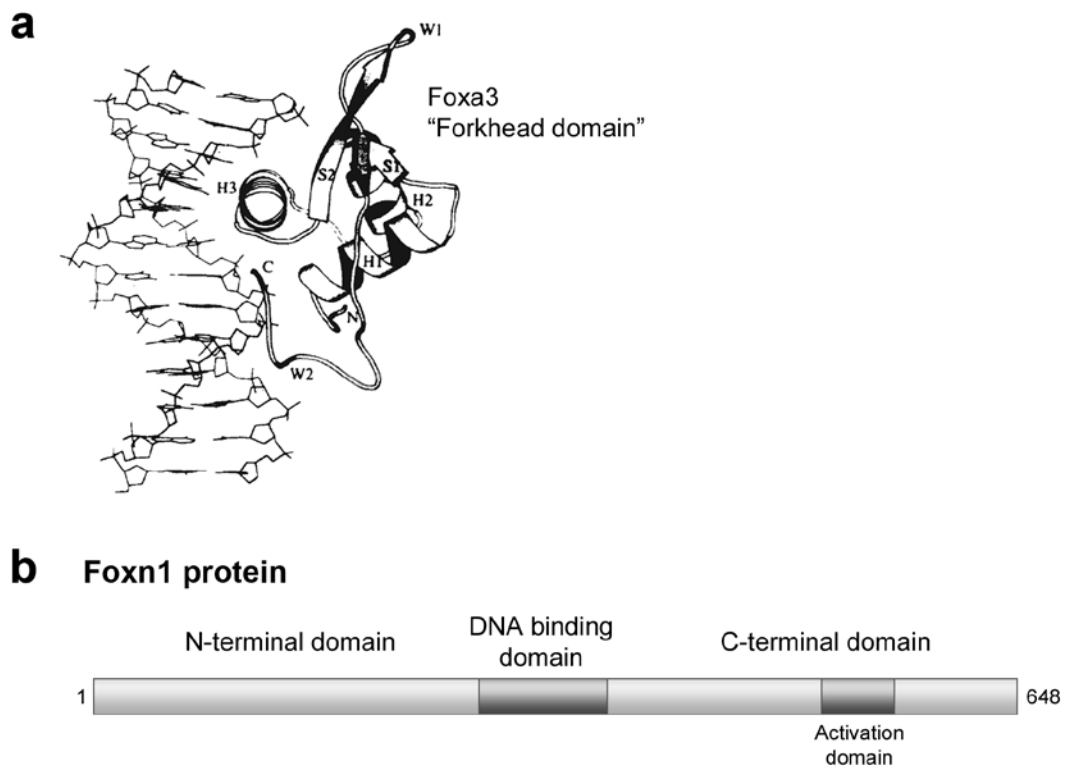


**Figure 1.4 Forkhead box transcription factors.**

**(a)** The structure of the Forkhead DNA-binding domain complexed with DNA was first resolved for HNF-3 $\gamma$  (Foxa3) (Clark et al., 1993). H,  $\alpha$ -helices; S,  $\beta$ -sheets; W, wings or loops. **(b)** Schematic representation of mouse *Foxn1* protein, showing the *in vitro*-determined activation domain (Schuddekopf et al., 1996).

Following initiation of a high level of transcription, Foxn1 is essentially expressed in all embryonic TECs and is indispensably and cell autonomously required for TEC differentiation and function; *Foxn1* null thymi completely fail to be colonised by hematopoietic cells (Blackburn et al., 1996; Flanagan, 1966; Gordon et al., 2007; Itoi et al., 2001; Nehls et al., 1996). The *Foxn1* null thymic rudiment consists of clusters and linear aggregates of TECs that appear to be trapped in an undifferentiated, progenitor cell-like state and express the progenitor cell marker, *Plet-1* (Blackburn et al., 1996; Depreter et al., 2008). Mechanistically, it appears that Foxn1 regulates the allocation into and/or the maintenance of the differentiated, *Plet-1*<sup>-</sup> TEC compartment during early organogenesis (Nowell et al., under review). Furthermore, clonal reactivation of Foxn1 in postnatal null TECs resulted in the formation of functional thymic units that could support T cell development, substantiating the notion that TECs are maintained in a progenitor-like state in the absence of Foxn1 (Bleul et al., 2006). Interestingly, it appears that Foxn1 is not required for the initial divergence into the medullary TEC sub-lineage as *Foxn1* null thymi contain Keratin 5<sup>hi</sup>/Claudin 4<sup>hi</sup> TEC clusters, which are the functionally determined precursors of the mTEC sub-lineage (Hamazaki et al., 2007; Nowell et al., under review). Taken together with the Bleul et al. findings, this suggests that a common thymic epithelial progenitor cell only persists in the postnatal *Foxn1* null thymus. Collectively, these data establish that *Foxn1* is critically required for proper TEC development from the thymic epithelial cell progenitor (TEPC) state.

An allelic series, generated using wildtype, hypomorphic (*Foxn1*<sup>R</sup>) and null *Foxn1* alleles, has revealed *Foxn1* as a potential master regulator of the thymic epithelial lineage differentiation programme (Nowell et al., under review) (Figure 1.5). In this series, Foxn1 is expressed at precisely defined levels allowing its role in TEC development to be dissected in detail. Firstly, Foxn1 appears to regulate most stages of cTEC and mTEC lineage progression, as defined by the absence or acquisition of phenotypic and functional markers in TECs at different Foxn1 levels (Figure 1.5). Secondly, a host of important TEC genes show Foxn1 dependent expression profiles. These include *Pax1*, *Pax9*, *FgfR2IIIb*, *Delta-like 4* (*Dll4*, a Notch ligand that is non-redundantly required for T cell lineage commitment) (Koch et al., 2008) and the chemokine *CCL25* (which regulates thymocyte colonization of the fetal thymus) (Liu et al., 2006). Thus, because Foxn1 regulates multiple aspects of TEC development, as opposed to a single trait, this suggests that it may function as a master regulator of TEC differentiation and function (Nowell et al., under review).



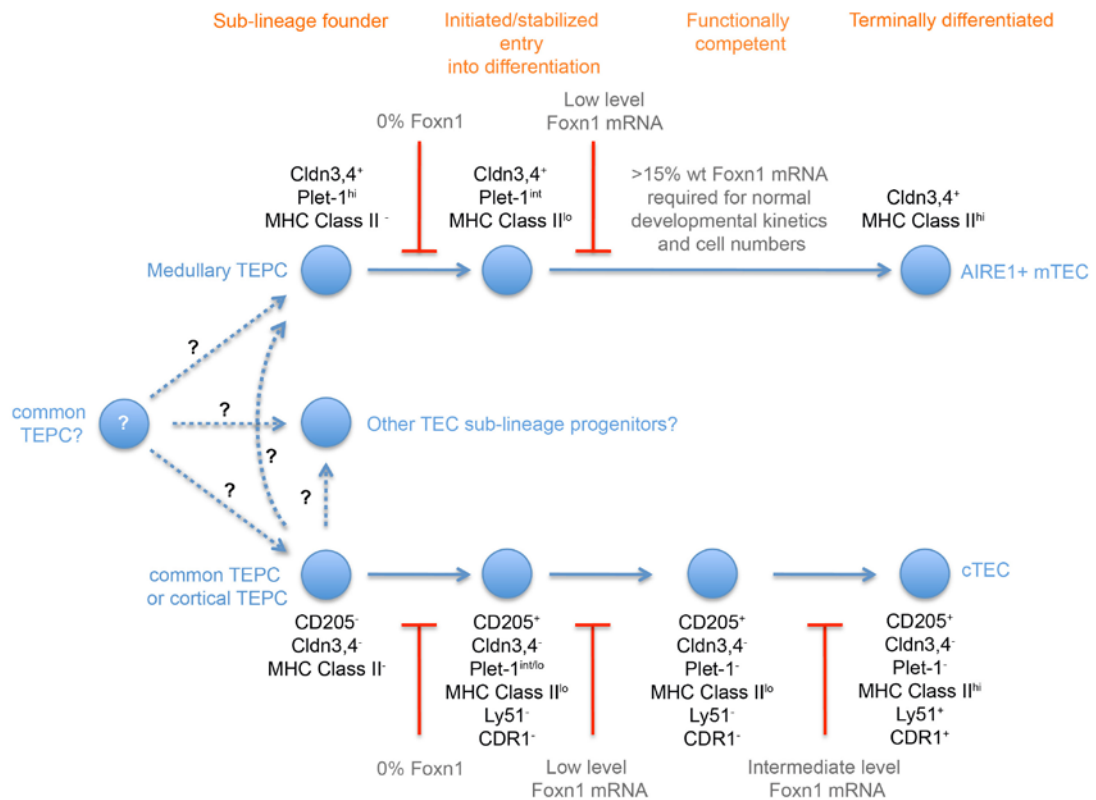


**Figure 1.5 Model of cellular hierarchies in Foxn1 lineage progression.**  
(Nowell et al., under review)

## 1.4 The postnatal thymus

T cell development in the postnatal thymus is mediated by a microenvironment of dynamic stromal populations. In mice, total thymus cellularity increases by 20-fold to approximately  $2 \times 10^8$  cells from birth until 1 month old (Gray et al., 2006). This primarily represents an increase in the number of haematopoietic cells, but the absolute stromal cell number also increases in a broadly proportional manner. From 1 month to 3 months, there is a decrease of thymus cellularity and then stabilisation at approximately  $1.2 \times 10^8$  cells. Following this the thymus gradually begins to degenerate from 3-4 months postnatally and thymic output is reduced, a process known as thymus involution (Manley et al., 2010).

### 1.4.1 Foxn1 in the postnatal thymus

The proportion of TECs that express Foxn1 in the postnatal thymus has been examined in a number of studies, with strikingly different results reported. An immunohistochemical assay with an  $\alpha$ -Foxn1 antibody determined that 24% of TECs in 2-4 week old thymi expressed

Foxn1 (Itoi et al., 2007). In contrast, flow cytometric analysis of a *Foxn1:eGFP* reporter model, in which a ~30kb fragment upstream exon 2 was used to drive GFP expression, showed Foxn1 expression in over 90% of TECs in the 10 day old thymus (Corbeaux et al., 2010). This discrepancy may be accounted for, at least in part, by the difference in sensitivity of detection between the two methods. Other factors that should be considered are the ability of the antibody or *Foxn1:eGFP* mouse line to faithfully detect or report Foxn1 expression respectively. These are worth considering as this was the first report that utilised this  $\alpha$ -Foxn1 antibody and, the *Foxn1:eGFP* reporter mice were generated by random insertion of the transgene into the genome which may result in integration-site specific effects on *Foxn1:eGFP* expression.

Foxn1 expression in thymic epithelium has been shown to decrease with age, suggesting a possible link between Foxn1 and thymus involution. Foxn1 mRNA levels in wildtype mice were reduced by 3-fold and 16-fold at 7 and 12 months, respectively, compared to levels in 1 month old mice (Ortman et al., 2002). However, because these analyses were performed on bulk thymic digests and not defined TEC populations, the actual fold changes are most likely inaccurate. Also, this approach cannot address changes in Foxn1 levels in specific TEC sub-populations.

Functionally, Foxn1 is required for proper terminal differentiation of both cTECs and mTECs in the postnatal thymus (Nowell et al., under review). In *Foxn1<sup>R/R</sup>* mice, which are homozygous for the revertible hypomorphic *Foxn1<sup>R</sup>* allele, cTEC differentiation is severely blocked, as shown by a marked reduction in expression of the mature cTEC markers, CDR1 and Ly51 (Nowell et al., under review). Additionally, the mature Aire<sup>+</sup> mTEC lineage, which is important for self-tolerance induction, does not develop normally. Following reversion of the *Foxn1<sup>R</sup>* allele to the wildtype allele, these markers are rapidly (after 2 days) acquired, indicating that Foxn1 is required for terminal differentiation in TECs.

The upstream regulation of Foxn1, in both the embryonic and postnatal contexts, is poorly understood. Wnt signalling has been shown to activate Foxn1 expression in *in vitro* reporter assays (Balciunaite et al., 2002). Additionally, a recent report has shown that Foxn1 may be regulated by Wnt signalling in the postnatal thymus (Osada et al., 2010). Disruption of Wnt signalling in the postnatal thymic epithelium, via up-regulation of the Wnt antagonist Dickkopf-related protein 1 (DKK1), resulted in reduced Foxn1 expression and disorganised TEC architecture. Furthermore, the TEC compartment and total thymus cellularity were also

reduced in size. Interestingly, Wnt4 expression is reported to decrease with age in the wildtype thymus (Kvell et al., 2010). However, a direct effect of Wnt signalling on Foxn1 expression was not demonstrated in this report and, thus the effect observed may be secondary to other Wnt-induced effects in the epithelium.

#### **1.4.2 Other genetic factors in the postnatal thymic epithelium**

The factors that regulate the cellular kinetics of the postnatal thymic epithelium are only poorly defined. This is partly due to the difficulty in interpreting postnatal phenotypes that are caused by perturbations in the thymic epithelium during organogenesis, and the lack of good genetic models that allow manipulation of the postnatal thymus. Ideally, experiments that aimed at investigating the effects of genetic modifications in the postnatal thymic epithelium would be designed such that the thymus was allowed to develop normally before perturbations were induced.

The cytokine and growth factor-responsive protein *Signal Transducer and Activator of Transcription 3 (Stat3)* has been shown to play a role in maintenance of postnatal thymic cellularity (Sano et al., 2001). When *Stat3* was deleted in TECs, postnatal thymus cellularity was reduced by three-fold from 5-7 weeks onwards. However, the TEC compartment appeared relatively unaltered and rather, it was an increase in T cell apoptosis that accounted for the reduced thymus cellularity. A number of genes have also been reported to regulate TEC proliferation in the postnatal thymus. Over-expression of a *Cyclin D1* transgene under control of a Keratin 5 promoter, that is active in TECs, resulted in severe thymus hyperplasia from 6 weeks of age (Robles et al., 1996). In contrast, the absence of the *Thymus, Brain and Testes-associated gene (Tbata)* resulted in an increase in thymus cellularity from 5 months of age (Flomerfelt et al., 2010). This increase in thymocyte cellularity was driven by a larger and more proliferative TEC compartment, indicating that *Tbata* may have a suppressive effect on TEC proliferation. That the effect of modulating *Cyclin D1* and *Tbata* was observed only during later postnatal stages (i.e. after the initial postnatal expansion in thymus cellularity) indicates that these genes may have role in maintaining the homeostatic thymic environment through mechanisms that regulate TECs.

*p63*, a homolog of the tumour suppressor gene *p53*, is expressed in human and mouse postnatal thymic epithelium; the predominant isoform expressed by TECs is  $\Delta Np63\alpha$  (Chilosi et al., 2003; Senoo et al., 2007). *p63* null thymi are hypoplastic, although the TECs proliferate, differentiate and support thymopoiesis as normal (Senoo et al., 2007). *In vitro*

assays, including clonal expansion and long term culture, indicated that p63 was essential for proliferative potential in TECs (Senoo et al., 2007). Lastly, while *Pax1* and *Pax9* genes are crucial for normal thymus organogenesis and are expressed in postnatal thymus – Pax1 in a subset of cTECs (Wallin et al., 1996) and Pax9 throughout the epithelium (Michelle Kelly, pers. comm.) – there are no reports investigating their function in the postnatal thymus.

### **1.5 Thymus involution**

One of the most striking consequences of aging is the degeneration or involution of the thymus. This is broadly characterised by a reduction in thymus size and T cell development (thymopoiesis) and the consequent reduction in naïve T cell thymic emigrants (Sempowski et al., 2002). In humans, the intrathymic lymphoid compartment begins to decrease shortly after birth at around 3% per year until middle age and then at 1% per year for the remainder of life (Steinmann et al., 1985). During involution the non-stromal, non-thymopoietic perivascular regions expand, such that the functional compartment constitutes less than 10% of the total thymic tissue by 70 years of age (Steinmann et al., 1985). In mice, the thymus begins to involute from approximately 3 months of age. This is initially evidenced by one of the early hallmarks of involution, the disorganisation of the CMJ; this is followed by the gradual decrease in the number of intrathymic hematopoietic cells (Chen et al., 2009; Gray et al., 2006; Manley et al., 2010; Sempowski et al., 2002). Very old mice (18 month and older) have over ten-fold fewer thymocytes than young mice, and by this age the CMJ has completely disintegrated and the cortio-medullary architecture is essentially lost (Chen et al., 2009; Sempowski et al., 2002) (Figure 1.6).

The fundamental reason why the thymus involutes is not clear. Some argue that thymus involution represents the conservation and redirection of energy towards reproduction in later life, while some have suggested that it is required to allow peripheral selection of a well-adapted T cell repertoire (Dowling and Hodgkin, 2009; George and Ritter, 1996).

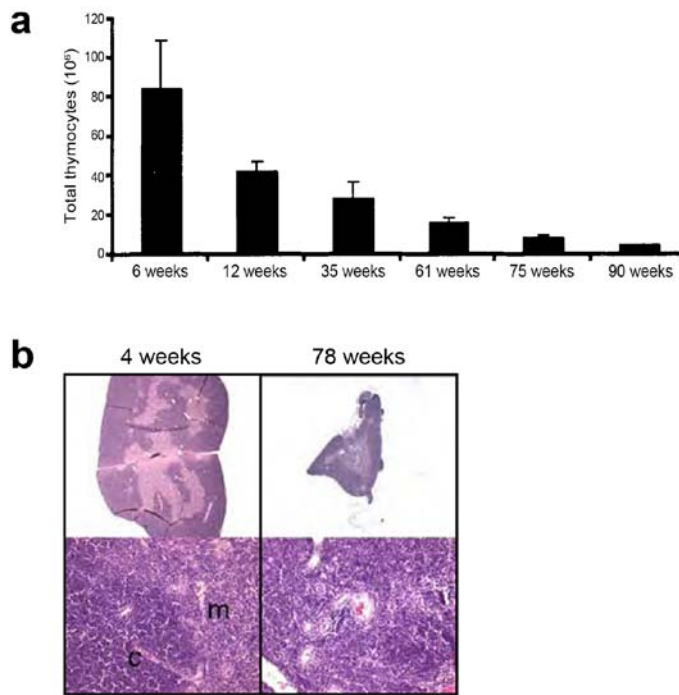


**Figure 1.6 Age-associated thymic atrophy in mice.**

**(a)** Total thymocyte numbers decrease with age (Sempowski et al., 2002). **(b)** Hematoxylin and eosin staining shows that the architecture of the thymus degenerates with age, including the disintegration of the cortico-medullary junction (c – cortex, m – medulla) (N. Manley, University of Georgia).

### 1.5.1 Mechanisms of thymus involution

Puberty-associated hormonal changes have long been proposed as the principle instigator of thymus involution (Henderson, 1904). This has been substantiated by a host of studies that have investigated the effects of various hormones and hormone-altering procedures on thymus output (Hince et al., 2008). However, as described above, the human thymus reaches peak sizes soon after birth and begins to decrease in size long before the onset of puberty (Steinmann et al., 1985). In contrast, thymus involution broadly corresponds with puberty in mice (Gray et al., 2006). Thus, the puberty-involution relationship remains controversial (Montecino-Rodriguez et al., 2005).

The underlying cellular mechanisms that drive thymus involution are poorly understood. While it is likely that age-related, functional defects in both the lymphoid and stromal compartments are causes of involution, it is unclear whether one compartment initially becomes defective and subsequently affects the functionality of the other. Several studies have investigated potential defects in the early hematopoietic precursor cells. The DN1 progenitor cell population decreases in size with age, and some studies have suggested that

these cells also exhibit a reduction in developmental potential and proliferative capacity with age (Heng et al., 2005; Min et al., 2004). This was demonstrated by assaying the characteristics of early T lineage precursors (ETPs) isolated from young and old mice in *in vitro* thymus reconstitution assays (Min et al., 2004). In contrast, other studies have reported no defect in the ETP population in the aged thymus (Zhu et al., 2007). Here, grafted allogenic fetal thymic lobes in young and old mice showed no difference in DN1 population size and proportion or in any other T cell population, following colonization by host HPCs. Caveats exist in both sets of experiments; in the former, the properties of the isolated ETPs may have already been defined by the stroma, and in the latter, the embryonic stromal niche may initially affect ETP characteristics. Further experiments have shown that when aged mice were reconstituted with BM from young mice, the thymic architecture was not restored, whereas reconstitution of young mice with BM from old mice did not diminish thymopoiesis (Mackall et al., 1998). Collectively, these data indicate that defects in the stromal compartment are, at least in part, responsible for the age-related decrease in thymic output.

The reduction in functionality of the stromal compartment with age is associated with an increase in adipose tissue in the perivascular, trabeculae and subcapsular regions of the thymus in mice and humans (Dixit, 2010; Flores et al., 1999). It is unclear whether thymic adipocytes arise as a consequence of thymic aging or are active instigators of the process. It has been proposed that adipocytes develop via an epithelial to mesenchymal transition (EMT) process (Dixit, 2010). Interestingly, cells identified as historically part of the Foxn1<sup>+</sup> TEC lineage (using a Foxn1<sup>Cre</sup> × R26-floxedSTOP-LacZ mouse model) expressed an EMT marker in the aged thymus (Youm et al., 2009). However, the extent of EMT in the aging thymus was not quantified and a significant proportion of the EMT positive cells were not derived from the Foxn1<sup>+</sup> epithelial lineage. Thus, while it appears that TECs do undergo EMT in the aging thymus, the extent and kinetics of this process remain unclear.

### **1.5.2 Consequences of thymus involution**

A complex array of mechanisms underlie the decline in the adaptive immune system function with age, and collectively are termed immunosenescence (Gruver et al., 2007). A primary cause of immunosenescence is age-associated thymic atrophy and the concurrent reduction in naïve T cell output. Homeostasis of the naïve and memory T cell populations in the periphery is maintained by an intricate balance between proliferation and the influx of new naïve T cells (Tanchot et al., 2000). In the aged, this homeostatic relationship is perturbed and becomes skewed towards memory T cells with a decline in the frequency of

naïve T cells also observed (Schwab et al., 1997). Additionally, the TCR diversity of both naïve and memory populations declines with age (Arstila et al., 1999; Goronzy and Weyand, 2005).

These age-associated changes to the immune system result in increased susceptibility and severity of infections and diseases, including cancer, poor responses to vaccines, and increased autoimmunity. In addition, the cytoablative effects of chemotherapy and radiation conditioning treatment in adult bone marrow transplant patients, further reduce thymic function, and are compounded by the reduced recovery capacity in the aged. Following HSC transplantation in older patients, the peripheral T cell compartment reconstituted slowly, if at all, and to only 25% of the levels observed in younger patients (Hakim et al., 2005). Additionally, some severe infections, such as HIV, also comprise immune system functionality. Thus it would be clinically beneficial to be able to improve immune system function in these instances. One of the approaches aimed at preventing or improving immunodeficiency is the enhancement of thymus function and the increased production of naïve T cells. Various treatments that improve thymus function in mice and humans have been reported, and are discussed below.

### **1.5.3 Models of immune reconstitution**

#### **1.5.3.1 Sex steroid modulation**

The link between sex steroid levels and thymus involution and regeneration has long been proposed and has been extensively investigated (Henderson, 1904; Hince et al., 2008). Most compellingly, sex steroid ablation by chemical or physical castration in aged rodents results in extensive thymus regeneration (Fitzpatrick et al., 1985; Greenstein et al., 1987). Atrophic thymi from aged mice that were surgically castrated, regenerated to the size observed in juvenile mice (Gray et al., 2006; Heng et al., 2005; Sutherland et al., 2005). This was driven by proliferative expansion and architectural restoration of the TEC compartment, including increased expression of MHC Class II. Correspondingly, absolute TN cell and T cell numbers increased to juvenile levels and showed increased proliferation rates and normalised distribution (Heng et al., 2005; Sutherland et al., 2005). BMT experiments in androgen resistant transgenic mice have suggested that the stromal component of the thymus and not the thymocytes are the essential for this regeneration (Olsen et al., 2001). Importantly, the increase in thymus size following of sex steroid ablation is transient; following an initial increase in thymus cellularity in castrated young mice, thymus cellularity returned to levels

comparable with those observed in age-matched mice that were not castrated (Min et al., 2006).

Similarly, chemical castration in humans via luteinising hormone-releasing hormone (LHRH) antagonist treatment, resulted in an increase in peripheral naïve T cells (including CD4<sup>+</sup> and CD8<sup>+</sup> subsets) and 60 % of patients showed an increase in thymus function as assayed by peripheral T cell receptor excision circles (TREC) levels (Sutherland et al., 2005). Similar results were observed following LHRH antagonist treatment prior to HSCT in humans (Sutherland et al., 2008). Taken together, these data establish sex steroid modulation as a potential approach for immune reconstitution, albeit in a transient manner.

### **1.5.3.2 Keratinocyte growth factor**

Keratinocyte growth factor (KGF) or fibroblast growth factor 7 (Fgf7) is an epithelial mitogen produced by range of mesenchymal cells, including fibroblasts in the thymus (Finch and Rubin, 2004; Gray et al., 2007). KGF functions exclusively through the IIIb isoform of FgfR2 (FgfR2IIIb), which is expressed on TECs and is required during development for normal thymus organogenesis (Revest et al., 2001; Rossi et al., 2002). *KGF*<sup>-/-</sup> mice have no altered thymus phenotype, with normal thymopoiesis and T cell numbers observed. However, *KGF* deficient thymi demonstrated an impaired recovery following sub-lethal irradiation (Alpdogan et al., 2006).

Experiments designed to test the effect of systemic administration KGF on thymus size have demonstrated that, similar to castration, this treatment results in an increase in thymus size. In young mice, systemic KGF treatment enhanced total thymus cellularity with an increase in number observed for all major thymocyte populations (Rossi et al., 2007). In 15 month old mice, KGF treatment transiently increased total thymus cellularity to near 1 month old levels (Min et al., 2007). Re-organisation and an increase in IL-7 expression were observed in the TEC compartment. In 18 month old mice, KGF treatment resulted in a 3-fold increase in thymic cellularity which was significantly less than juvenile levels; however this probably represents the shorter time period between KGF treatment and analysis (14 days compared to 1 month in Min et al., 2007) (Alpdogan et al., 2006). Currently, no published clinical studies exist for KGF treatment as an approach for immune reconstitution. However, other clinical data suggest that KGF is cytoprotective and it is currently used as a drug for oral mucositis prophylaxis in patients receiving myeloablative conditioning prior to HSCT (Radtke and Kolesar, 2005).



### 1.5.3.3 Interleukin-7

Interleukin-7 (IL-7) is a cytokine that is produced by thymic and bone marrow stromal cells and is essential for both T and B cell development in mice (Sakata et al., 1990; Zamisch et al., 2005). Its receptor, IL-7R, is expressed by a range of cells in the immune system including thymocytes and developing B cells (Alpdogan and van den Brink, 2005). *IL-7* and *IL-7R* knockout mice have drastically reduced thymic cellularity and impaired thymocyte development (Peschon et al., 1994; von Freeden-Jeffry et al., 1995). IL-7 promotes the survival of TN progenitor thymocytes and thymocytes undergoing transition through the  $\beta$ -selection checkpoint to the CD4<sup>+</sup>CD8<sup>+</sup> DP stage (Morrissey et al., 1994; Trigueros et al., 2003). It also promotes the proliferation of intrathymic CD4<sup>+</sup> and CD8<sup>+</sup> SP T cells and the production of  $\gamma\delta$  T cells (Hare et al., 2000; Maki et al., 1996). Due to these effects of IL-7 on a number of thymocyte populations, it has been extensively investigated as an approach to immune reconstitution.

Studies into the treatment of aged mice with IL-7, as a means of reversing thymus involution, have reported mixed success. While some reports observed an increase in TN thymocytes, others showed no increase in thymic output and thymus size following IL-7 treatment (Andrew and Aspinall, 2001; Pido-Lopez et al., 2002; Sempowski et al., 2002). In contrast, IL-7 treatment in HSCT models has been used successfully to enhance T cell reconstitution (in young and old mice) through increased T cell development and homeostatic proliferation and decreased T cell apoptosis (Abdul-Hai et al., 1996; Alpdogan et al., 2003a; Bolotin et al., 1996; Mackall et al., 2001). However, one concern that has been raised is the magnifying effect of IL-7 on graft-versus-host disease in allogenic HSCT models (Sinha et al., 2002). Nonetheless, various human forms of IL-7 are currently in clinical trials aimed at enhancing immune reconstitution in various situations, including following bone marrow transplants and in HIV-infected patients (Cytheris).

### 1.5.3.4 Growth Hormone

Growth hormone (GH), predominantly produced in the anterior pituitary, acts on the immune system via stimulatory or direct effects on insulin-like growth factor 1 (IGF-1), production of which has been observed in TECs (Timsit et al., 1992; Welniak et al., 2002). In young mice, IGF-1 treatment increased thymopoiesis, including increased intrathymic and peripheral T cell numbers, via a proportional increase in TEC compartment size through the enhancement of TEC proliferation (Chu et al., 2008). Additionally, treatment of mice with GH and IGF-1 following allogenic HSCT procedures in mice resulted in increased thymic cellularity and

peripheral T cells (Alpdogan et al., 2003b; Chen et al., 2003). In a clinical study of GH treatment in HIV-infected adults, an increase in thymic mass, thymic output (as measured by TREC) and circulating CD4<sup>+</sup> T cells was observed. However, side effects of significant drug toxicity were also observed (Napolitano et al., 2008).

#### **1.5.3.5 *In vitro* T cell development**

One proposed approach to immune reconstitution is the generation of *in vitro* T cells for transplantation. Both thymic stromal elements and isolated fetal epithelial progenitor cells have the ability to support T cell differentiation *in vitro* reaggregated thymic organoids (Anderson et al., 1993; Sheridan, 2007). However, the application of these methods is limited due to the requirement of fresh thymus tissue. Another approach is the differentiation of T cells by stromal cell lines that express Delta-like 1 or 4 (OP9-D111 or OP9-D114 cells). In this Notch1-based culture system, murine and human hematopoietic and embryonic stem cells developed into T cells in the presence of various cytokines (La Motte-Mohs et al., 2005; Schmitt et al., 2004b; Schmitt and Zuniga-Pflucker, 2002). Additionally, OP9-D111 cells have been shown to facilitate the expansion of T cell progenitors from human umbilical cord blood HSCs, which when grafted into immunodeficient mice, were able to reconstitute the thymus (Awong et al., 2009). However, the *in vitro* facilitation of both the development of MHC classes I and II restricted thymocytes and the deletion of self-reactive thymocytes has yet to be achieved.

#### **1.5.3.6 Thymus transplantation**

Thymus transplantation has recently been developed as a treatment for patients with DiGeorge anomaly, which is characterised by congenital heart disease and severe hypoplasia or athymia (Kirkpatrick and DiGeorge, 1968). Cultured postnatal, allogenic thymus tissue was transplanted into the quadriceps muscles of DiGeorge patients and resulted in T cell reconstitution and function, with peripheral naïve T cells observed 3-5 months post-transplantation (Markert et al., 2007; Markert et al., 2010). A 10-year follow up in these patients indicated that outcome was still positive. However, this approach is severely limited by fresh thymus tissue donation and is complicated by donor/recipient major histocompatibility matching.

As described above, numerous treatments, at various stages of development, are currently being pursued as potential clinical approaches to reconstitute the immune system.

### 1.5.4 *Foxn1* and thymus involution

A potential role for *Foxn1* in postnatal thymus maintenance and involution has been highlighted in a number of recent reports. Firstly, a novel *Foxn1* allele, *Foxn1<sup>LacZ</sup>*, where IRES-LacZ was inserted into the 3'UTR of *Foxn1*, exhibited a phenotype that mimicked early thymus involution, including premature thymic atrophy and a corresponding decrease in T cell output (Chen et al., 2009; Figure 1.7). In these mice, *Foxn1* expression is prematurely down-regulated from 1 week postnatally such that *Foxn1* is only expressed at 20-30% of wildtype levels at 5 weeks of age. The reduction in *Foxn1* expression in the *Foxn1<sup>LacZ</sup>* mice was proposed to be as a result of hypermethylation of the *Foxn1* promoter caused by the insertion of the LacZ cDNA (Strathdee et al., 2008). This was confirmed in the study by the *in vitro* treatment of isolated *Foxn1<sup>LacZ</sup>* TECs with a demethylating agent, which restored *Foxn1* expression to normal levels.

The reduction in *Foxn1* expression in postnatal *Foxn1<sup>LacZ</sup>* thymi led to an early decrease in the number of thymocytes compared to normal thymi. Additionally, there was deterioration of the TEC compartment, including the disintegration of the normal epithelial architecture, a reduction in the number of TECs and loss of mature medullary (UEA1<sup>hi</sup>) and functional (MHC Class II<sup>hi</sup>) TEC subpopulations. Furthermore, there were fewer proliferating TECs in thymi *Foxn1<sup>LacZ/LacZ</sup>* thymi compared to controls. These data indicated for the first time that *Foxn1* is required to maintain the postnatal thymic microenvironment.

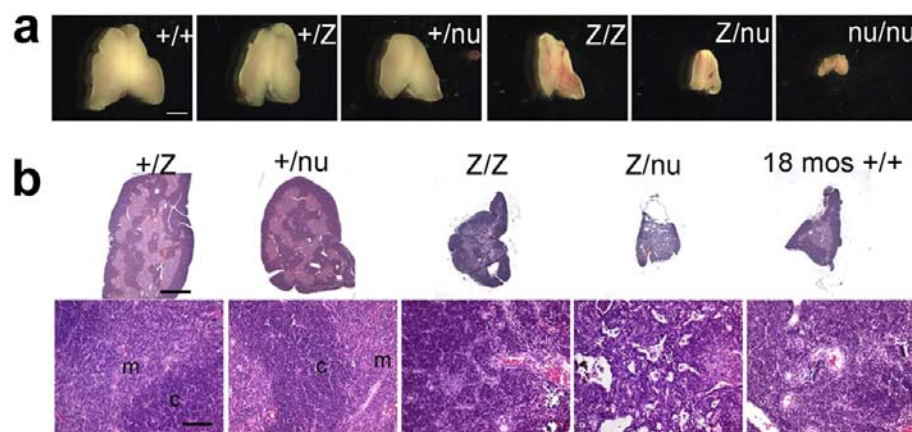


**Figure 1.7 *Foxn1* is required to maintain the postnatal thymic microenvironment.**

A *Foxn1* allelic series, using *wildtype* (+), *Foxn1<sup>LacZ</sup>* (Z) and *null* (nu) alleles, demonstrated that *Foxn1* is required to maintain the postnatal thymus in a dosage-dependent manner. **(a)** Whole thymic lobes from 5 week old mice. **(b)** Hematoxylin and eosin staining of 10 week old thymic lobes shows that *Foxn1* is required to maintain the thymic architecture. Image from Chen et al., 2009.

Further studies have also examined the reduction or loss of Foxn1 expression in the postnatal thymic epithelium using different approaches. A phenotype of premature involution was also observed in a mouse model where the *Foxn1* genomic locus was disrupted; here, loxP sites were introduced into exons 5 and 6 of *Foxn1*, rendering the locus susceptible to Cre-mediated recombination (Cheng et al., 2010). A Tamoxifen inducible, ubiquitous CreER<sup>tm</sup> mouse strain was then utilized to disrupt the *Foxn1* locus postnatally, which resulted in thymic atrophy and loss of TEC architecture. A caveat in this analysis is the inability to unequivocally distinguish between the effect of loss of Foxn1 and the general effect of ubiquitous Cre induction. Indeed, postnatal induction of ubiquitous Cre expression resulted in a host of defects in multiple haematopoietic lineages, including reduced proliferation, increased apoptosis and chromosomal abnormalities (Higashi et al., 2009). Most notably, significant thymus atrophy and defects in T cell distribution were also observed (Higashi et al., 2009). This is particularly noteworthy as data for Cre<sup>ER</sup> control mice treated with Tamoxifen, which would establish the general effect of ubiquitous Cre induction on the parameters measured, were not presented in this report.

A further mouse model has been described in which Foxn1 positive TECs were ablated in the postnatal thymus, due to the expression of a toxic form of the Foxn1 protein that contained an N-terminal fusion of 82 glutamine residues (Corbeaux et al., 2010). Unsurprisingly, the loss of Foxn1 positive TEC lineage in the postnatal thymus resulted in decreased T cell output and epithelial disintegration. This analysis does not directly address the effect of the loss of Foxn1 expression in the postnatal thymus but rather the effect of the loss of Foxn1 positive TECs at a cellular level. Nonetheless, it confirms that the Foxn1<sup>+</sup> TEC lineage is important for thymopoiesis in the postnatal thymus, although it cannot account for a role in thymopoiesis of a potential Foxn1<sup>-</sup> TEC lineage that may develop from the Foxn1<sup>+</sup> lineage.

Collectively, data from these three mouse models show that *Foxn1* plays a role in the maintenance of the postnatal thymic microenvironment, and suggest that *Foxn1* may be a primary target for thymic involution.

## **1.6 Aims**

The recent reports described above have shown that the premature loss of Foxn1 expression in the postnatal thymus results in a reduction in thymopoiesis. This suggests that Foxn1 may be a primary target of thymus involution. Thus, the initial aim of this work was to determine whether Foxn1 was differentially expressed in the postnatal thymic epithelium in the context of different involution states and different TEC subpopulations (Chapter 3). A further aim was to determine whether thymus involution could be delayed or prevented by up-regulation and maintenance of Foxn1 expression from the onset of involution (Chapter 5). The last aim was to determine whether increased Foxn1 expression in the aged, involuted thymus was able to induce a reversal of involution (Chapter 6). To modulate Foxn1 expression in this manner, I generated a conditional, regulatable Foxn1 mouse model which is described in Chapter 4. Thus, the overall aim of this thesis was to determine whether over-expression of Foxn1 was sufficient to prevent or reverse thymus involution as a novel approach to immune reconstitution.

## Chapter 2: Materials and methods

---

### 2.1 Mice

All animal work was conducted according to UK Home Office guidelines, as established in the ANIMALS (SCIENTIFIC PROCEDURES) ACT 1986. For timed matings, noon of the day of the vaginal plug was taken as day 0.5 (E0.5).

#### 2.1.1 Mice strains

##### 2.1.1.1 *Foxn1*<sup>Cre</sup>

*Foxn1*<sup>Cre</sup> mice were generated in the Manley laboratory at the University of Georgia, USA (Gordon et al., 2007). An IRES-Cre cassette was knocked-in to the 3' UTR of *Foxn1*, generating a *Foxn1*-Cre bicistronic mRNA that was shown not to affect *Foxn1* function. These mice have been backcrossed onto the C57BL/6 background for at least 5 generations and subsequently maintained via intercrossing.

##### 2.1.1.2 Tg(CAG-FLPe)

Tg(CAG-FLPe) mice were generated by Andrew Smith at the University of Edinburgh by random insertion of a CAG-FLPe transgene into the genome (Wallace et al., 2007). These mice have been backcrossed onto the C57BL/6 background for at least 5 generations and subsequently maintained via intercrossing.

##### 2.1.1.3 *Foxn1*<sup>GFP</sup>

*Foxn1*<sup>GFP</sup> mice were generated in the Blackburn laboratory at the University of Edinburgh. A splice acceptor-eGFP-polyA cassette was inserted into intron 2 (upstream of the first coding exon) of the *Foxn1* locus such that GFP faithfully reports *Foxn1* expression (Figure 2.1). These mice have been backcrossed onto the C57BL/6 background for 2 generations.



**Figure 2.1 *Foxn1*<sup>GFP</sup> allele.**

A splice acceptor (SA)-eGFP cassette was inserted into intron 2 of the *Foxn1* genomic locus. E – exon, start – transcriptional start.

#### **2.1.1.4 ROSA26<sup>CAG-STOP-Foxn1ERT2</sup>**

The generation of ROSA26<sup>CAG-STOP-Foxn1ERT2</sup> mice are described in this thesis. These mice were backcrossed onto the C57BL/6 background for 2 generations.

#### **2.1.2 Tamoxifen treatment**

For short term experiments (two weeks or less) mice were treated with single or repeated intraperitoneal (IP) injections of tamoxifen (Sigma-Aldrich). Tamoxifen was dissolved in ethanol and diluted in a cremophor (Sigma-Aldrich)/PBS carrier. Repeated IP dose was 3mg every second day for 2 weeks. For long term experiments tamoxifen was delivered to mice in their drinking water. Tamoxifen citrate salt (Sigma-Aldrich) was prepared in ethanol and diluted in the drinking water to 0.05mg/ml. Tamoxifen/drinking water supply was changed weekly. Mice treated with tamoxifen citrate (at 0.1mg/ml) have been shown to be viable in long term experiments (up to 300 days) (Blyth et al., 2000).

#### **2.1.3 5-Bromo-2'-deoxyuridine (BrdU) treatment**

Mice were injected once intraperitoneally with 1mg of BrdU (BD Biosciences) and then BrdU was administered via drinking water for 3 days (0.5mg/ml).

### **2.2 Molecular biology**

Basic molecular biology techniques were performed as described in (Sambrook and Russell, 2001)

#### **2.2.1 Isolation of nucleic acids**

##### **2.2.1.1 Plasmid DNA**

Small scale plasmid purification was performed using the QIAprep miniprep spin kit (Qiagen). Large scale plasmid purification was performed using the standard plasmid maxi kit (Qiagen).

##### **2.2.1.2 Genomic DNA**

*ES cell DNA:* lysis buffer (100mM Tris pH 8.5, 5mM EDTA, 0.2% SDS, 200mM NaCl, 100µg/ml proteinase K) was added to confluent ES cells in 96-well plates and incubated overnight at 37°C. DNA was precipitated by centrifugation following the addition of an equal volume isopropanol, washed with 70% ethanol, and resuspended in TE buffer (pH 8).  
*Mouse ear punch DNA:* lysis buffer was added to ear punches and incubated overnight at 56°C. Proteinase K was denatured by incubation at 95°C for 10 minutes and total cell lysate

was used in subsequent reactions. *Mouse tail DNA*: lysis buffer was added to tail bopsies and incubated at 56°C overnight. DNA was purified using conventional phenol extraction, precipitated using an equal volume of isopropanol, washed with 70% ethanol and resuspended in TE buffer.

### 2.2.1.3 RNA

RNA isolation was performed using the RNeasy mini kit (Qiagen). Tissue was homogenised by mechanical disruption with a syringe and needle; cells were homogenised by vortexing. DNase treatment was performed on the spin columns using RNase-free DNase (Qiagen).

## 2.2.2 Molecular cloning

### 2.2.2.1 Conventional cloning

DNA plasmids were digested with the appropriate restriction enzymes and resolved by gel electrophoresis on 0.8-1% agarose gels. Relevant DNA fragments were excised and purified using the QIAquick gel extraction kit (Qiagen). Plasmids and inserts were ligated at ratios of 1:1 to 1:5 using 1-2U of T4 DNA ligase (Roche) with an overnight incubation at 16°C.

#### 2.2.2.1.1 Oligonucleotide sequences

New restriction sites were introduced into plasmids by ligation of annealed, complementary oligonucleotides that contained the required restriction site into the relevant plasmid. Sequences for these oligonucleotides are shown below. All oligonucleotides were synthesised by Sigma-Aldrich.

Oligonucleotide	Sequence (5' -3')
IPC260-BbsI-a	CGCAATCTCGAAGACTTGGCCCTAGACGGTGCA
IPC260-BbsI-b	CCGTCTAGGGCCAAGTCTTCGAGATTGCG
ROSA26-1-PacI/MluI-a	CTAGGCAGTCTTAATTAAGGACAGCCTGTAACCA CGCGTGGTTAC
ROSA26-1-PacI/MluI-b	CTAGGTAACCACGCGTGGTTACAGGCTGTCCTTAA TTAAGACTGC



### 2.2.2.2 PCR cloning

PCR products were resolved by gel electrophoresis and purified using the QIA quick gel extraction kit (Qiagen). Purified PCR products were cloned using the pGEM-T Easy plasmid according to the manufactures instructions (Promega).

### 2.2.2.3 Transformation of chemically competent *E. coli*

Subcloning-efficiency DH5 $\alpha$  competent cells were used for routine cloning ligation reactions. One shot TOP10 competent cells were used for PCR product ligation reactions. Max efficiency Stbl2 competent cells were used to propagate the large, unstable plasmids. All cells were purchased from Invitrogen and used according to the manufacturer's instructions. Transformation mixtures were plated onto agar plates containing the appropriate antibiotic selection.

## 2.2.3 PCR

### 2.2.3.1 PCR Primers

The list below shows the primers used for genotyping, sequencing and PCR cloning, as described in the relevant sections herein.

PCR primer	Sequence (5' - 3')
CAG210R	CGTAAATAGTCCACCCATTGACGTC
CagIPC270	GTTCGGCTTCTGGCGTGTGA
Cre145F	GACCAGGTTTCGTTCACTCATGG
Cre817R	CCTTAGCGCCGTAAATCAATCG
FEIG1f	TGGGCTCACCTCACTATCC
FEIG1r	TGGGAAGAGTGGCTGGTGAC
FEIG2f	GGGAGCAGCTGAAGGATGAC
FEIG2r	GGCAACATGGAGGATGACG
FEIG3f	CGGTTCCGCATGATGAATC
FEIG3r	GACTTCAGGGTGCTGGACAG
FEIG4f	CGTCTGTAGCGACCCTTTGC
FEIG4r	CGCTTGAGGAGAGCCATTTG
FEIG5f	GGAGTACAAGGGCCGCAACT
FEIG5' r	AAGTTAGCATGCTTGTCTGTGG
FRTf	GCTGGTTCGACGAAGTTCCTATAC
ROSA3 <sup>geno2</sup> -R	CATTCTCAGTGGCTCAACAACACTTG

ROSA <sup>prmt</sup> r720F	CCTAAAGAAGAGGCTGTGCTTTG
ROSA <sup>seq</sup> F	AGGGAGCTGCAGTGGAGTAG

---

### 2.2.3.2 Conventional PCR

Routine PCR was performed using Taq DNA polymerase according to the manufacturer's instructions (Qiagen). PCR cloned products were amplified using Expand High Fidelity PCR System according to the manufacturer's instructions (Roche).

### 2.2.3.3 Genotyping PCR

Genotyping of mice was performed on genomic DNA isolated from ear punch biopsies. R26-CAG-Foxn1<sup>ER</sup> mice were genotyped using FEIG3f and FEIG4r primers with an expected product size of 897bp for transgenic mice. Foxn1<sup>Cre</sup> mice were genotyped using CRE145F and CRE817R with an expected product size of 403bp for transgenic mice. Targeted ES cell recombinants were genotyped as described in 4.3.2.

### 2.2.3.4 Quantitative RT-PCR

First strand cDNA was synthesised from up to 5µg of total RNA using oligo dT primer with Superscript II reverse transcriptase following the manufacturer's instructions (Invitrogen). cDNA was diluted five-fold with PCR grade water and 2.5µl was added to the following reaction: 5µl of 2× Lightcycler 480 Probes Master, 0.05µl of each 10 µM primer, 0.1µl of 100× UPL probe, PCR grade water to 10µl. Reactions were performed on a Roche LightCycler 480 instrument (384 System) using the standard run protocol. At least 3 technical repeats were performed per sample and data were analysed using the LightCycler 480 software (v1.5). Standard curves were established for each gene analysed using E14.5 EpCAM<sup>+</sup> TEC cDNA and a serial dilution series of 10, 10<sup>-1</sup>, 10<sup>-2</sup>, 10<sup>-3</sup>, 10<sup>-4</sup> (where 10 represents the undiluted cDNA sample).

Primers for qRT-PCR were designed using the Universal Probe Library (UPL) Assay Design Software (Roche) and are listed below:

<b>Primer</b>	<b>Sequence (5' -3')</b>	<b>UPL probe</b>
$\alpha$ -tubulin F	CGGACCACTTCAAGGACTAAA	58
$\alpha$ -tubulin R	ATTGCCGATCTGGACACC	
EVA F	TGTGCTTCCACTTCTCCTGA	100
EVA R	TCCACAGCTTCTGTAGGACAAA	
Foxn1 F	TGACGGAGCACTTCCCTTAC	68
Foxn1 R	GACAGGTTATGGCGAACAGAA	
Dll4 F	AGGTGCCACTTCGGTTACAC	106
Dll4 R	GGGAGAGCAAATGGCTGATA	
CCL25 F	GAGTGCCACCCTAGGTCATC	9
CCL25 R	CCAGCTGGTGCTTACTCTGA	
Pax1 F	CTCCGCACATTCAGTCAGC	105
Pax1 R	TCTTCCATCTTGGGGGAGTA	
Pax9 F	AGCAGGAAGCCAAGTACGG	33
Pax9 R	TGGATGCTGAGACGAAACTG	
Foxn1-3'UTR F	CTTAAAGGTCAAAGAAGGAAAACACT	94
Foxn1-3'UTR R	GGCTAACAAATAAGTTGGCTGAG	
Foxn1ER F	AGGACTTCCCCGAGTACCAC	42
Foxn1ER R	CGTCCTCCACGTACCTCTTC	

#### 2.2.4 DNA sequencing

Sequencing reactions were performed on plasmid DNA. 250ng DNA template and 1 $\mu$ l of 3.2 $\mu$ M sequencing primer were added together and the volume adjusted to 6 $\mu$ l with dH<sub>2</sub>O. BigDye sequencing, clean-up and capillary analysis reactions were performed on a Sanger ABI3730 instrument at the Genepool facility at the University of Edinburgh. Sequences were analysed with Chromas Lite (v2.01) and BioEdit (v7.0.5).

#### 2.2.5 Southern blotting

The strategy used for Southern blotting analyses of targeted R26<sup>CAG-STOP-Foxn1ERT2</sup> transgenic ES cell clones and mice is described in Figure 2.2. Genomic DNA was prepared as described and digested with EcoRI, EcoRV and PacI restriction enzymes for 5', 3' and internal Southern probe assays, respectively.

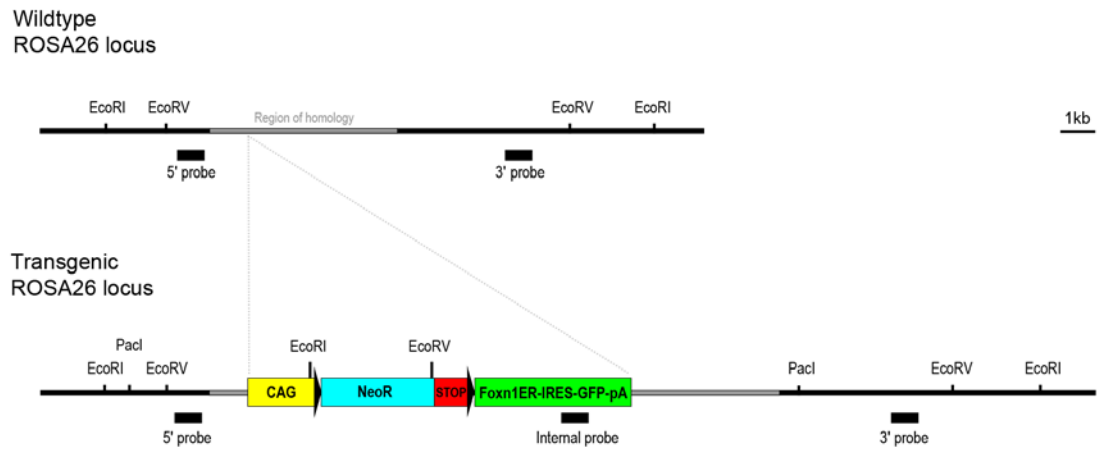


**Figure 2.2 Strategy for Southern blot analysis of transgenic R26<sup>CAG-STOP-Foxn1ERt2</sup> ES cell clones and mice.**

The position of restriction enzyme sites and Southern blot hybridisation probes are shown for the wildtype and transgenic ROSA26 locus. EcoRI, EcoRV and PacI restriction enzyme digests were used for 5', 3' and internal Southern blot analyses, respectively.

### 2.2.5.1 Generation of Southern blotting probes by PCR

Southern blot probes were generated by PCR using the primers listed below. The PCR reaction products were resolved by gel electrophoresis and purified using the QIAquick gel extraction kit (Qiagen). 25ng of probe was then radiolabelled with dCTP-<sup>32</sup>P using the Rediprime II kit (GE Healthcare), following the manufacturer's instructions. The labelled probe was then separated from unincorporated nucleotides using the ProbeQuant G-50 micro columns (GE Healthcare).

Probe	PCR primer	Sequence (5' - 3')
5'	ROSA5'F	GGCCTCTCCTGAAAAGGGTA
	ROSA5'R	GAGACTCACGCAGCCCTAGT
3'	ROSA3'F	CTGACTATGGTGCCAATGTGGATTC
	ROSA3'R	CCCAAAGTGCCTGTCAGTCTTAGG
Internal	InternalF	TGGTTGCCGAACAGGATGTTG
	InternalR	GATCTCCATTCGCCATTCAGG

### **2.2.5.2 Southern blot preparation**

80U of the appropriate restriction enzyme (as described in Figure 4.5) was added to 5-8 $\mu$ g of genomic DNA and incubated overnight at 37°C. The following day the reaction mixture was “spiked” with a further 40U of restriction enzyme and incubated for 2 hours at 37°C.

Restricted genomic DNA was resolved on 0.8% agarose gel overnight. The gel was then soaked for 20 minutes in depurination buffer (0.25M HCl), washed with water, soaked for 2 $\times$  20 minutes in denaturation buffer (1.5M NaCl, 0.5M NaOH), washed with water, and lastly soaked for 2 $\times$  20 minutes in neutralization buffer (1.5M NaCl, 0.5M Tris, pH7). The DNA was then transferred onto an Amersham Hybond-N nylon membrane (GE Healthcare) using conventional capillary action protocols and immobilised by baking the membrane for 1 hour at 120°C.

### **2.2.5.3 Southern blot hybridisation**

Hybridisations were performed using Amersham Rapid-hyb buffer (GE Healthcare) in Techne hybridisation bottles rotating in a Techne HB-1 oven. All steps were carried out at 65°C. Southern blots were pre-hybridised in Rapid-hyb buffer for 15 minutes, then 25ng of labelled probe was added and allowed to hybridise for 2 hours. Blots were then washed for 2 $\times$  15 minutes in 2 $\times$  SSC, 0.1% SDS and 2 $\times$  15 minutes in 1 $\times$  SSC, 0.1% SDS. Blots were then wrapped in Saran wrap and exposed to autoradiographic film at -80°C for 1 day to 3 weeks.

### **2.2.6 Western blotting**

*Sample processing.* Whole thymic lobes were dissociated using the ProteoExtract tissue dissociation buffer kit (Calbiochem) according to the manufacturer’s instructions.

Cytoplasmic and nuclear protein fractions were extracted using a nuclear extract kit (Active Motif) following the manufacturer’s instructions for tissue extraction. Protein samples were quantified following a 1:200 dilution in Bio-Rad protein assay dye and a spectrophotometric absorbance assay at 595nm. A standard curve derived from a series of BSA protein standard concentrations (halving dilutions from 1mg/ml to 0.05mg/ml) was used to determine sample concentration from absorbance read-outs.

*Electrophoresis and transfer.* 6mg of cytoplasmic protein sample or 3mg of nuclear protein sample were added to 5 $\mu$ l sample loading buffer (50 mM Tris pH 6.8, 2% SDS, 10% Glycerol, 1%  $\beta$ -Mercaptoethanol, 12.5 mM EDTA , 0.02 % Bromophenol Blue) and the volume was adjusted to 20 $\mu$ l with water. Protein samples and a SeeBlue Plus2 pre-stained

standard were run on a NuPAGE 4-12% Bis-Tris gel in NuPAGE MOPS SDS running buffer using an XCell SureLock electrophoresis unit (all Invitrogen). Separated protein samples were transferred onto PVDF membrane (Roche) in transfer buffer (25mM Tris, 190mM glycine, 20% methanol (v/v)) using an XCell SureLock unit.

*Detection.* Membranes were blocked overnight at 4°C in 10% skim milk (Marvel) in PBS-Tween 20 (0.05%). Primary incubation was performed for 2 hours at room temperature using  $\alpha$ -Foxn1 (G20, Goat IgG, 1:500, Santa Cruz Biotechnology) in 5% skim milk/PBS Tween 20. Membranes were then washed for 4× 10 minutes and incubated for 1 hour at room temperature with a rabbit anti-goat IgG-HRP conjugated secondary antibody (Sigma-Aldrich, 1:20000). Membranes were washed for 4× 10 minutes and then signal was detected using ECL Plus kit (GE Healthcare) following the manufacturer's instructions. Blots were then wrapped in Saran wrap and exposed to autoradiographic film for 10 seconds to 5 minutes. For loading control analyses blots were stripped in stripping buffer (25mM glycine pH 2, 2% SDS) for 30 minutes at room temperature. Blots were then processed as described above using an anti- $\alpha$ -tubulin (B-7, Mouse IgG2a, 1:3000, Santa Cruz Biotechnology) primary antibody and a sheep anti-mouse IgG-HRP conjugated secondary antibody (GE Healthcare, 1:5000).

### **2.2.7 Luciferase assay**

The wildtype and mutated Foxn1 minimal responsive reporter cassettes, detailed in Figure 4.7a (obtained from Dr. David Prowse, Queen Mary University of London) were stably transfected into COS-7 cells using Lipofectamine 2000 (Invitrogen) following the manufacturer's instructions. CAG-Empty, CAG-Foxn1 and CAG-Foxn1ER were transiently transfected into COS7-WT-FRE-luc and COS7-Mut-FRE-luc cells using Lipofectamine 2000. Cells were cultured for 48 hours with or without 4-hydroxytamoxifen (1 $\mu$ M) and assayed for luciferase expression using a Luciferase Assay System (Promega) according to the manufacturer's instructions and analysed on a Mediators PhL Luminometer (ImmTech).

## **2.3 Immunohistochemistry**

### **2.3.1 Sample processing and staining**

Freshly dissected tissues were embedded in OCT compound (Agar Scientific), snap frozen on dry ice and stored at -80°C. Sections were cut from frozen tissue blocks at 8 $\mu$ m, collected on poly-L-lysine coated glass slides (VWR International) and stored at -80°C. Frozen sections were equilibrated to room temperature (RT) and then fixed in acetone (-20°C) for 2

minutes or in 4% PFA (Sigma-Aldrich) for 5 minutes at room temperature. Sections were then air dried and rinsed in PBS. Blocking was performed with 1-5% serum (secondary antibody host species) in PBS-Tween 20 (0.05%) for at least 30 minutes. Primary antibodies were diluted at the appropriate concentration in the blocking solution and incubated on the sections at room temperature for 1 hour. Sections were then washed for 3× 5 minutes in PBS-Tween 20 and incubated with the appropriately diluted secondary antibody at room temperature for 1 hour. Next, sections were washed for 2× 5 minutes, incubated with DAPI (4',6-Diamidino-2-phenylindole, 5µg/ml) for 2 minutes and washed for 5 minutes. Sections were then air-dried and mounted using Vectashield (Vector Laboratories). Staining was analyzed using a Leica AOBS confocal microscope.

In some instances, immunohistochemistry with  $\alpha$ -Foxn1 (Section 4.4.3) was performed using the tyramide signal amplification kit (Invitrogen) following the manufacturer's instructions.

### 2.3.2 Cytospin preparation

Approximately 1000-5000 cells were resuspended in 100µl of PBS and loaded into a cytospin chamber attached to a poly-L-lysine coated slide (VWR International) and a filter card (ThermoFisher Scientific). Chambers were centrifuged at 500rpm (Cytospin 3, Shandon) for 5 minutes at room temperature. Slides were removed from the chamber, air-dried and fixed in acetone (-20°C) for 2 minutes. Following fixation slides were air-dried for 5 minutes and stored at -80°C until required.

### 2.3.3 Antibodies

The antibodies used for immunohistochemistry are listed below:

Antibody	Clone	Isotype	Source	Working conc.
Pancytokeratin	Polyclonal	Rabbit IgG	DAKO	17µg/ml
Cytokeratin 5	AF138	Rabbit IgG	Covance	2.5µg/ml
Cytokeratin 8	Troma 1	Rat IgG2a	DSHB	Hybridoma stock (1:5)
Cytokeratin 14	AF64	Rabbit IgG	Covance	2.5µg/ml
CDR1	CDR1	Rat IgG2a	Gift from B. Kyewski	Hybridoma stock (1:10)
ER $\alpha$ (HC-20)	Polyclonal	Rabbit IgG	Santa Cruz	0.4-10µg/ml

Foxn1 (G-20)	Polyclonal	Goat IgG	Santa Cruz	4µg/ml
p63	4A4	Mouse IgG2a	Millipore	4µg/ml
ΔNp63 (N-16)	Polyclonal	Goat IgG	Santa Cruz	2µg/ml

Additionally, the biotin conjugated lectin, Ulex Europaeus Agglutinin 1 (UEA1) (Vector laboratories) was also utilised in fluorescence assays. For detection of primary antibodies the following secondary antibodies were used: donkey anti-goat IgG-Alexa488, goat anti-rat IgG-Alexa488, donkey anti-goat IgG-Alexa647, donkey anti-rabbit IgG-Alexa647, goat anti-rabbit IgG-Alexa647, goat anti-mouse IgG2a-Alexa647 and streptavidin-Alexa488 (all Molecular Probes, all used at 2 µg/ml). The following isotype controls were used: rat IgG2a, rabbit IgG, mouse IgG2a (BD Pharmingen) and goat IgG (Santa Cruz Biotechnology).

## 2.4 Flow cytometry

### 2.4.1 Cell preparation

*Embryonic thymus dissociation.* Dissected thymi were dissociated at 37°C for 1 hour in an enzyme mix solution (2mg/ml Hyaluronidase (Sigma-Alrich), 0.7mg/ml Collagenase, 0.05mg/ml DNase (all Roche) in PBS).

*Postnatal thymus dissociation.* Dissected thymi were finely minced with scissors and dissociated at 37°C for 3× 15 minute with 1.25mg/ml Collagenase and 0.05mg/ml DNase in RPMI-1640 (following each 15 minute digestion the dissociated cells were removed and fresh enzyme solution was added). A final digest of remaining cell fragments was performed at 37°C for 30-45 minutes with 1.25mg/ml Collagenase/Dispase (Roche) and 0.05mg/ml DNase in RPMI-1640 (Gray et al., 2008).

#### 2.4.1.1 Postnatal TEC enrichment

*Magnetic enrichment.* Total postnatal thymic cell suspensions were incubated with α-CD45 labelled microbeads (Miltenyi Biotech) following the manufacturer's instructions (5µl of microbeads per 10<sup>7</sup> cells) (Gray et al., 2008). The cell suspension was then run on an AutoMACS (Miltenyi Biotech) using the DepleteS programme. CD45<sup>+</sup> cells recovered were rerun on the machine to recover any remaining unlabelled cells. CD45<sup>-</sup> fractions were pooled and collected by centrifugation

*Density gradient enrichment.* Percoll media (GE Healthcare) was used to create a density gradient for enrichment of TECs by centrifugation (Derbinski et al., 2008). Thymic cell suspensions (<10<sup>9</sup> cells) in 2.41ml of RPMI-1640 where added to 3.59ml of Percoll solution (density ρ=1.07) in a 50ml Falcon tube. Two further 6ml layers, ρ=1.045 layer (3.69ml



RPMI-1640 and 2.31ml Percoll) and  $\rho=1.0$  layer (6ml RPMI-1640) were overlaid to create the density gradient. Tubes were centrifuged at 3500×g at 4°C for 30 minutes. Enriched TECs were recovered from the upper interphase.

### 2.4.2 Cell staining

Cells were washed with cell wash/staining buffer (5% foetal calf serum in PBS). Cells were counted using a Neubauer hemocytometer; an average of 3 technical count repeats were used to determine the cell number for each sample. For thymocyte or enriched CD45<sup>+</sup> fraction analyses,  $1 \times 10^6$  cells were incubated with primary antibody for 15 minutes at 4°C. For flow cytometric analyses of TECs from unenriched thymic digests,  $1 \times 10^7$  cells with incubated with primary antibody for 15 minutes at 4°C. Next, cells were washed and incubated with secondary antibodies when necessary. Following this, cells were washed again and resuspended in 0.2-1ml for flow cytometric analysis. Dead cells were excluding based on DAPI staining (1µg/ml). Intracellular analyses for BrdU incorporation were performed using an APC BrdU flow kit (BD Bioscience) according to the manufacturer's instructions.

### 2.4.3 Antibodies

The following conjugated antibodies were used for flow cytometry assays:

Ab.	Clone	Isotype	Conjugate	Source	Conc.
EpCAM	G8.8	Rat IgG2a	FITC, PE, APC	Biologend	2µg/ml
Ly51	6C3	Rat IgG2a	Biotin	Biologend	5µg/ml
MHC II	M5/ 114.15.2	Rat IgG2b	PE	BD Pharmingen	1µg/ml
CD3	145- 2C11	Hamster IgG1	FITC	BD Pharmingen	2.5µg/ml
CD4	H129.19	Rat IgG2a	FITC, PE, PerCP/Cy5.5	BD Pharmingen	2.5µg/ml
CD8	53-6.7	Rat IgG2a	FITC, PerCP/Cy5.5	BD Pharmingen	2.5µg/ml
CD11b	M1/70	Rat IgG2b	FITC	BD Pharmingen	2.5µg/ml
CD11c	HL3	Hamster IgG1	FITC, PerCP/Cy5.5	BD Pharmingen	2.5µg/ml
CD19	1D3	Rat IgG2a	FITC	BD Pharmingen	2.5µg/ml
CD31	390	Rat IgG2a	FITC	BD Pharmingen	2.5µg/ml
CD25	3C7	Rat IgG2b	PE	eBioscience	1µg/ml

CD44	1M7	Rat IgG2b	APC	eBioscience	2µg/ml
CD45	30-F11	Rat IgG2b	APC, PerCP/Cy5.5	BD Pharmingen	2.5µg/ml
NK1.1	PK136	Mouse IgG2a	FITC	BD Pharmingen	2.5µg/ml
Gr-1	RB6-8C5	Rat IgG2b	FITC	BD Pharmingen	2.5µg/ml
Ter119	Ter119	Rat IgG2b	APC, PerCP/Cy5.5	BD Pharmingen	1µg/ml

Additionally, UEA1-biotin lectin (Vector laboratories) was utilised in flow cytometric assays (5µg/ml). Secondary detection of biotin conjugated primary antibodies was performed using streptavidin-APC or PE/Cy7 (BD Pharmingen, 4µg/ml). The relevant directly conjugated isotype control antibodies were used for all experiments (all BD Pharmingen).

#### 2.4.4 Flow cytometry instruments

Cells were analysed on a BD Bioscience LSR Fortessa SORP instrument. Cell sorting was performed by Jan Vrana or Simon Monard on a BD Bioscience Aria II or a Beckman Coulter MoFlo MLS instrument at the Institute for Stem Cell Research. Laser wavelength specifications for these instruments are as follows: 405nm (V), 488nm (B), 561nm (YG) and 640nm (R). The following laser and filter combinations were used to detect the following fluorochromes: DAPI – V450/50, FITC – B530/30, PerCPCy5.5 – B695/40, PE – YG582/15, PECy7 – YG780/60, and APC – R670/30. Flow cytometric data collected were analysed using FlowJo analysis software.

#### 2.5 Cell culture

Cells were thawed, passaged, expanded and frozen using standard tissue culture techniques in sterile laminar flow hoods. ES cells were maintained in 1× Glasgow minimum essential medium (GMEM) (Invitrogen) containing: 10% foetal calf serum, 1× nonessential amino acids, 4mM glutamine, 2mM sodium pyruvate, 0.1mM 2-mercaptoethanol, 1× leukaemia inhibitory factor (LIF). COS-7 cells were maintained in the same media without LIF.

##### 2.5.1 ES cell electroporation and isolation of targeted clones

For gene targeting experiments, 100µg of XhoI linearised R26-CAG-STOP-Foxn1ER targeting vector was added to a cell suspension of E14Tg2A ES cells. Cells were electroporated at 0.8kV, 3µF in a BioRad GenePulser. Cells were left to recover for 10 minutes and the plated in 100mm tissue culture dishes at densities of  $5 \times 10^6$ ,  $1 \times 10^6$  and  $1 \times 10^5$  cells per plate. G418 selection medium (200µg/ml) was applied to the cells for 7 days until

G418 resistant colonies appeared. A non-transfected control was used to monitor the duration of complete cell death in G418 sensitive colonies. G418 resistant colonies were picked into 96-well plates using a pipette and yellow tip. Once confluent potential clones were replica plated into 96-well plates, one plate was frozen and the other was used for isolation of genomic DNA.

### **2.5.2 Karyotyping and transgenic mouse generation**

Correctly targeted ES cell clones were karyotyped by Jonathan Rans (Tissue Culture Service, Institute for Stem Cell Research, University of Edinburgh). Blastocyst injection and transfer were performed by the Transgenic Service Facility (Institute for Stem Cell Research, University of Edinburgh).

### **2.6 Statistical analyses**

Statistical analyses were performed using the one-way ANOVA test (two tailed), as appropriate for normally distributed data (normal distribution was tested using Chi<sup>2</sup> goodness of fit), using OpenEpi software (Dean and Sullivan, 2010). The  $\alpha$  level is taken as 0.05. Deviation values shown are standard errors throughout. The number of biological and technical repeats is indicated for each experiment.

## Chapter 3: Transcriptional profile of Foxn1 in the thymic epithelium

---

### 3.1 Introduction

Mice homozygous for the hypomorphic *Foxn1* allele, *Foxn1<sup>R</sup>*, display a block in postnatal TEC terminal differentiation, which is more severe in cTECs than mTECs (Nowell et al., under review). This suggests differential dosage requirements for Foxn1 in cTEC and mTEC lineage progression, specifically that a higher level of Foxn1 is required in cTECs than in mTECs to permit proper terminal differentiation. Additionally, Foxn1 is required to maintain the postnatal thymus in a dosage specific manner (Chen et al., 2009). Published data for Foxn1 transcript expression levels in the postnatal thymus shows that there is a decline of Foxn1 with age, with an approximate 16-fold reduction at 12 months compared to 1 month (Ortman et al., 2002). However, these data were obtained from bulk thymic lobe digests and, thus differential effects of thymic involution on populations such as thymocytes, non-epithelial stroma and vasculature may have distorted the results.

In this chapter I test the hypothesis that Foxn1 is differentially expressed in the two major TEC compartments in wildtype mice by quantifying Foxn1 transcript levels in postnatal cTECs and mTECs. I then extend these data and relate them to the previous finding of Ortman et al. by determining Foxn1 transcript levels in defined TEC populations from aged mice. Additionally, I use a recently generated *Foxn1* allele (where GFP reports Foxn1 expression) to examine the proportion of TECs that express Foxn1 in the postnatal thymus. Thus, the overall aim of this chapter is to better understand the dynamics of Foxn1 expression in the postnatal thymus, with respect to the major TEC subpopulations and normal aging.

### 3.2 Results

#### 3.2.1 Isolation of defined TEC subpopulations

I initially analysed Foxn1 transcript levels in the thymic epithelium of 4-8 week old mice. During this window, the thymus is relatively homeostatic, as it is no longer increasing in total cell number but has not yet begun to involute (Gray et al., 2006). In order to obtain purified TEC subpopulations for subsequent analyses, I used established protocols for flow cytometric isolation of TECs (Derbinski et al., 2008; Gray et al., 2008).

The percentage of stromal cells (including TECs) in the postnatal thymus is approximately 1-2% of the total cellularity, with the remainder being hematopoietic cells (Gray et al., 2006). The most efficient manner by which to isolate postnatal TECs is thus to initially deplete single cell suspensions of total thymic cells of CD45<sup>+</sup> cells. This has been achieved by either centrifugation of total thymic digests over a discontinuous density gradient (Derbinski et al., 2008) or depletion of magnetically labelled CD45 cells (Gray et al., 2008). In the experiments performed here I have used both techniques; Figure 3.1a,b show representative plots of thymi cell suspensions from 4-8 week old thymi before and after CD45 depletion.

The CD45<sup>-</sup> cellular component in 4-8 week old postnatal thymi is approximately 2.5% of total cellularity (Figure 3.1a,b), which is comparable to 2-7.5% observed in Gray et al., 2008). After CD45 depletion, the CD45<sup>-</sup> component is enriched to 60-80% of the total cells, of which approximately half are TECs, as defined by staining for the epithelial cell adhesion molecule, EpCAM (Farr et al., 1991) (Figure 3.1b,c). The epithelium can be phenotypically separated into cTEC and mTEC fractions using the antibody Ly51, which reacts with a cell surface glycoprotein on cTECs (Adkins et al., 1988) (Figure 3.1d); thus, cTECs are defined as EpCAM<sup>+</sup>Ly51<sup>+</sup> and mTECs as EpCAM<sup>+</sup>Ly51<sup>-</sup>. TECs can be further characterised by their expression of the functional marker, MHC class II (MHCII), which is essential for T cell development (Figure 3.1d). MHC class II<sup>lo</sup> and MHC class II<sup>hi</sup> expression profiles define immature and mature TEC subpopulations, respectively (Gray et al., 2006). Of note is that MHC class II expression on TECs decreases with age and is absent on cTECs in the *Foxn1*<sup>R/R</sup> hypomorphic thymus (Gray et al., 2006; Nowell et al., under review) indicating that it is directly or indirectly regulated by Foxn1.

To verify the accuracy of the TEC isolation procedure, I immunostained cytopun, sorted cells with epithelial sub-compartment specific antibodies. Representative images show that almost all cells isolated as mTECs (phenotype: EpCAM<sup>+</sup>, Ly51<sup>-</sup>) expressed the medullary marker, Keratin 5 (K5) (Figure 3.1e). Similarly, all cTECs (phenotype: EpCAM<sup>+</sup>, Ly51<sup>+</sup>) expressed the cortical marker CDR1 (Rouse et al., 1988) (Figure 3.1e). The validity of all immunostaining signals were confirmed by comparison against the corresponding isotype antibody controls (Figure 3.1e). These results confirm that the procedure used to isolate TECs is robust and specific.

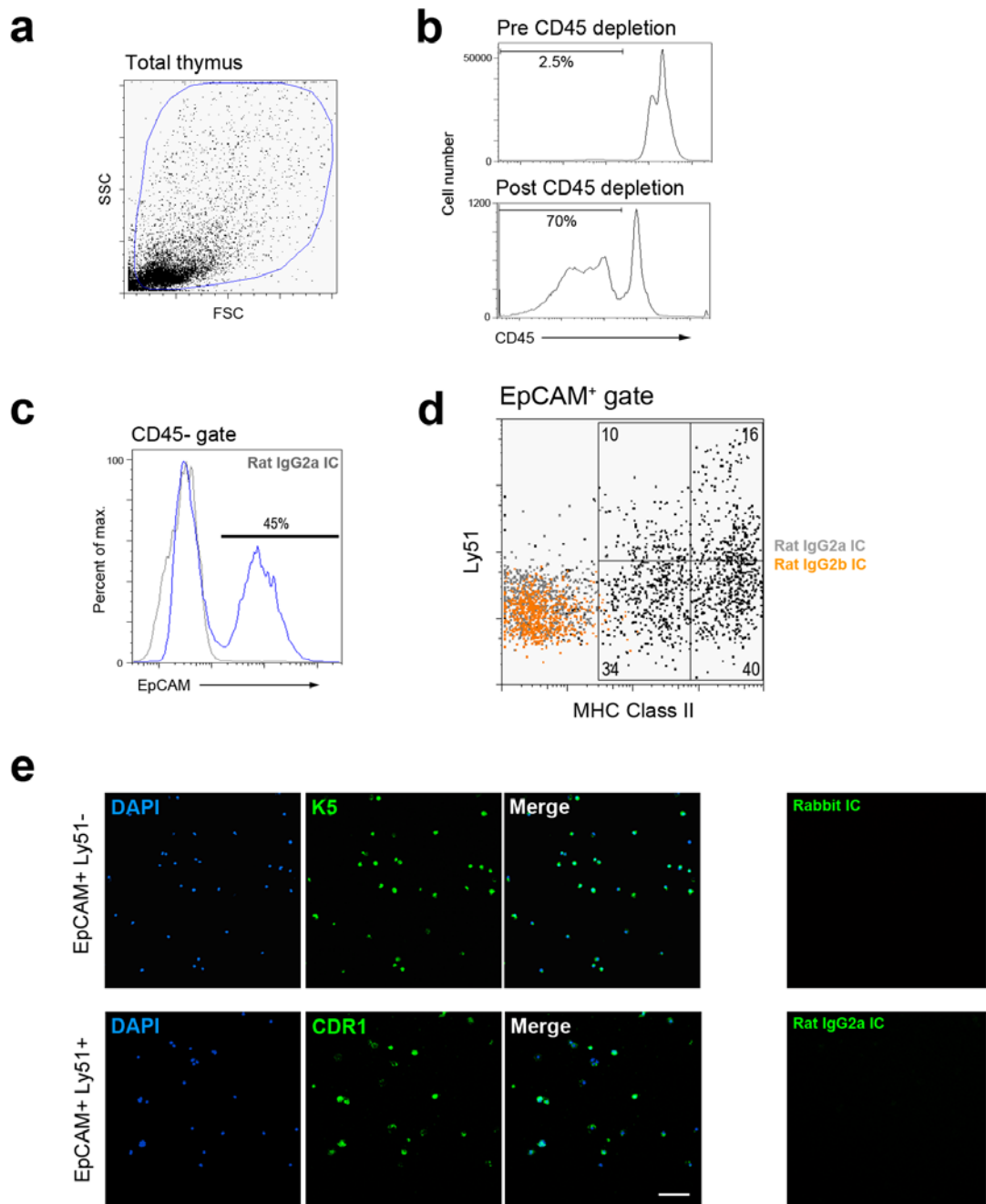


**Figure 3.1 Robust isolation of TECs from postnatal mice thymi.**

Representative plots from a procedure for TEC isolation from postnatal mice thymi using **(a, b)** CD45<sup>-</sup> cells make up a small proportion of total postnatal thymus cellularity, such that CD45<sup>+</sup> cells need to initially be depleted, to make flow cytometric isolation of TECs efficient. In the representative example shown, CD45 cells were labelled and magnetically depleted. **(c)** Approximately half of the post-CD45 depletion fraction is TECs, as marked by EpCAM. **(d)** The epithelial component can then be phenotypically divided into mTECs (Ly51<sup>-</sup>) and cTECs (Ly51<sup>+</sup>) that express high or low levels of the functional molecule MHC class II. **(e)** Isolated TECs were verified by immunocytochemistry. Almost all isolated mTECs (EpCAM<sup>+</sup> Ly51<sup>-</sup>) express the medulla specific keratin, Keratin 5 (K5), while all cTECs (EpCAM<sup>+</sup> Ly51<sup>+</sup>) express the cortex specific marker, CDR1. All signals were determined as above isotype (IC) controls. Images show single optical sections. Scale bar represents 100µm.

### 3.2.2 Foxn1 is differentially expressed in the major TEC compartments

To test whether Foxn1 was expressed at different levels in different TEC subpopulations, quantitative real-time (qRT) PCR was used to analyse *Foxn1* transcript levels in the isolated TEC subsets. *Foxn1* levels were normalised to  *$\alpha$ -tubulin* expression, which has been determined as the optimal reference gene for TEC gene expression analysis (Nowell et al., under review). Initially, total cortex and medullary subsets were compared from wildtype 4-8 week old mice. *Foxn1* was expressed at approximately twice the level in cTECs as in mTECs (Figure 3.2a). A caveat of this qRT-PCR analysis is that more cTECs than mTECs may express Foxn1, while Foxn1-positive cells express comparable levels of Foxn1 across the two compartments.

To address this potential caveat, I utilised the Foxn1<sup>GFP/+</sup> mice to obtain a direct read-out of Foxn1 expression in homeostatic, 8 week old TECs (Figure 3.2b). Foxn1<sup>GFP</sup> is a newly generated Foxn1 reporter strain in which GFP is knocked into the Foxn1 locus (see Materials and Methods 2.1.1.3). Three Foxn1 expression states were evident by GFP levels: negative/low, intermediate and high (neg/lo, int, hi). The precise classification of the Foxn1<sup>neg/lo</sup> population as either negative or low may be restricted by the detection limits of analysis method used (flow cytometry). Indeed, the observed distribution of the GFP<sup>neg/lo</sup> population suggested that this population may be GFP<sup>lo</sup> rather than GFP<sup>neg</sup>, as it did not align precisely with the wildtype, GFP<sup>neg</sup> population (Figure 3.2b).

The Foxn1<sup>lo</sup> proportions in each subpopulation were comparable (cTECs, 10%; mTECs, 12%), indicating that the differential mRNA expression observed above probably stems primarily from differences in the Foxn1<sup>int/hi</sup> populations across the two compartments (Figure 3.2b). Indeed, the medullary compartment contained a higher proportion of Foxn1<sup>int</sup> TECs (cTECs, 19%; mTECs, 24%) and a lower proportion of Foxn1<sup>hi</sup> (cTECs, 71%; mTECs, 64%) than the cortical compartment (Figure 3.2b).

Thus, a combination of the direct read-out of Foxn1 expression levels, using the *Foxn1*<sup>GFP/+</sup> allele, and quantification of *Foxn1* transcript by qRT-PCR, showed that Foxn1 is expressed at a higher level in cTECs compared to mTECs. This most likely reflects a higher proportion of Foxn1<sup>hi</sup> TECs in the cortex than the medulla rather than a higher Foxn1 expression level on a per cell basis.

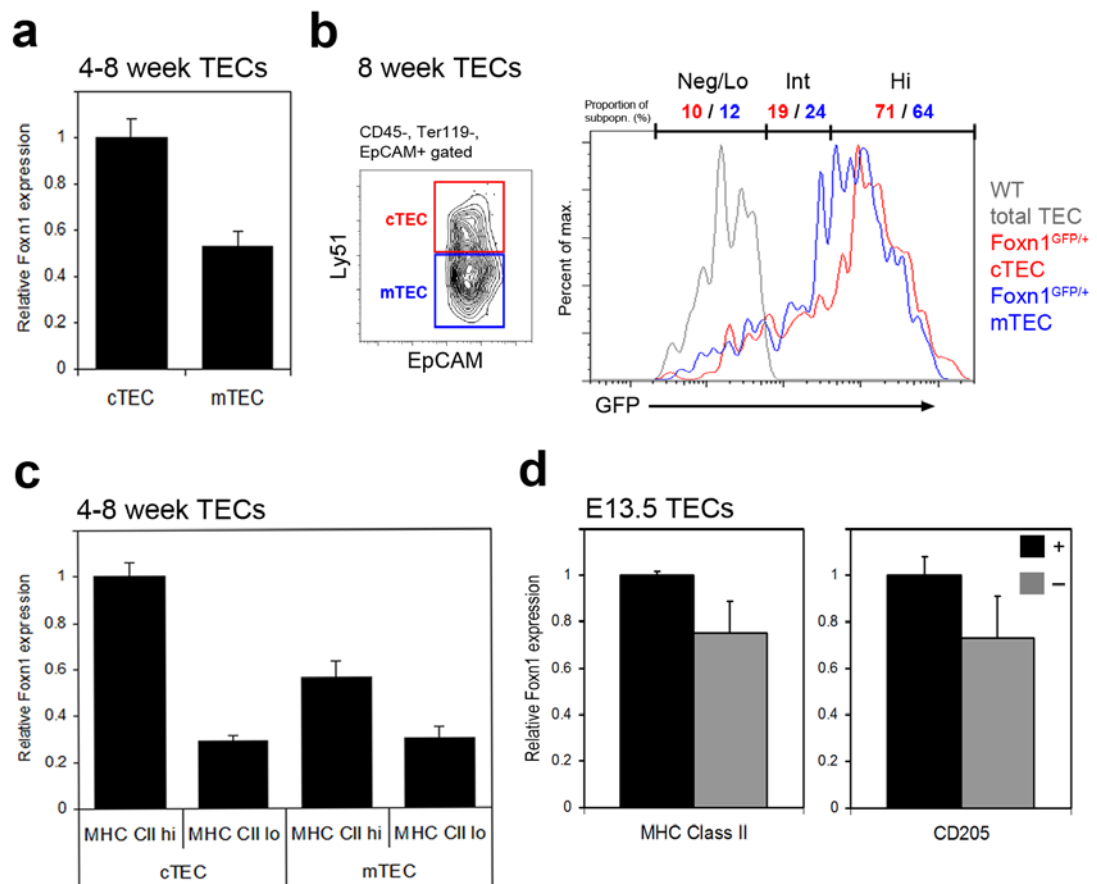


**Figure 3.2 Foxn1 is differentially expressed in major TEC subpopulations.**

**(a)** Foxn1 transcript levels were quantified by qRT-PCR in mTEC and cTEC populations (EpCAM<sup>+</sup>Ly51<sup>-</sup> and EpCAM<sup>+</sup>Ly51<sup>+</sup>, respectively) isolated by flow cytometry from at least 3 pooled thymi. Foxn1 is expressed at higher levels in cTECs compared to mTECs (n=3, p=0.009). **(b)** Flow cytometric analysis, without thymocyte depletion, was performed on 8 week old Foxn1<sup>GFP/+</sup> thymi where total TECs were analysed using EpCAM and Ly51 after gating on CD45<sup>-</sup> and Ter119<sup>-</sup> cells. Histogram shows GFP expression profile for cTECs (Ly51<sup>+</sup>, red line) and mTECs (Ly51<sup>-</sup>, blue line). Data shown are from 3 pooled mice (n=1). **(c)** Foxn1 transcript levels were quantified by qRT-PCR for MHC class II high and low subpopulations in the cortex and medulla. Foxn1 is expressed at higher levels in cTEC/MHCII<sup>hi</sup> compared to mTEC/MHCII<sup>hi</sup> populations (p=0.001) and at higher levels within the cortical and medullary MHCII<sup>hi</sup> populations compared to the MHCII<sup>lo</sup> populations (p=0.0004 and p=0.037, respectively). Foxn1 is expressed at similar levels in the cTEC/MHCII<sup>lo</sup> and mTEC/MHCII<sup>lo</sup> populations (all n=4). **(d)** Analysis of Foxn1 levels in embryonic day 13.5 (E13.5) TECs suggested that Foxn1 may be expressed at higher levels in mature TECs (MHCII<sup>+</sup>) and cTECs (CD205<sup>+</sup>) compared to the relevant negative populations, however, these differences were not significant (n=3, p=0.064 and p=0.28, respectively).



Next, I quantified *Foxn1* mRNA levels in different mTEC and cTEC subpopulations. All cortical and medullary postnatal TECs express MHC class II as a function of their role in mediating selection of the TCR repertoire of thymocytes (Figure 3.1d) (Gray et al., 2006; Shakib et al., 2009; Surh et al., 1992). MHC class II expression on TECs can be used as a marker for immature (low) and mature, functional (high) TECs. This is supported by, among other data, the superior *in vitro* T cell-stimulatory capacity of MHCII<sup>hi</sup> compared to MHCII<sup>lo</sup> mTECs and, the preferential loss of MHCII<sup>hi</sup> TECs during thymus involution (Gray et al., 2006). Thus, I quantified *Foxn1* transcript levels in MHC class II high and low populations in the cortex and medulla.

*Foxn1* expression in MHCII<sup>hi</sup> populations in the cortex and medulla, showed a similar trend to total populations, with *Foxn1* being expressed at approximately double the level in the cTEC/MHCII<sup>hi</sup> than the mTEC/MHCII<sup>hi</sup> populations (Figure 3.2c). However, *Foxn1* was expressed at similar levels in the cortical and medullary MHCII<sup>lo</sup> populations. Within each of the major compartments, *Foxn1* was expressed at higher levels in the MHCII<sup>hi</sup> populations than the MHCII<sup>lo</sup> populations, and was approximately 3-fold and 2-fold higher in the MHCII<sup>hi</sup> cTECs and mTECs than the MHCII<sup>lo</sup> cTECs and mTECs, respectively. These data confirm the differential expression of *Foxn1* in cTECs and mTECs and also show that *Foxn1* is expressed at higher levels in mature TEC populations in the two main compartments.

To test if this differential expression of *Foxn1* was established during thymus organogenesis, I analyzed *Foxn1* expression in the equivalent embryonic TEC subpopulations. Prominent mature (MHCII<sup>+</sup>) and cortical/medullary (CD205<sup>+/-</sup>) TEC populations emerge at embryonic day 13.5 (E13.5) (Nowell et al., under review; Shakib et al., 2009). MHCII<sup>+</sup>/MHCII<sup>-</sup> and CD205<sup>+</sup>/CD205<sup>-</sup> TEC populations were isolated by flow cytometry and analyzed for *Foxn1* mRNA levels by qRT-PCR. As in the postnatal thymus, *Foxn1* mRNA was detected at higher levels in mature than in immature TECs and at slightly higher levels in cTECs compared to mTECs (Figure 3.2d). However, these differences only approached significance for the MHCII<sup>+</sup> and MHCII<sup>-</sup> populations (p=0.064) and were not significant for CD205<sup>+</sup> and CD205<sup>-</sup> populations (p=0.28) (both n=3). Thus, while there was some evidence for higher *Foxn1* expression levels in cortical E13.5 TECs, these differences were not determined to be significant.

### 3.2.3 Foxn1 expression decreases with age in the thymic epithelium

To date, Foxn1 expression has not been accurately quantified in aged postnatal TECs. However, because premature down-regulation of Foxn1 in postnatal TECs results in an early thymus involution phenotype (Chen et al., 2009), it was important to determine if involution in wildtype mice correlated with a decrease in Foxn1 expression. Thus, I analyzed *Foxn1* transcript levels in isolated TECs, and used the Foxn1<sup>GFP</sup> mouse model to track Foxn1 expression in TECs in aging mice.

At 12 months of age total thymus cellularity has decreased drastically compared to that in 4 week old mice ( $5 \times 10^7$  and  $2 \times 10^8$  cells, respectively; Gray et al., 2006). This reduction in total cellularity is possibly driven by a reduction in the size of the stromal compartment with age (defined as CD45<sup>-</sup> cells; 4 weeks,  $5 \times 10^5$  cells and 12 months,  $2 \times 10^5$  cells; Gray et al., 2006). To determine how *Foxn1* expression levels in TECs varies with age I isolated TECs from 4 week and 12 month mice and compared *Foxn1* mRNA levels in cortical and medullary populations by qRT-PCR. *Foxn1* mRNA expression was approximately 10-fold lower in the medullary compartment and 12-fold lower in the cortical compartment, at 12 months than at 4 weeks of age (Figure 3.3a). At 12 months the difference in *Foxn1* levels between cTECs and mTECs was not as pronounced as at 4 weeks, with the expression of *Foxn1* at two thirds the level in mTECs compared to cTECs (although these differences were not significant,  $p=0.11$ ). These data show, for the first time, the accurate quantification of *Foxn1* in aged TECs with a greater than 10-fold reduction in mRNA expression at 12 months compared to 4 weeks.

In addition to *Foxn1* message quantification, I utilised the *Foxn1*<sup>GFP</sup> allele to track Foxn1 expression in aging TECs. For this analysis I compared the GFP expression profiles of total TECs from 3, 6 and 12 month old Foxn1<sup>GFP/+</sup> mice by flow cytometry. The majority of TECs from 3 month old Foxn1<sup>GFP/+</sup> thymi expressed Foxn1 at high levels (76%), while the remainder expressed Foxn1 at low or intermediate levels (10% and 14%, respectively; Figure 3.3b,c). Notably, the proportion of the Foxn1<sup>hi</sup> TECs decreased by 20% in 6 month old thymi to constitute 56% of total TECs. The reduction of the Foxn1<sup>hi</sup> population corresponded with an approximate doubling in Foxn1<sup>lo</sup> and Foxn1<sup>int</sup> TEC proportions at 6 months (to 20% and 24%, respectively; Figure 3.3b,c). At 12 months the Foxn1<sup>hi</sup> TEC population had decreased even further, to levels that were 60% and 85% of those observed at 3 months and 6 months, respectively (Figure 3.3b,c). The proportion of Foxn1<sup>lo</sup> TECs increased from 3 to 6 months but thereafter remained similar while the proportion of Foxn1<sup>int</sup> TECs increased

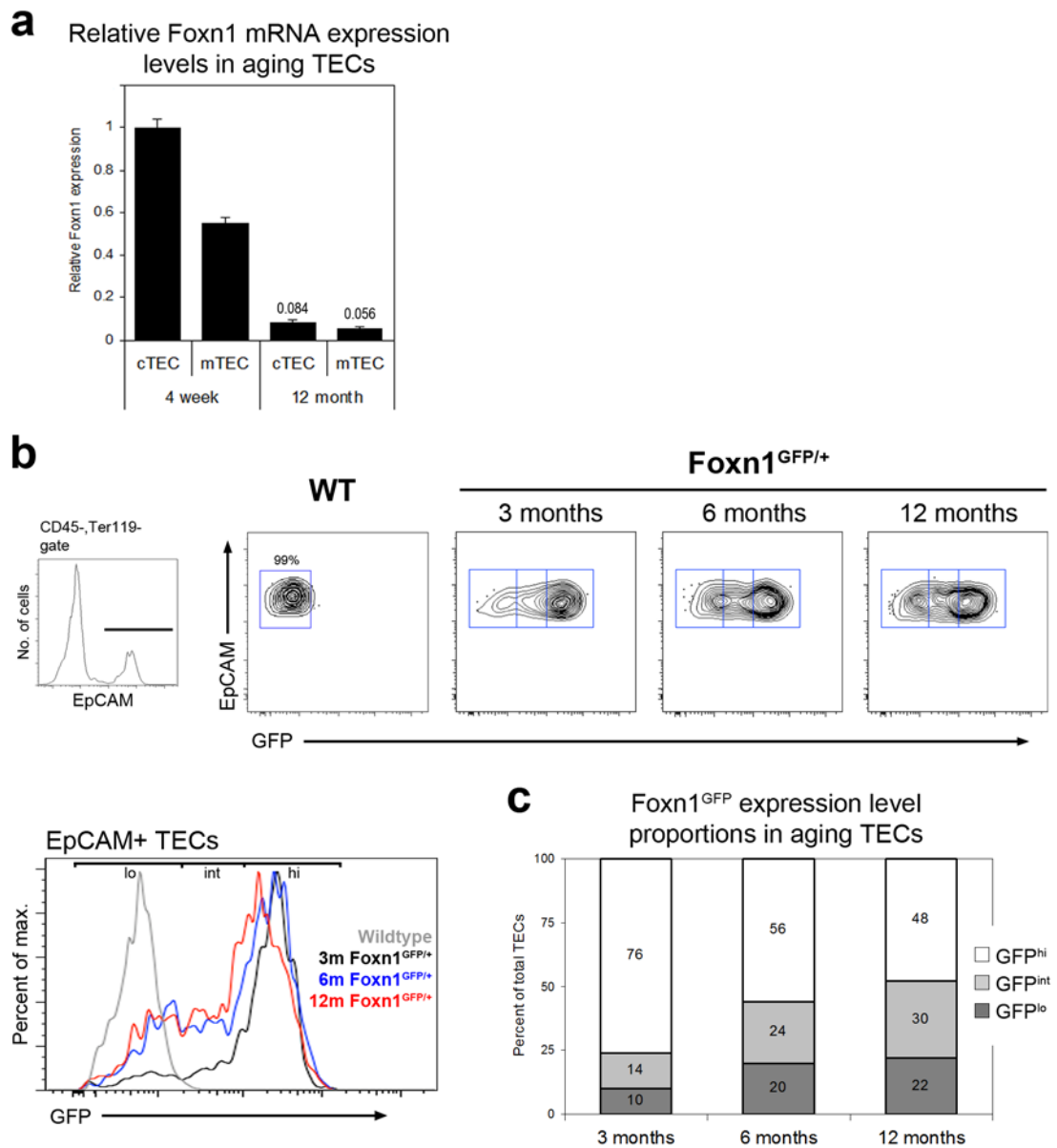


**Figure 3.3 Foxn1 expression decreases with age in the thymic epithelium.**

(a) Foxn1 transcript levels were quantified by qRT-PCR in flow cytometrically isolated mTEC and cTEC populations (EpCAM<sup>+</sup>Ly51<sup>-</sup> and EpCAM<sup>+</sup>Ly51<sup>+</sup>, respectively) at 4 weeks and 12 months of age. Foxn1 is expressed at higher levels at 4 weeks than at 12 months ( $n=2$ ,  $p<0.001$ ). (b) Flow cytometric analyses of EpCAM<sup>+</sup> TECs after gating on CD45<sup>-</sup>Ter119<sup>-</sup> cells. WT and Foxn1<sup>GFP/+</sup> TECs were analyzed for GFP expression and showed that Foxn1 expression decreased from 3 months to 6 months to 12 months. Plots show analysis of 3 pooled mice ( $n=1$ ). Histogram shows GFP profile of EpCAM<sup>+</sup> TECs from WT and 3, 6 and 12 month old Foxn1<sup>GFP/+</sup> mice (c) Graphical representation of data shown in (b), showing low, intermediate and high GFP expression level proportions in total TECs at 3, 6 and 12 months.

progressively with age. Thus, through the combination of *Foxn1* mRNA quantification in defined aging TEC populations, and direct analysis of *Foxn1* expression levels in total aging TECs, I have shown, in the most accurate manner to date, that *Foxn1* expression progressively decreases with age in the thymic epithelium.

### 3.3 Discussion

Here, I show that *Foxn1* is differentially expressed among the major TEC compartments in the homeostatic postnatal thymus, with approximately double the level of transcript detected in cTECs compared to mTECs. Additionally, analysis of the *Foxn1*<sup>GFP</sup> allele showed that at 2 months of age, a higher proportion of *Foxn1*<sup>hi</sup> TECs is found in the cortex than in the medulla. Previous observations show that TECs that express only ~15% of wildtype levels of *Foxn1* mRNA, exhibit a partial block in cTEC and mTEC differentiation (Nowell et al., under review). In these mice, the effect on cTEC differentiation is more pronounced, suggesting that normal cTEC development may require higher levels of *Foxn1* than in mTECs. Data presented here, showing higher *Foxn1* mRNA levels in wildtype cTECs than in mTECs, support this hypothesis.

The biological significance of different *Foxn1* expression levels in different TEC compartments is unclear. *Foxn1* up-regulation may, for example, be required in cTECs to promote progression to a more mature state, or increased *Foxn1* levels may be required in matured cTECs in order to maintain this population. A relationship between *Foxn1* levels and the maturity state of the TEC is evident when comparing *Foxn1* levels in high and low MHC class II populations. There is no difference in *Foxn1* expression between the MHCII<sup>lo</sup> population in the cortex and medulla, but *Foxn1* is up-regulated in MHCII<sup>hi</sup> populations, suggesting that it may be important for entry into or maintenance of differentiated TECs. Thus, up-regulation of *Foxn1* levels may be important for maturation of TECs within the cortex and the medulla, with a further requirement of higher levels of expression in the cortex.

It may be that the differences in *Foxn1* expression between the cortex and medulla are indicative of different modes of action. Analysis of the allelic series of *Foxn1* shows that there are two gene expression response patterns in embryonic TECs: one titrates with *Foxn1* and the other is a binary response, where even at very low levels of *Foxn1*, responsive genes are expressed at wildtype levels (Nowell et al., under review). This mechanism may also operate in the wildtype postnatal situation; for example, *Foxn1* may regulate a binary

response programme in mTECs but needs to be expressed at higher levels in cTECs, where its functionality is dependent on reaching a critical expression level. Or it might be possible that mTECs depend less on genes which require high levels of Foxn1 to activate them. Furthermore, different mechanistic actions may explain the response programmes; for example Foxn1 protein may need to be present at high concentration if it functions by binding to a co-factor with a low binding affinity, or conversely, only at low levels if it functions as a transcription factor that binds to a small number of regulatory sites, or visa versa. Thus, in the one instance Foxn1 is limiting and in the other, it is not.

It should be noted that a caveat of the data presented and conclusions discussed here, is that Foxn1 was only quantified at the transcriptional level. Thus, any regulation of Foxn1 expression by post-translation modification cannot be accounted for here. However, no evidence for post-translational modification of Foxn1 has been detected to date and, furthermore, data from our lab show that Foxn1 protein tracks with mRNA expression levels (Nowell et al., under review).

Lastly, I accurately quantified the down-regulation of Foxn1 transcript expression in wildtype TECs with age. Recent reports have shown that a postnatal decrease in Foxn1 expression is associated with accelerated thymic involution in several mouse models (Chen et al., 2009; Cheng et al., 2010; Corbeaux et al., 2010; Sun et al., 2010). While one report attempts to quantify Foxn1 in aging wildtype TECs, the experimental approach adopted was sub-optimal as Foxn1 expression was not quantified in pure TEC populations (Ortman et al., 2002). Here, I show that Foxn1 is indeed down-regulated in wildtype, aged TECs, by approximately 10-fold at 12 months compared to 2 months. Additionally, I tracked the Foxn1 expression profile in aging TECs using a Foxn1<sup>GFP</sup> reporter mouse model. The TEC compartment in thymi at the onset of involution (3 months old) was comprised mainly (over 75%) of TECs that expressed high levels of Foxn1. In the aging TEC compartment (6 months and 12 months old), this proportion decreased significantly with an increase in Foxn1 low and intermediate populations observed. These data clearly show that Foxn1 expression decreases in aging wildtype TECs, providing support for its role in the maintenance of the postnatal thymus.

## Chapter 4: Generation of a conditional, inducible Foxn1 mouse model

---

### 4.1 Introduction

A number of recent studies have revealed the dosage-dependent mode of action of Foxn1 in the postnatal thymic epithelium. Firstly, Foxn1 mRNA is expressed at different levels in different wildtype TEC subpopulations, suggesting that the level of Foxn1 is important for the development and function of different TEC sub-populations (Chapter 3). Additionally, a Foxn1 allelic series – generated using null, hypomorphic (*Foxn1<sup>R</sup>*) and wildtype alleles – demonstrated different roles for Foxn1 dependent on its expression levels (Nowell et al., under review). These roles include regulation of exit from a TEC progenitor state and entry into the cortical and medullary differentiation programmes, and roles in postnatal maturation of TECs. Lastly, a number of recent reports indicate that Foxn1 is required for maintenance of postnatal TECs and thymic homeostasis (Chen et al., 2009; Cheng et al., 2010; Corbeaux et al., 2010; Sun et al., 2010). Mice in these studies, where different approaches were used to prematurely reduce or stop Foxn1 expression in postnatal TECs, had consistent thymic phenotypes of early TEC architecture degeneration and reduced T cell output. Collectively, these studies establish the importance of Foxn1 dosage in TEC development and maintenance.

In order to address this function of *Foxn1* further, I generated a transgenic mouse model which permitted tissue specific, regulatable expression of Foxn1. In this model, a Tamoxifen inducible form of Foxn1 (Foxn1ER<sup>t2</sup>) is expressed within the ROSA26 locus under control of the CAG compound promoter. To add tissue specificity of expression to this system I placed a floxed MAZ stop cassette (Ashfield et al., 1994) between the promoter and the Foxn1 cDNA. Additionally, IRES-GFP was placed downstream of Foxn1 to report expression. This generates a Foxn1ER<sup>t2</sup>-GFP bicistronic mRNA upon transcription following tissue-specific, Cre-mediated excision of the stop cassette (Figure 4.1). The Foxn1ER<sup>t2</sup> fusion protein produced from this mRNA is then maintained in the cytoplasm until treatment with Tamoxifen, whereupon it is released from the cell membrane and translocates to the nucleus. Thus, in this model Foxn1 expression is conditional and regulatable by Tamoxifen treatment.

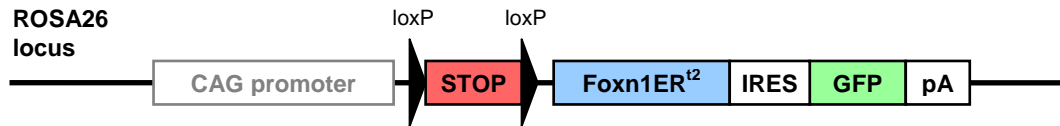


**Figure 4.1 The R26-CAG-STOP-Foxn1ER<sup>t2</sup> transgene.** A targeting cassette designed to permit tissue specific, regulatable expression of Foxn1 was generated as shown here. Mouse Foxn1 was fused to the mutated Tamoxifen responsive ligand binding domain of the estrogen receptor (ER<sup>t2</sup>) and placed under control of the compound CAG promoter. A floxed MAZ transcriptional STOP cassette and IRES-GFP component were included to permit Cre-mediated induction and to report transgene expression, respectively. This cassette was inserted into a vector containing 5' (1.1kb) and 3' (4.2kb) homology arms (Soriano, 1999). The cassette was then inserted into the ROSA26 locus by homologous recombination in ES cells.

## 4.2 Evaluation of experimental approach

Initially, two possible Foxn1 regulatable systems were evaluated: (1) Rosa26<sup>CAG-STOP-Foxn1ER</sup>, as described above and, (2) a doxycycline (Dox) regulatable Tet-On system (Gossen et al., 1995). In the latter system, Foxn1 would be placed under control of a Dox-responsive regulatory element, such that Dox treatment would induce Foxn1 expression via a transactivator (rtTA). I chose not to develop this system as it had been reported at the time that Dox-dependent induction of gene expression in the thymus was poor compared to other tissues (Hochedlinger et al., 2005). Furthermore, it is well established that ER fusion proteins are titratable (Hayashi and McMahon, 2002), which would permit Tamoxifen-dosage dependent induction of Foxn1ER, if required. Additionally, a functional Foxn1ER fusion protein had previously been described and characterised which, at least at the outset, abated concerns that ER might alter or inhibit Foxn1 function (Janes et al., 2004). Lastly, reagents were available to me that would permit Foxn1ER expression all TECs in Rosa26<sup>CAG-STOP-Foxn1ER</sup> mice (i.e. Foxn1<sup>Cre</sup> mice, Gordon et al., 2007) while similar reagents did not exist for the Tet-On system (e.g. Foxn1rtTA). Thus, I chose to generate the Rosa26<sup>CAG-STOP-Foxn1ER</sup> mouse model for conditional, regulatable Foxn1 expression.

### **4.3 Generation of R26-CAG-STOP-Foxn1ER transgenic mouse line**

#### **4.3.1 Targeting vector construction**

The targeting vector was assembled from four components: (1) the Foxn1ER<sup>t2</sup>-IRES-GFP component, (2) the CAG promoter and loxP-flanked MAZ transcriptional stop cassette (Ashfield et al., 1994), (3) a frt-flanked neomycin cassette for positive selection, and (4) the host pROSA26-1 vector containing the ROSA26 homology arms (Friedrich and Soriano, 1991; Soriano, 1999).

##### **4.3.1.1 Foxn1ER<sup>t2</sup>-IRES-GFP construction**

Firstly, the full length mouse Foxn1 cDNA was fused in-frame to a mutated ligand binding domain of the human estrogen receptor (ER<sup>t2</sup>) (Feil et al., 1997) with a glycine-rich linker (GGAGSGDP) (Zeisig et al., 2004). Mouse Foxn1 cDNA (in pBlueScript, obtained from Professor Nancy Manley, University of Georgia, USA) was amplified by PCR, with a sense primer that spanned the start codon and an anti-sense primer that spanned the stop codon. The anti-sense primer contained a non-homologous tail made up of part of the linker sequence, which incorporated a BamHI restriction site and also introduced a single nucleotide mutation such that the stop codon of Foxn1 subsequently coded for the first glycine of the linker. This Foxn1 fragment was then cloned into pGEMT-Easy (Figure 4.2a). Similarly, ER<sup>t2</sup> was amplified from a Cre-ER<sup>t2</sup> plasmid with a sense primer that contained the remainder of the linker sequence/BamHI restriction site and an anti-sense primer that contained a BstEII restriction site, and sub-cloned in pGEMT-Easy (Figure 4.2b). The Foxn1 and ER<sup>t2</sup> components were excised from pGEMT-Easy by NotI/BamHI and BamHI/BstEII restriction digests, respectively. These two fragments, together with an IRES-hrGFP-polyA component (humanised renilla form (hr) of GFP, excised from pIRES-hrGFP-1a (Stratagene) with BstEII and MluI (Figure 4.2c)) were ligated into the NotI and MluI sites of the pSP72 vector (Promega), in a four-way, directional, sticky-ended reaction, generating the pSP72-Foxn1ER<sup>t2</sup>-IRES-GFP construct (Figure 4.2d). The ligation mix was transformed into DH5α *E. coli* competent cells and clones were positively selected using ampicillin resistance. Plasmids were extracted from positively selected clones and sequenced to confirm identity. Both strands of the Foxn1ER<sup>t2</sup>-IRES-GFP insertion (FEIG) were sequenced using overlapping primer sets (Figure 4.2e) and confirmed to be correct.



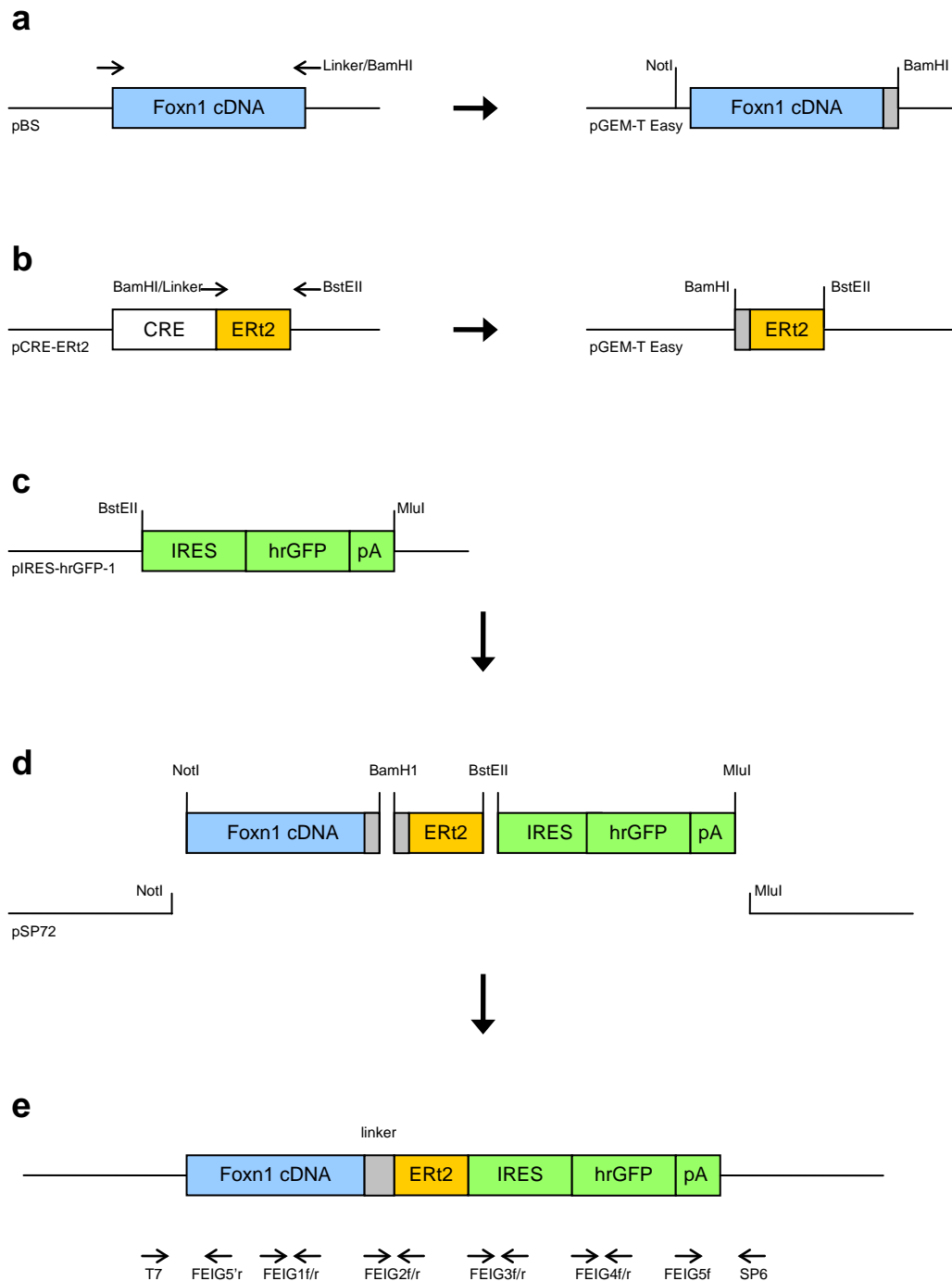


**Figure 4.2 Construction of the Foxn1ER<sup>t2</sup>-IRES-hrGFP cassette.**

**(a, b)** Foxn1 cDNA (blue) and ER<sup>t2</sup> (yellow) were amplified by PCR using primers (arrows) that contained restriction sites and linker (grey) sequences as indicated, and were cloned into the pGEM-T Easy vector (Promega). **(c)** An IRES-hrGFP-pA (humanised renilla GFP) (green) component was excised from the pIRES-hrGFP-1 vector (Stratagene). **(d)** The three components were ligated into a host pSP72 vector (Promega) and clones recovered after transformation and positive selection were sequenced through both strands using primers (arrows), as indicated **(e)**.

#### 4.3.1.2 CAG-floxed STOP construction

The next major component of the targeting vector that was constructed was the CAG-floxed STOP and the selection cassette. A vector containing the CAG compound promoter and a floxed MAZ transcriptional stop component was utilised as the host vector for this construction step (obtained from Professor Ian Chambers, Institute for Stem Cell Research, University of Edinburgh) (Figure 4.3a). An unwanted IRES/Puro fragment was removed by HindIII/ClaI digestion and vector was religated. Next, the vector was digested with AclI and PstI and ligated with complementary-ended, annealed oligonucleotides that contained a BbsI restricted site (Figure 4.3b). The BbsI recognition sequence (GAAGACNN<sup>y</sup>NNNN) was manipulated such that the overhang generated was 5' -GGCC and complementary to the NotI-generated overhang, which was used in the next construction steps (Figure 4.4). Next, a unique PmeI site between the first loxP site and the stop cassette was used to insert the frt/PGK-neoR/frt selection cassette (obtained from Dr Andrew Smith, Institute for Stem Cell Research, University of Edinburgh) by blunt-end ligation (Figure 4.3c). The selection cassette is composed of a neomycin resistance (neoR) gene driven by a PGK promoter and is frt-site flanked, allowing downstream excision of the cassette using FLPe mediated recombination.

#### 4.3.1.3 Final targeting vector assembly

The pROSA26-1 targeting vector (obtained from Professor Phillippe Soriano, Mount Sinai School of Medicine) (Soriano, 1999) – which contains a 1.1kb 5' homology arm and a 4.2kb 3' homology arm, separated by a unique XbaI cloning site – was used to target the CAG-STOP-Foxn1ER transgene to the ROSA26 locus. Firstly, the single XbaI cloning site was manipulated to include two further unique restriction sites. Annealed oligonucleotides with XbaI overhangs, that contained PacI and MluI restriction sites, were introduced into the ROSA26-1 vector by ligation into the XbaI cloning site. Next, a three-way ligation reaction was used to construct the final targeting vector from the following components: (1) the 9.8kb pROSA26-1 host vector, digested with PacI and MluI, (2) the 6.3kb CAG-frt/neoR/frt-floxed STOP component, excised with PvuI and BbsI (Figure 4.3c), and (3) the 3.7kb Foxn1ER-IRES-GFP, excised with NotI and MluI (Figure 4.2e) (Figure 4.4). PacI and PvuI digested ends are compatible, while the BbsI-generated overhang was designed to be complementary to the NotI-generated overhang, thus generating a directional, three-way, sticky-ended ligation reaction. The final vector was verified by restriction enzyme digestion and sequenced using FEIG (Figure 4.2e), CagIPC270, ROSAseqF and FRTf primers (primer details are shown in Section 2.2.3.1).

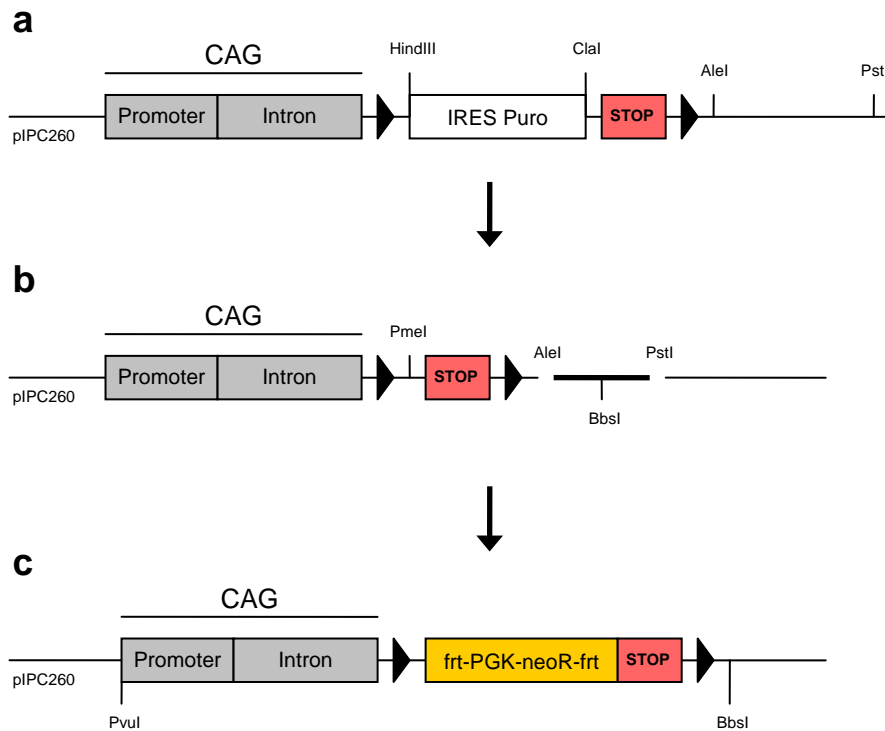


**Figure 4.3 Construction of CAG-frt/neoR/frt-floxed STOP component.**

**(a)** A vector, pIPC260, that contained the CAG compound promoter (grey) and a loxP-flanked (black arrows) MAZ STOP cassette (red) was digested with HindIII and ClaI to remove the unwanted IRES-Puro component (white). **(b)** A BbsI site, required for subsequent sub-cloning steps, was inserted between AleI and PstI sites, using complementary annealed oligonucleotides. **(c)** Lastly, a frt-flanked PGK promoter/neomycin resistance (neoR) cassette (yellow) was inserted into a PmeI site, generating the final CAG-frt/neoR/frt-floxed STOP vector.

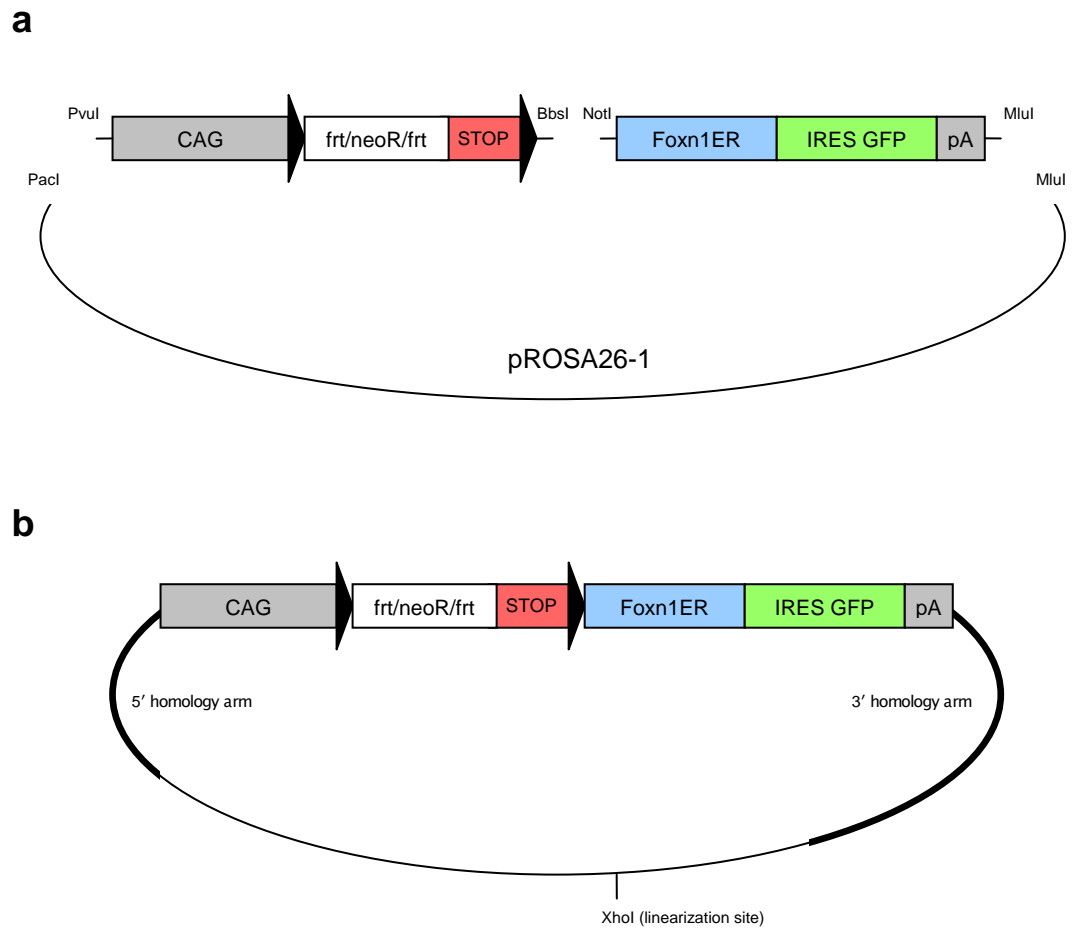


**Figure 4.4 Assembly of the final pR26-CAG-STOP-Foxn1ER targeting vector**  
**(a)** The final targeting vector was assembled by ligation of the CAG-floxed STOP (from Figure 4.3) and Foxn1ER-IRES-GFP components (from Figure 4.2) into the pROSA26-1 vector (Soriano, 1999) **(b)**.

### 4.3.2 ES cell targeting, selection and screening

The pR26-CAG-STOP-Foxn1ER targeting vector was linearised at the unique XhoI site (Figure 4.4), precipitated and electroporated into E14Tg2a mouse ES cells as described in Materials and Methods (Section 2.5.1). Cell colonies resistant to G418 treatment after 7 days were picked into 96 well plates and screened for homologous recombination at the ROSA26 locus. Initially, 5' PCR was used to screen potential recombinants, with an expected PCR product of 1.4kb in recombinants (Figure 4.5a, b) (Primers: ROSAprmtr720F and CAG210R). This identified 18 positive clones in the first 48 clones analyzed, which gave a recombination rate of 38% in G418 resistant clones – which falls within the rate of 25-50% reported by the Soriano lab (Soriano, 1999). Next, 3' PCR was used to confirm the correct integration of the full targeting vector in the 5' PCR -positive clones. All except one of the clones were positive by 3' PCR as indicated by a 4.9kb PCR product (Figure 4.5c) (Primers: FEIG5f and ROSA3geno2-R).

Of the 17 positive recombinant ES cell clones that successfully recovered from storage, 3 were selected to generate the R26-CAG-STOP-Foxn1ER mouse line. Southern blotting was used to confirm homologous recombination in the 3 selected positive ES cell clones (A12, C1 and D9) using 5', 3' and internal probes (Figure 4.5a). For the 5' Southern blot analysis, genomic DNA was digested with EcoRI and probed with a 5' probe which yielded a 15.6kb wildtype ROSA26 locus fragment and a 5.8kb transgenic ROSA26 locus fragment (Figure 4.5d). Similarly, an EcoRV restriction digestion and 3' probe detection, yielded an 11.5kb wildtype fragment and a 14.3kb transgenic fragment (Figure 4.5e). Further, PacI sites on either side of the targeted, transgenic locus generated a single 18.6kb fragment, indicating the single, site-specific integration of the CAG-STOP-Foxn1ER transgene (Figure 4.5f). Lastly, the karyotypes of selected ES cells recombinants, A12, C1 and D9, were tested and were found to be normal (Jonathan Rans, Tissue Culture Service, Institute of Stem Cell Research, University of Edinburgh).

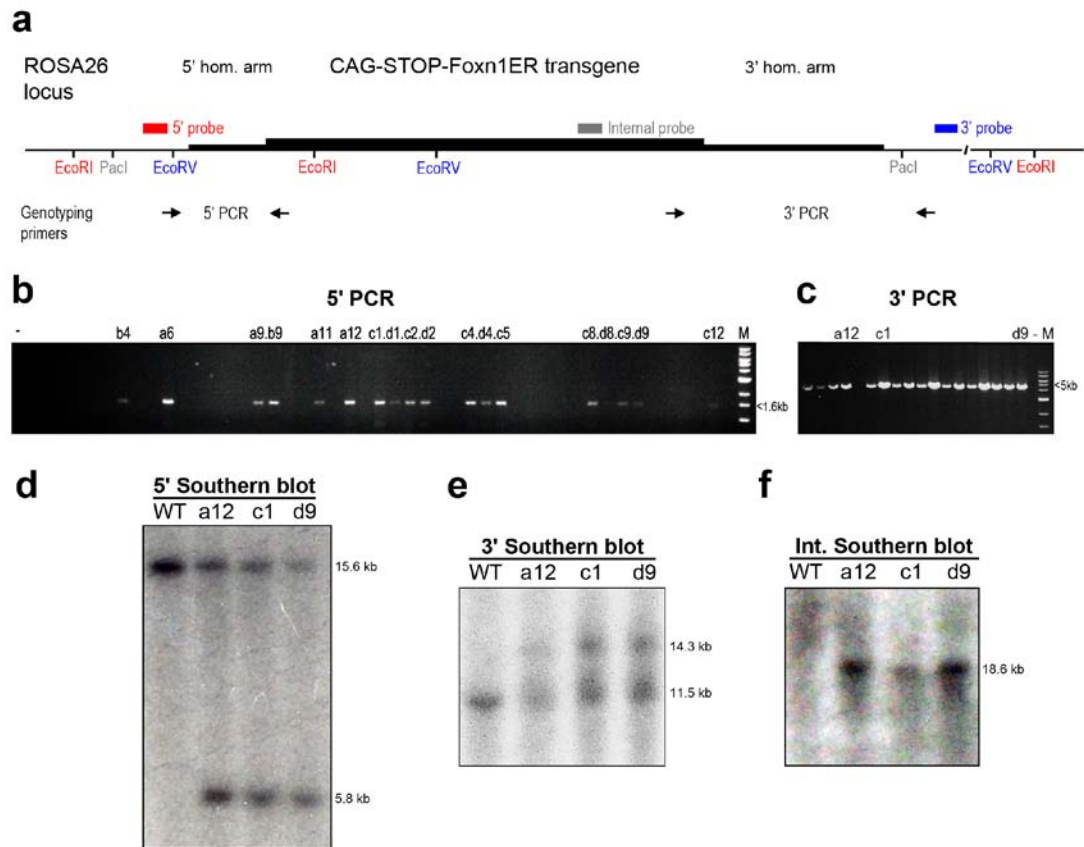


**Figure 4.5 Verification of R26-CAG-STOP-Foxn1ER ES cell clones by PCR and Southern blotting.**

(a) The strategy used for PCR and Southern blot screening of potential R26-CAG-STOP-Foxn1ER ES cell clones is illustrated. The CAG-STOP-Foxn1ER transgene (thick black line) is shown targeted to the ROSA26 locus (thin black line), with the 5' and 3' homology (hom.) regions for homologous recombination also shown. Positions of Southern blot probes and restriction sites (colour matched) and PCR primers (arrows) are indicated. (b, c) 5' PCR was initially used to identify positive recombinants by a 1.4kb PCR product (labeled lanes); which were confirmed by 3' PCR and a 4.9kb product (M, DNA ladder marker with relevant band size labeled; -, negative control). Three clones, A12, C1 and D9, were selected to generate the mouse line and were confirmed as correctly targeted by Southern blotting. (d) Genomic DNA from A12, C1 and D9 ES cell clones was digested with EcoRI and probed with a 5' probe (red), generating transgenic and wildtype (WT) restriction fragments. (e, f) Similarly, genomic DNA digestions with EcoRV and PacI, were probed with a 3' probe (blue) and internal probe (grey), respectively, revealing wildtype and transgenic restriction fragments.

### **4.3.3 Generation of R26-CAG-STOP-Foxn1ER transgenic mice**

Cells from the three selected CAG-STOP-Foxn1ER ES cell clones (A12, C1, D9) were used to generate transgenic mouse lines by conventional blastocyst injection protocols (performed by the Transgenic Service Facility, Institute for Stem Cell Research, University of Edinburgh). All ES cell clones generated chimeric mice with the transgene transmitted to the germline, as initially tracked by coat colour. Potential R26-CAG-STOP-Foxn1ER mice (generated from ES cell clones C1 and D9) were confirmed by Southern blotting, using the same strategies outlined above (Figure 4.6). Next, the *frt*-flanked, neomycin<sup>R</sup> cassette used for ES cell clone selection was removed by FLPe recombination by breeding R26-CAG-STOP-Foxn1ER mice with ubiquitous FLPe expressing mouse strain (Figure 4.6; obtained from Dr Andrew Smith, Institute for Stem Cell Research, University of Edinburgh). Collectively, these data describe the generation and verification of the R26-CAG-STOP-Foxn1ER mouse line.

## **4.4 Preliminary characterisation of R26-CAG-STOP-Foxn1ER mice**

### **4.4.1 The Foxn1ER<sup>t2</sup> fusion protein is transcriptionally active and Tamoxifen responsive *in vitro***

Before the transgenic mouse line was generated, the transcriptional activity of the Foxn1ER<sup>t2</sup> fusion protein was investigated, as the direct fusion of ER<sup>t2</sup> to the carboxy (C)-terminal of Foxn1 could result in impaired or blocked functionality of the Foxn1 protein. Two reports were important in this regard. Firstly, I chose to fuse ER<sup>t2</sup> to Foxn1 via a linker that has shown to produce a functional protein when ER<sup>TM</sup> was fused to the C-terminal of the transcription factor MLL (Zeisig et al., 2004). Secondly, a Foxn1ER fusion protein has previously been generated and expressed in keratinocytes (Janes et al., 2004). Here, the authors showed the Foxn1ER fusion protein was functional, and developed a system to test the transcriptional activity of Foxn1ER compared to Foxn1. Thus, the system from Janes et al. was used to test the activity of the Foxn1ER<sup>t2</sup> fusion protein that was generated here. In this reporter system, the core binding sites required for Foxn1 binding (Schlake et al., 1997) were placed upstream of a luciferase gene, such that luciferase transcription is regulated by Foxn1 (Figure 4.7a). Thus, the transcriptional activity of Foxn1 and Foxn1ER can be compared by co-expressing either with the luciferase response element and determining luciferase levels. The specificity of the binding sites for Foxn1 in this system was confirmed by a control element that contained mutated binding sites (Figure 4.7a).

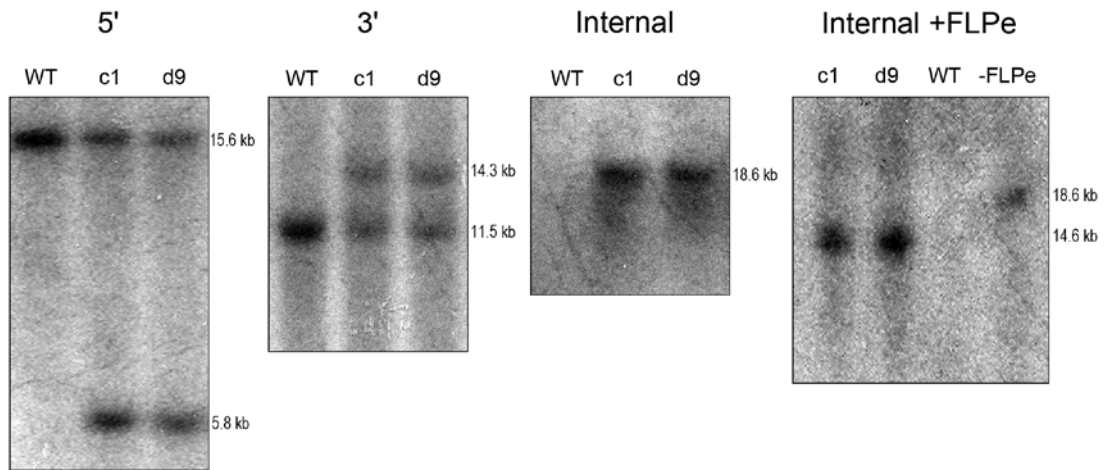
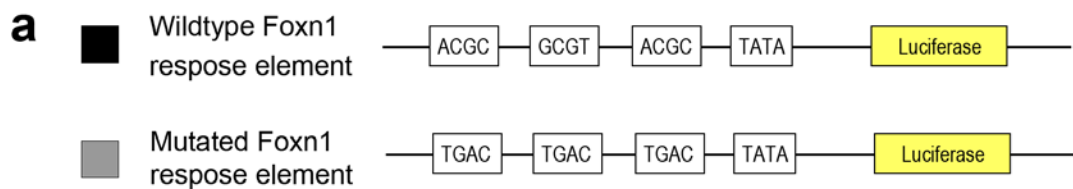


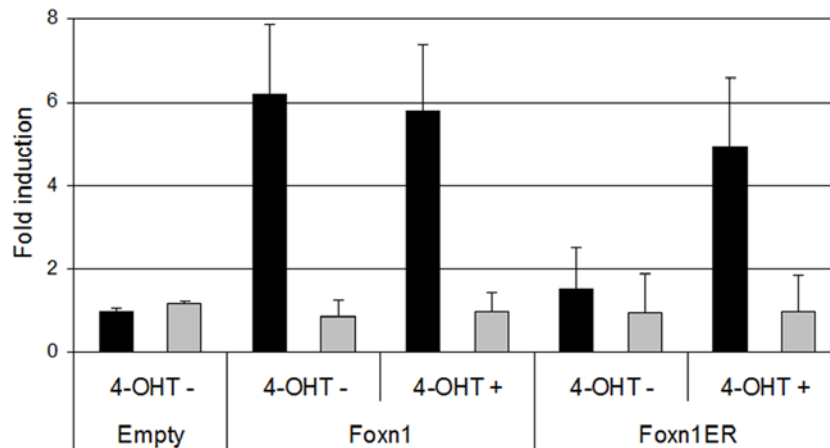
**Figure 4.6 Confirmation of R26-CAG-STOP-Foxn1ER transgenic mouse line by Southern blotting.**

The R26-CAG-STOP-Foxn1ER mouse line was generated from 2 separate ES cell clones, C1 and D9. The correct genetic identity of the mice generated from these clones was confirmed by 5', 3' and internal Southern blotting, using the strategies outline d in Figure 4.5. These mice were then crossed with FLPe expressing mice to remove the selectable marker from the transgene by FLPe-mediated recombination; this was confirmed by the 14.6kb restriction fragment observed on probing with the internal probe (+FLPe panel).





**b** Luciferase induction levels for Foxn1 and Foxn1ER transcription factors



**c**

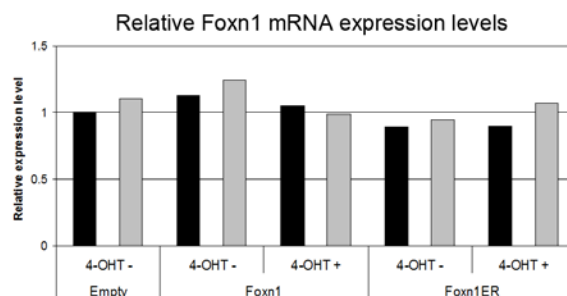


**Figure 4.7 The Foxn1ER fusion protein is transcriptionally active.**

(a) Wildtype and mutated Foxn1 transcriptional response elements upstream of a luciferase reporter were stably transfected into COS-7 cells. (b) Empty, Foxn1 or Foxn1ER vectors (all under control of the CAG promoter) were transfected into these cells and then assayed for luciferase expression. Luciferase expression was not detected for the mutated response element (grey) under any condition. Foxn1 and Foxn1ER induced luciferase at a similar level for the wildtype response element (black), indicating a comparable transcription activity. Foxn1ER was also regulatable by 4-hydroxy-tamoxifen (4-OHT). Data represent 2 biological repeats. (c) Transfection efficiency was controlled by quantification of Foxn1 mRNA expression in transfected cells by qRT-PCR. Data represents average of 2 biological repeats (with 3 technical repeats each).

Therefore to test the transcriptional activity of the Foxn1ER fusion protein generated here, I transfected cells that contained the wildtype and mutated Foxn1 response element reporter with Foxn1 and Foxn1ER plasmids and assayed for luciferase expression. Foxn1 and Foxn1ER were found to have comparable transcriptional activity, with a slightly lower, but insignificant, luciferase induction for Foxn1ER compared to Foxn1 (Figure 4.7b,c). Importantly, the mutated binding sites showed no response to Foxn1 or Foxn1ER, showing similar luciferase induction levels to the empty vector controls. Additionally, the Tamoxifen-mediated regulation of Foxn1ER could be tested *in vitro* using this system. In the absence of Tamoxifen, the Foxn1ER protein was maintained in the cytoplasm and thus could not bind to and activate the luciferase response element, confirmed by near background luciferase levels for this experimental condition (Figure 4.7b,c). However, upon addition of 4-hydroxy-tamoxifen (4-OHT), luciferase expression increased, indicating that Foxn1ER is responsive to Tamoxifen. Thus, the Foxn1ER<sup>2</sup> fusion protein generated here is transcriptionally active and is efficiently regulated by Tamoxifen.

#### **4.4.2 Foxn1ER-IRES-GFP is expressed after Cre mediated excision of the STOP cassette in CAG-STOP-Foxn1ER mice**

The floxed STOP cassette in the R26-CAG-STOP-Foxn1ER mice line permits tissue specific expression of Foxn1ER by crossing these mice with relevant Cre-expressing mouse strains. In order to express Foxn1ER in TECs the newly generated R26-CAG-STOP-Foxn1ER mice were crossed with a Foxn1<sup>Cre</sup> mouse strain. This Foxn1 allele has an IRES-Cre component targeted to the 3' UTR of Foxn1, such that Cre is expressed from a Foxn1-IRES-Cre bicistronic mRNA that is faithfully transcribed from the Foxn1 locus (Gordon et al., 2007).

In Foxn1<sup>Cre/+</sup>;CAG-STOP-Foxn1ER mice (called Foxn1<sup>Cre/+</sup>;CAG-Foxn1ER), the stop cassette should be excised in cells that express Foxn1. To investigate the efficiency of this Cre-mediated recombination, GFP expression (translated from the Foxn1ER-IRES-GFP bicistronic mRNA) was examined in E12.5 EpCAM<sup>+</sup> TECs; most, if not all, TECs express Foxn1 at E12.5 (Gordon et al., 2007; Nehls et al., 1996). In E12.5 Foxn1<sup>Cre/+</sup>;CAG-Foxn1ER TECs over 95% of the cells expressed GFP. In contrast, no GFP expression was detected in TECs from wildtype and Cre negative controls, indicating that Foxn1ER-IRES-GFP transcription is effectively blocked by the STOP cassette and that Cre activity efficiently excised the STOP cassette from the CAG-STOP-Foxn1ER transgene (Figure 4.8a). Furthermore, GFP was detected in approximately 90% of TECs at 8 months, representing current and historical Foxn1 expression/Cre activity in these TECs (Figure 4.8b).

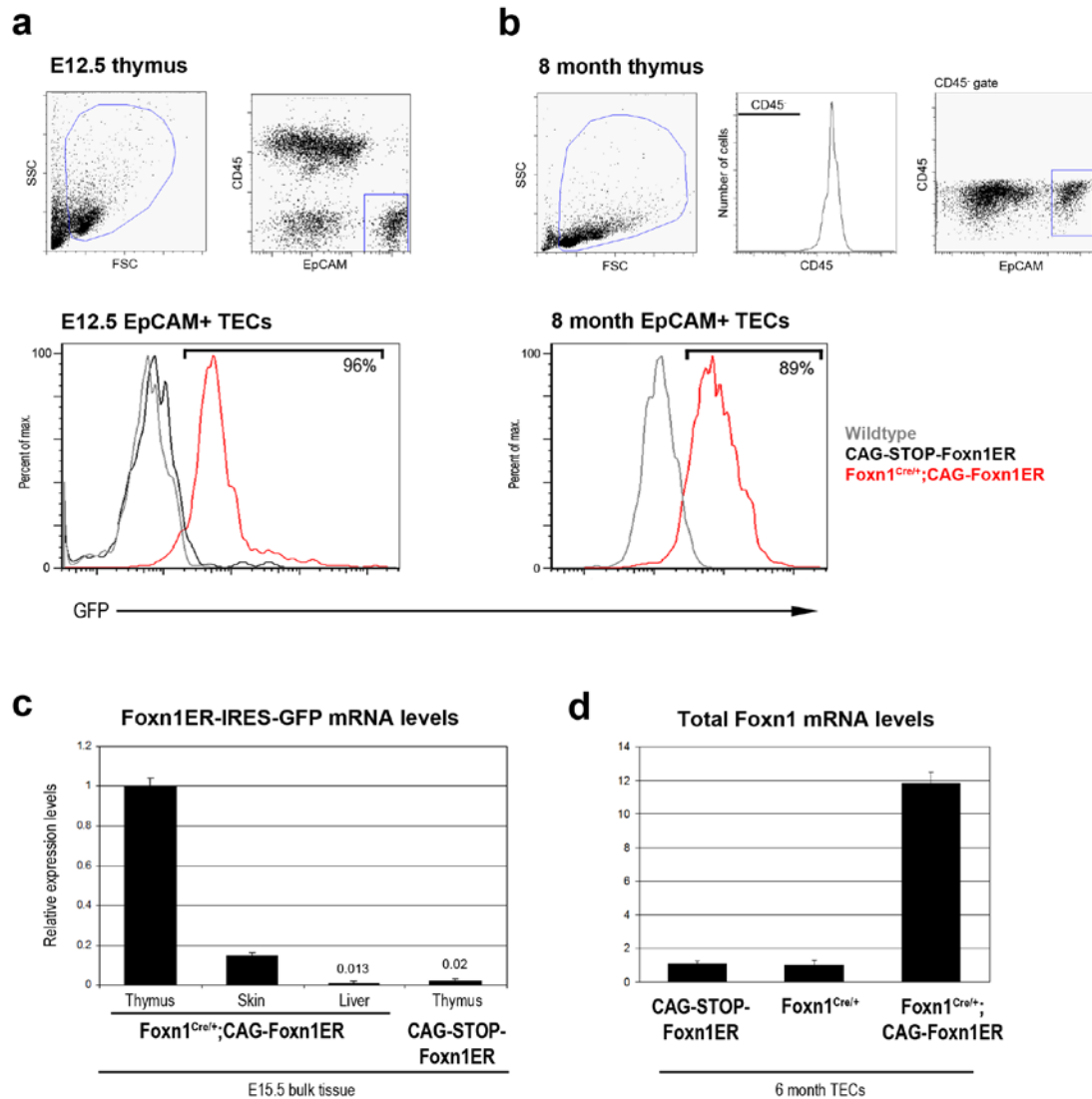


**Figure 4.8 Foxn1ER is expressed following Cre-mediated excision of the STOP cassette in TECs.**

(a) R26-CAG-STOP-Foxn1ER mice were crossed with Foxn1<sup>Cre/+</sup> mice to test the efficiency of Cre-mediated excision of the STOP cassette in the thymic epithelium. This was assayed by flow cytometric analysis of GFP expression (translated from the Foxn1ER-IRES-GFP mRNA) in EpCAM<sup>+</sup> TECs. E12.5 TECs from CAG-STOP-Foxn1ER mice (no Cre, black line) have an indistinguishable GFP profile to wildtype TECs (grey line). Conversely, almost all Foxn1<sup>Cre/+</sup>;CAG-Foxn1ER TECs express GFP (red line) following excision of the STOP cassette. Histograms show data from at least two pooled samples (b) Similarly, almost all 8 month Foxn1<sup>Cre/+</sup>;CAG-Foxn1ER TECs express GFP (red line) while wildtype TECs show no GFP expression (grey line). (c) Foxn1-IRES-GFP mRNA levels were quantified, normalised to  $\alpha$ -tubulin, by qRT-PCR on bulk embryonic tissues. Foxn1<sup>Cre/+</sup>;CAG-Foxn1ER thymi and skin express Foxn1-CAG-Foxn1ER at high levels, demonstrating the Foxn1<sup>Cre</sup> activity in these tissues, while little, if any, Foxn1-IRES-GFP mRNA is detected in the liver of Foxn1<sup>Cre/+</sup>;CAG-Foxn1ER mice and in the thymi of R26-CAG-STOP-Foxn1ER (without Cre). (d) Total Foxn1 mRNA levels (endogenous and Foxn1ER mRNA) were also quantified in TECs populations. Postnatal Foxn1<sup>Cre/+</sup>;CAG-Foxn1ER TECs express Foxn1 at significantly higher levels than wildtype embryonic and postnatal TECs. Data for qRT-PCR represent 3 or more biological repeats.

Thus, Foxn1-IRES-GFP is expressed in almost all embryonic and postnatal TECs in Foxn1<sup>Cre/+</sup>;CAG-Foxn1ER mice.

Next, Foxn1ER and total Foxn1 (Foxn1ER and endogenous Foxn1) mRNA levels were investigated to quantify background (e.g. caused by a transcriptional leak through the STOP cassette) and total Foxn1 levels (after STOP cassette excision) as well as the specificity of Foxn1<sup>Cre</sup> activity. Firstly, qRT-PCR analysis, using primers that specifically detect the Foxn1ER-IRES-GFP mRNA, showed that this transcript was expressed at significant levels in the thymus and skin at E15.5 in Foxn1<sup>Cre/+</sup>;CAG-Foxn1ER mice, in line with Foxn1 expression in these tissues at this age (Figure 4.8c) (Gordon et al., 2007; Lee et al., 1999). That no expression of Foxn1ER-IRES-GFP was detected in a tissue where Foxn1 is not expressed (liver), demonstrated the specificity of the Cre activity (Figure 4.8c). Additionally, there was little, if any, Foxn1ER-IRES-GFP mRNA in Cre negative thymi where the STOP cassette remained in tact (Figure 4.8c). Lastly, the Foxn1 levels were quantified in postnatal TEC. The total Foxn1 mRNA expression level in 6 month old Foxn1<sup>Cre/+</sup>;CAG-Foxn1ER TECs was greater than 10-fold higher compared to Foxn1<sup>Cre/+</sup> and Cre negative (CAG-STOP-Foxn1ER) controls (Figure 4.8d). These data establish that Foxn1<sup>Cre</sup> efficiently induces Foxn1ER-IRES-GFP expression in TECs following Cre-mediated excision of the transcriptional STOP cassette in the CAG-STOP-Foxn1ER transgene.

#### **4.4.3 Foxn1ER is regulatable by Tamoxifen treatment *in vivo***

While the above data confirm that Foxn1ER expression is effectively induced following Foxn1<sup>Cre</sup>-mediated excision of the STOP cassette, it cannot address the localization of the Foxn1ER protein (and thus the corresponding ability of Foxn1ER to perform its function). The ER component of Foxn1ER should maintain the protein in the cytoplasm in the absence of Tamoxifen, while the protein should translocate into the nucleus after Tamoxifen treatment.

Foxn1 immunohistochemistry was initially used to investigate whether or not a change in localization of Foxn1ER could be detected following Tamoxifen treatment. Although this method cannot differentiate between endogenous Foxn1 and Foxn1ER, Foxn1 protein was clearly detected in the cytoplasm of E15.5 Foxn1<sup>Cre/+</sup>;CAG-Foxn1ER TECs in the absence of Tamoxifen (Figure 4.9a). In comparison, Foxn1 in the wildtype thymus was exclusively nuclear (Figure 4.9a). After Tamoxifen treatment (a single 1.5mg dose at E14.5) most Foxn1 protein in Foxn1<sup>Cre/+</sup>;CAG-Foxn1ER TECs was nuclear, suggesting that the cytoplasmic

Foxn1ER had translocated into the nucleus (Figure 4.9a). A similar scenario was observed in the postnatal thymus. In Foxn1<sup>Cre/+</sup>;CAG-Foxn1ER mice that had not been treated with Tamoxifen, some Foxn1 protein was detected in the cytoplasm of TECs while following Tamoxifen treatment (a single 2mg dose and next day analysis) Foxn1 protein was predominantly nuclear (Figure 4.9b). An antibody against the ER region of Foxn1ER was also utilised in an attempt to track Foxn1ER translocation; however this method was not successful. Thus, by tracking total Foxn1 protein localization in the presence and absence of Tamoxifen, it appears that Foxn1ER is regulatable by Tamoxifen.

Also, while this method could be used to compare Foxn1 levels in wildtype and Foxn1<sup>Cre/+</sup>;CAG-Foxn1ER TECs, it should be noted that Foxn1 immunohistochemistry was performed here using an amplification protocol, such any Foxn1-positive signal is saturated meaning that linear expression relationships between samples is probably lost.

To definitively track Foxn1ER translocation following Tamoxifen treatment Western blot analysis of nuclear and cytoplasmic protein extracts from embryonic thymi was performed, as this permits distinction between the endogenous Foxn1 protein (~68kD) and the larger Foxn1ER protein (~95kD; ER is approximately 30kD). Foxn1ER was detected in the cytoplasm of Foxn1<sup>Cre/+</sup>;CAG-Foxn1ER TECs in the absence of Tamoxifen at a level that was markedly reduced following Tamoxifen treatment (Figure 4.9c) – indicating that the Foxn1ER protein is regulatable by Tamoxifen. Correspondingly, increased Tamoxifen dosage (0.5mg and 2.5mg) resulted in increased Foxn1ER in the nuclear fraction – indicating that Foxn1ER was regulated by Tamoxifen in a titratable manner (Figure 4.9c). In the absence of Tamoxifen, some Foxn1ER is detectable in the nucleus, indicating that there may be some background induction of Foxn1ER. However, this may also be as a result of contaminating cytoplasmic protein in the nuclear fraction. Thus, the data presented in Figure 4.9 verify that Foxn1ER is regulatable by Tamoxifen *in vivo*.

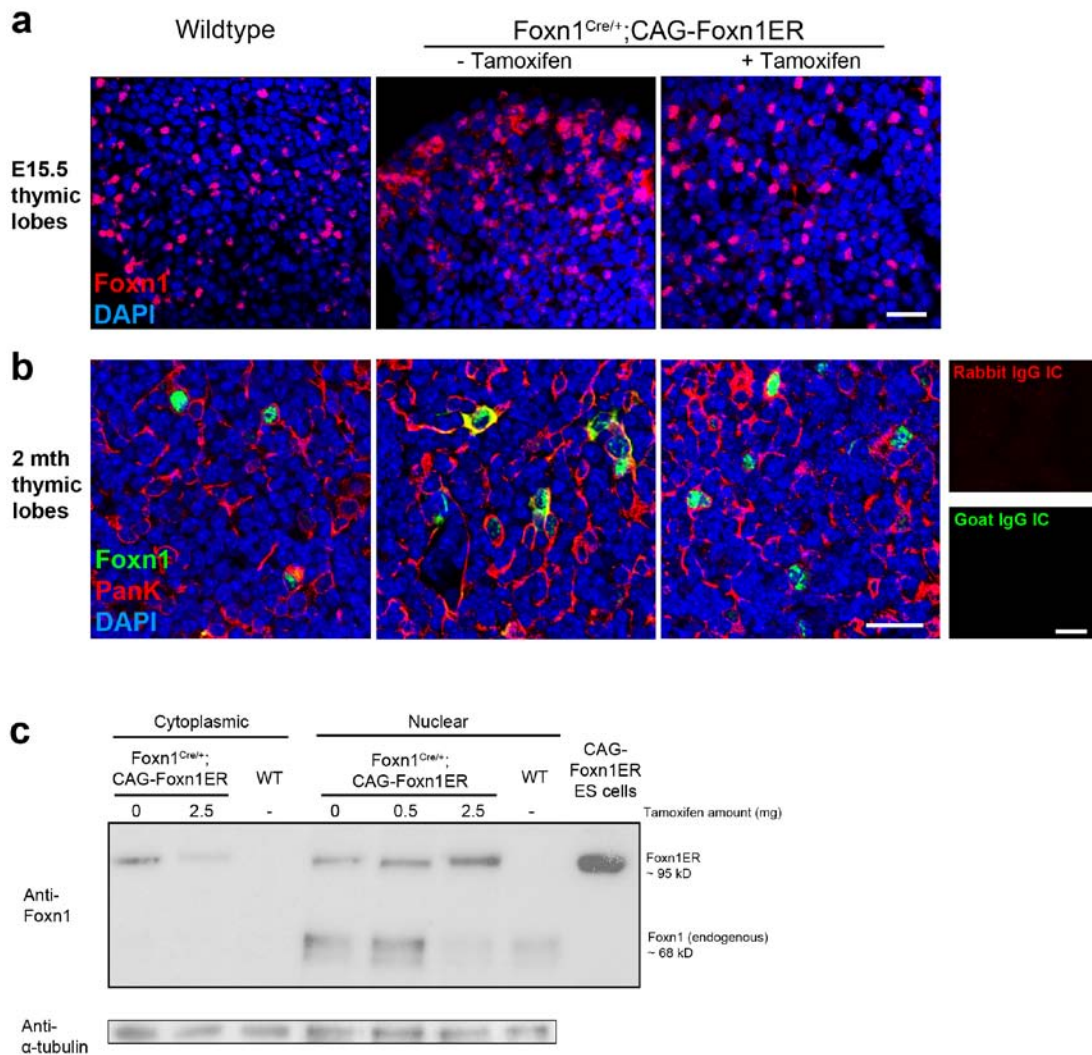


**Figure 4.9 Foxn1ER is regulatable by Tamoxifen *in vivo*.**

**(a)** Foxn1 localization was analysed in E15.5 wildtype and Foxn1<sup>Cre/+</sup>;CAG-Foxn1ER thymic lobes in the presence and absence of Tamoxifen by immunohistochemistry. Pregnant female mice were treated with 1.5mg Tamoxifen or carrier only at E14.5 and the embryos were analysed at E15.5. In wildtype mice, Foxn1 expression was exclusively nuclear, however in Foxn1<sup>Cre/+</sup>; CAG-Foxn1ER thymi (-Tamoxifen), Foxn1 is detectable in the cytoplasm, which probably represents Foxn1ER expression. After Tamoxifen treatment, Foxn1 expression is primarily nuclear, indicating that Foxn1ER is Tamoxifen responsive. **(b)** A similar scenario was observed in the postnatal thymus following a single 2mg dose of Tamoxifen and Foxn1 immunohistochemical analysis the following day. Scale bars represent 50 $\mu$ m. **(c)** To distinguish between endogenous Foxn1 and Foxn1ER Western blot analyses with  $\alpha$ -Foxn1 (G-20) was performed on cytoplasmic and nuclear protein fractions from E14.5 thymi lobes after various single dose Tamoxifen treatments at E13.5. 6mg or 3mg of protein were loaded for cytoplasmic or nuclear fractions, respectively. Foxn1ER shows a dosage dependent response to Tamoxifen (n=2).

#### **4.5 Concluding remarks**

This chapter details the generation of a transgenic mouse model that permits tissue specific, regulatable expression of Foxn1. By crossing these R26-CAG-STOP-Foxn1ER mice with Foxn1<sup>Cre</sup> mice, it was shown that Foxn1ER expression is efficiently induced in the thymic epithelium. Further, Foxn1ER functionality is regulatable by Tamoxifen which results in nuclear translocation of the fusion protein. Collectively, these data describe the generation and preliminary validation of the Foxn1<sup>Cre/+</sup>;CAG-Foxn1ER mouse line, which allows the effects of regulated Foxn1 expression in TECs to be investigated.

## Chapter 5: Maintained expression of Foxn1 prevents thymus involution

---

### 5.1 Introduction

Thymus involution is characterised by a series of stereotypical morphological and cellular changes. After a postnatal period of thymus expansion and homeostasis (until approximately 3-4 months), the thymus begins to decrease in size and exhibit early signs of involution, including disorganisation of the cortico-medullary junction (CMJ) and a reduction in MHC Class II and UEA1 expression (Gray et al., 2006; Manley et al., 2010). These changes correlate with a decrease in Foxn1 expression: in 6 and 12 month old thymi, there are a higher proportion of Foxn1<sup>lo</sup> and Foxn1<sup>int</sup> TECs than in 3 month thymi (Figure 3.3). Additionally, premature down-regulation or loss of Foxn1 expression in the postnatal thymus results in an early involution and decrease in thymic output (Chen et al., 2009; Cheng et al., 2010; Corbeaux et al., 2010; Sun et al., 2010). Collectively, these observations suggest that down-regulation of Foxn1 may play a role, primary or otherwise, in the involution of the thymus.

To probe this notion, I used the R26-CAG-STOP-Foxn1ER mouse model to over-express Foxn1 at the onset of involution (3-4 months postnatally) for a prolonged period of time (3 months) and investigated whether this delayed or prevented thymus involution. Therefore, while Foxn1 expression naturally decreases with age, this model allowed Foxn1 expression to be maintained at higher levels relative to wildtype from the onset of involution. R26-CAG-STOP-Foxn1ER mice were crossed with Foxn1<sup>Cre</sup> mice, such that Foxn1ER was expressed only in TECs and some keratinocytes; then, 3-4 month old CAG-Foxn1ER;Foxn1<sup>Cre</sup> mice were treated with Tamoxifen to induce Foxn1ER activity. The thymi from these mice and littermate controls were compared and analysed with regard to conventional involution hallmarks, including T cell number and composition and TEC phenotypes. Thus, in this Chapter I test the hypothesis that maintained expression of Foxn1 from the onset of involution is able to delay or prevent thymic involution.



## 5.2. Experimental strategy and preliminary validation

### 5.2.1 Experimental mice

$R26^{CAG-Foxn1ER/+};Foxn1^{Cre/+}$  mice treated with Tamoxifen (called **CAG-Foxn1ER +Tam hereafter**) were the experimental mice. CAG-Foxn1ER +Tam mice were 3-4 months old mice that were treated with Tamoxifen for 3 months and then analysed.

### 5.2.2 Control mice

Three control conditions were analysed as described below:

$R26^{+/+};Foxn1^{Cre/+}$  mice treated with carrier only (called **Cre control –Tam hereafter**).

Cre control –Tam mice were 3-4 months old mice that were treated with carrier only for 3 months and then analysed; these mice established the normal characteristics of thymus involution in my hands. Additionally, 3-4 month old Cre control –Tam mice were also analysed, where available, as the t=0 control.

$R26^{+/+};Foxn1^{Cre/+}$  mice treated with Tamoxifen (called **Cre control +Tam hereafter**)

Cre control +Tam mice were 3-4 months old mice that were treated with Tamoxifen for 3 months and then analysed; these mice established the effects of Tamoxifen on thymus involution.

$R26^{CAG-Foxn1ER/+};Foxn1^{Cre/+}$  mice treated with carrier only (called **CAG-Foxn1ER –Tam hereafter**).

CAG-Foxn1ER –Tam mice were 3-4 months old mice that were treated with Tamoxifen for 3 months and then analysed; these mice were used to determine if the background induction of Foxn1ER in the absence of Tamoxifen was significant.

### 5.2.3 Foxn1 mRNA levels in experimental and control mice

To confirm that Foxn1 was over-expressed in CAG-Foxn1ER TECs compared to Cre control TECs, total *Foxn1* mRNA levels (endogenous and transgenic) were quantified by qRT-PCR. Relative to 3-4 month Cre control mice –Tam mice, 6-7 month old Cre control +/-Tam mice expressed approximately half of the level of *Foxn1* mRNA in their thymi, while, CAG-Foxn1ER +/-Tam 6-7 month expressed greater than 6-fold more *Foxn1* mRNA (Figure 5.1a). This establishes that CAG-Foxn1ER thymi significantly over-express *Foxn1*, relative to t=0 and age-matched Cre control thymi. The specificity and efficiency of Cre-mediated deletion of the STOP cassette in the CAG-STOP-Foxn1ER transgene is described in Figure 4.8.

### 5.2.4 Hair phenotype

A hair pigment phenotype was consistently observed in 6-7 month old CAG-Foxn1ER mice that had been treated with Tamoxifen for 3 months. The ventral hair pigment of black-haired,

3-4 month old CAG-Foxn1ER mice changed to a light brown colour following 3 months of Tamoxifen administration (Figure 5.1b). No hair pigment changes were observed in Cre control +/-Tam and CAG-Foxn1ER -Tam mice.

This phenotype is particularly interesting as ectopic expression of Foxn1 in the mouse skin epidermis induced pigmentation through the recruitment of melanocytes (Weiner et al., 2007). Additionally, Foxn1 is normally expressed in the precursor cells of the hair cortex, which are the target cells of melanocytes in the hair follicle, with Foxn1 null mice exhibiting a lack of pigmentation in their hair cortex regions (Lee et al., 1999; Weiner et al., 2007). Thus, the macroscopic phenotype observed here is consistent with a proposed role for Foxn1 in hair pigmentation, and provides a preliminary indication that the experimental approach adopted here is valid.

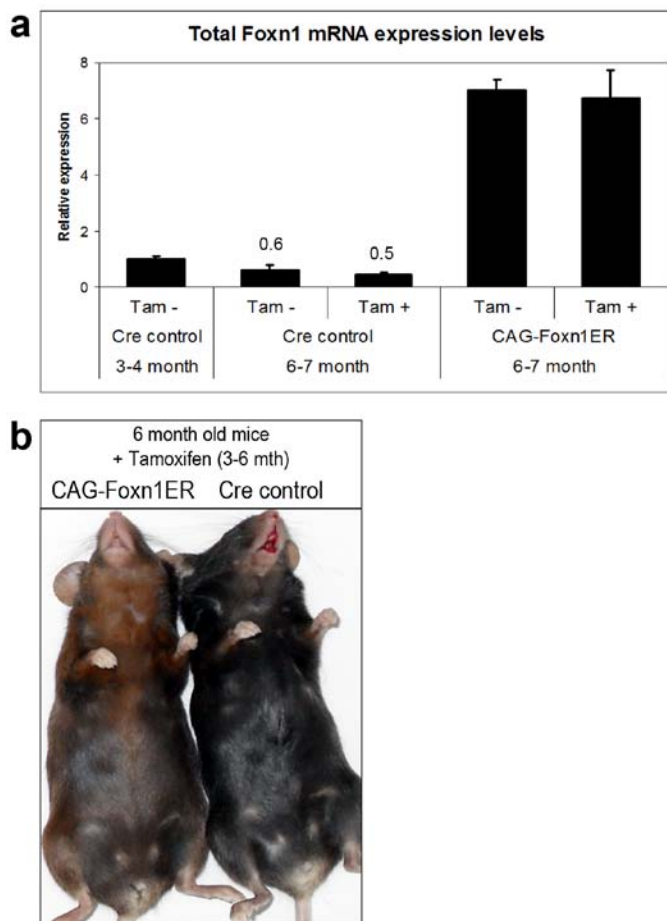


**Figure 5.1 Preliminary validation of the experimental system.**

**(a)** *Foxn1* mRNA expression levels were quantified by qRT-PCR in thymocyte-depleted bulk thymic digests from Cre control and CAG-Foxn1ER mice. Foxn1 was normalised to EVA (n=4). **(b)** CAG-Foxn1ER mice treated with Tamoxifen for 3 months showed changes in their hair pigment compared to Cre control mice.

## 5.3 Results

### 5.3.1 Thymus size

As an overt test of the effect of Foxn1 up-regulation during thymus involution, I first analysed thymus size. Thymi from 3-4 month old Cre control –Tam mice at the onset of thymus involution were overtly larger than thymi from 6-7 month old Cre control –Tam mice, indicating the overt effect of involution on thymus size (Figure 5.2a). Cre control thymi from 6-7 month old mice with and without Tamoxifen treatment were comparable in size, suggesting that Tamoxifen does not effect thymus involution, at least overtly (Figure 5.2a). Similarly, thymi from 6-7 month old CAG-Foxn1ER mice that had no Tamoxifen treatment were comparable in size to age-matched Cre control –Tam thymi, indicating that there was minimal background induction of Foxn1ER in the absence of Tamoxifen (Figure 5.2a).

Thymi from mice that over-expressed Foxn1 from 3-4 months of age for 3 months showed distinct overt differences, compared to control thymi. Thymi from CAG-Foxn1ER +Tam mice were overtly larger than all age-matched control conditions (Figure 5.2a). Furthermore, 6-7 month old CAG-Foxn1ER +Tam thymi were comparable size in size to 3-4 month old Cre control thymi at the onset of involution (Figure 5.2a). These data establish, at least overtly, that over-expression of Foxn1 from the onset of involution is able to maintain thymus size.

To correct for the general effect of mouse size/weight on the above data, thymi weights were determined relative to mouse body weight. Here, female and male mice are analysed separately due the greater weight of male mice. The average thymus to body weight ratio for 6-7 month old mice across all control conditions (Cre control +/-Tam and Foxn1ER –Tam) were comparable within male and female datasets (Figure 5.2b). In 6-7 month old male Foxn1 over-expressing mice (CAG-Foxn1ER +Tam) the average thymus to body weight ratio was significantly higher than male littermate control mice (Cre control +/-Tam and CAG-Foxn1ER –Tam) ( $n=3$ ,  $p\leq 0.05$ ) and was not significantly different from 3-4 month Cre control mice ( $n=3$ ,  $p=0.46$ ) (Figure 5.2b). Similarly, 6-7 month old female CAG-Foxn1ER +Tam mice had significantly higher thymus to body weight ratios compared to the control mice ( $n=5$ ,  $p<0.03$ ) and were not significantly different from 3-4 month female Cre control mice ( $n=3$ ,  $p=0.063$ ). Thus, maintained over-expression of Foxn1, at the onset of involution, when its expression would normally begin to decrease, results in a thymus size and thymus/

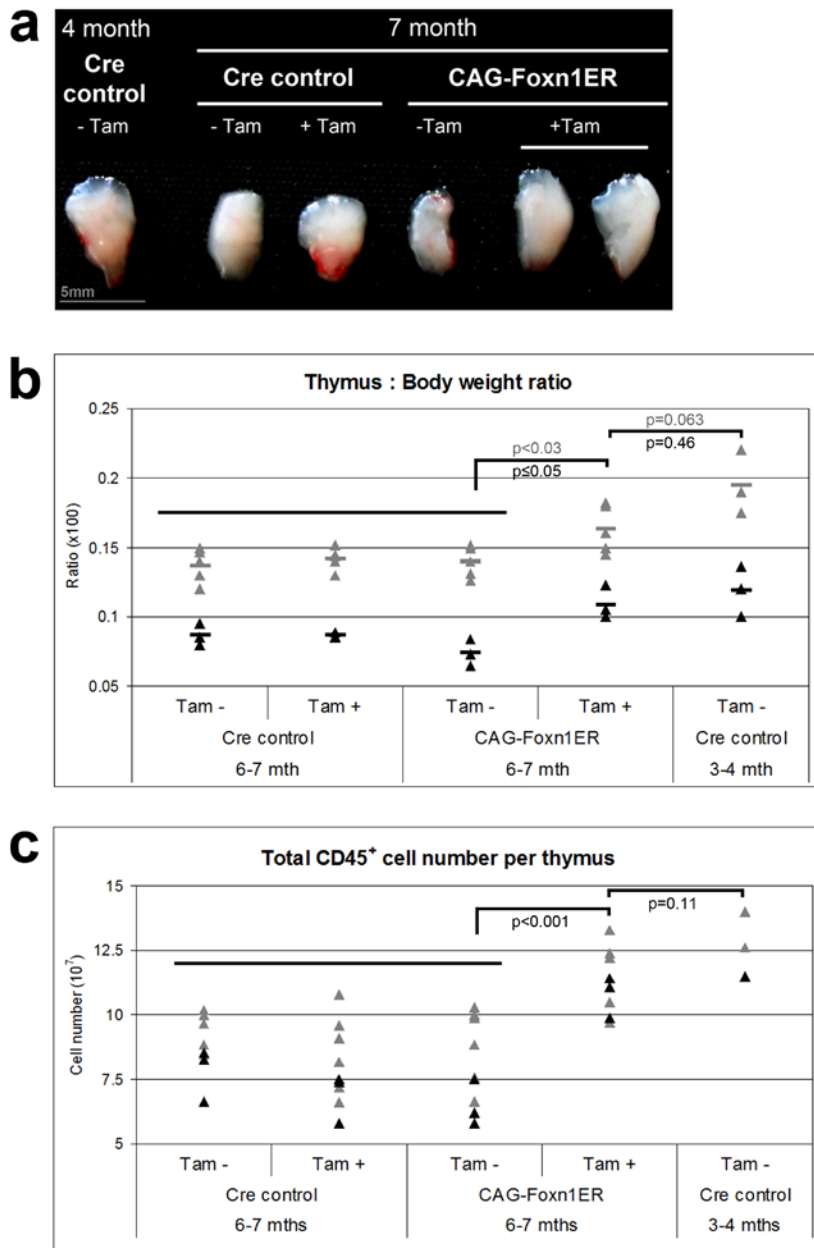


**Figure 5.2 Maintained expression of Foxn1 prevents thymus involution.**

(a) When Foxn1 expression was maintained in TECs from the onset of involution for 3 months (7 month CAG-Foxn1ER +Tam) the thymus was overtly larger than littermate control thymi (7 month CAG-Foxn1ER -Tam, Cre control +/-Tam) and comparable in size to a thymus at the onset of involution (4 month Cre control). Image shows single thymus lobes from male mice and is representative of 3 independent experiments. (b) The thymus (mg) to body weight (g) ratio for 6-7 mth CAG-Foxn1ER +Tam mice is higher than all age-matched controls. Each data point represents a single mouse. (c) CAG-Foxn1ER +Tam thymi contained significantly more CD45<sup>+</sup> cells than age-matched controls (n=9, p<0.001) but not 3-4 mth Cre control thymi (n=3, p=0.11). (▲) Male mouse, (▲) female mouse, (-) average for each data set.

body weight ratio that is comparable to the t=0 thymus (i.e. at 3-4 months) and larger than control littermate thymi.

### 5.3.2 T cells numbers and composition

The fundamental function of the thymus is the generation of the pool of naïve T cells that emigrate from the organ and perform critical immune functions. Consequently, the most important feature that defines thymic involution is the reduction in thymic activity and output as determined by number and composition of developing and mature T cells. The number of intrathymic CD45<sup>+</sup> cells, which accounts for all the hematopoietic cells in the thymus (of which, T cells constitute the majority) can be used as a general read-out of thymic activity (Chen et al., 2009; Gray et al., 2006).

Thymi from 6-7 month old Cre control –Tam, Cre control +Tam and CAG-Foxn1ER –Tam mice contained a comparable number of total intrathymic CD45<sup>+</sup> hematopoietic cells ( $8.8 \times 10^7 \pm 3.6 \times 10^6$ ,  $8.0 \times 10^7 \pm 5.2 \times 10^6$  and  $8.1 \times 10^7 \pm 5.8 \times 10^6$  cells, respectively) (Figure 5.2c). In contrast, thymi from 6-7 month old CAG-Foxn1ER +Tam mice contained, on average, significantly more CD45<sup>+</sup> cells than all control conditions ( $1.13 \times 10^8 \pm 4.0 \times 10^6$  cells, n=9, p<0.001) (Figure 5.2c). Moreover, the number of CD45<sup>+</sup> cells in 6-7 month old Tamoxifen treated mice were not significantly different from 3-4 month old Cre control thymi ( $1.27 \times 10^8 \pm 7.2 \times 10^6$  cells, n=3, p=0.11) (Figure 5.2c). The hematopoietic cellularity of 3-4 month old thymi presented here are in line with data reported in the literature of approximately  $1.2 \times 10^8$  cells in 3 month old thymi (Gray et al., 2006). This indicates that maintenance of Foxn1 expression is sufficient to prevent the reduction in total intrathymic hematopoietic cells associated with normal involution.

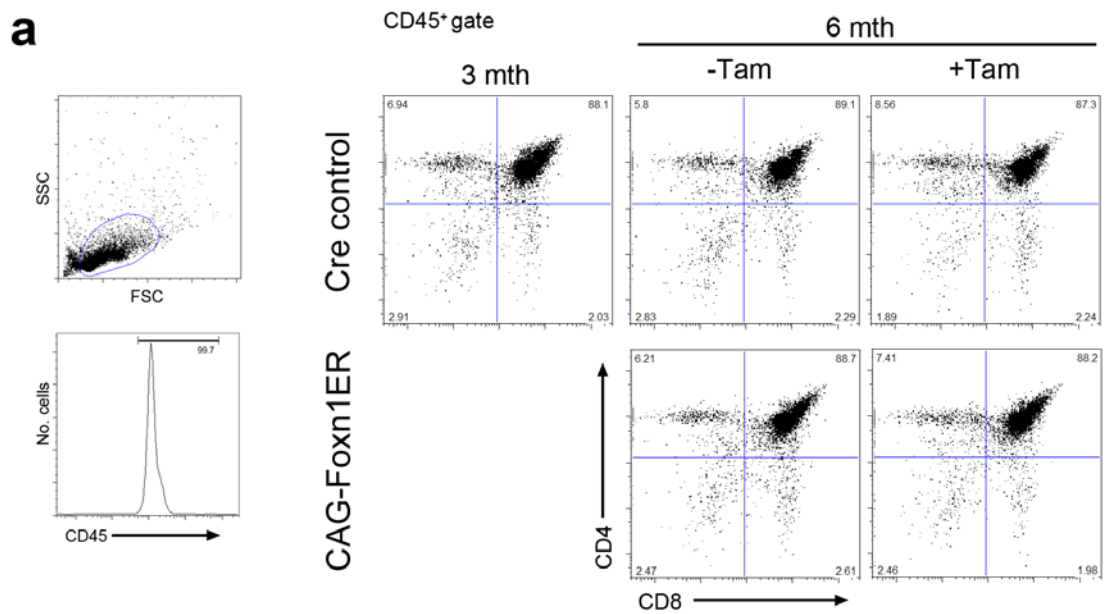
Next, different T cell sub-populations were analysed in more detail. Firstly, the major T cell development stages corresponding to CD4 and CD8 expression profiles were examined. There was no reproducible difference detected in the proportions of the four CD4/CD8 populations (CD4 and CD8 double negative (DN), double positive (DP) and the two more mature populations of CD4 and CD8 single positive cells (SP)) across all control and experimental conditions (Figure 5.3a). However, differences in the absolute numbers of these T cells populations were observed.

Firstly, all 6-7 month old control thymi contained a comparable number of CD4<sup>+</sup>CD8<sup>+</sup> DP cells (Cre control –Tam,  $7.38 \times 10^7 \pm 4.0 \times 10^6$ ; Cre control +Tam,  $6.56 \times 10^7 \pm 3.0 \times 10^6$ ; CAG-

Foxn1ER –Tam  $7.12 \times 10^7 \pm 6.0 \times 10^6$ ) (Figure 5.3b). Compared to these controls, CAG-Foxn1ER +Tam thymi contained over 20% and significantly more DP T cells ( $9.13 \times 10^7 \pm 4.0 \times 10^6$ , n=6, p<0.02) (Figure 5.3b). Furthermore, the number of DP T cells in 6-7 month old CAG-Foxn1ER +Tam thymi was not significantly different from 3-4 month Cre control –Tam thymi ( $10.5 \times 10^7 \pm 4.0 \times 10^6$ , n=2, p=0.12) (Figure 5.3b). Similarly, 6-7 month old control thymi contained comparable numbers of CD4<sup>+</sup> SP cells (Cre control –Tam,  $5.79 \times 10^6 \pm 6.0 \times 10^5$ ; Cre control +Tam,  $5.26 \times 10^6 \pm 7.0 \times 10^5$ ; CAG-Foxn1ER –Tam  $5.16 \times 10^6 \pm 8.2 \times 10^5$ ); while 6-7 month old CAG-Foxn1ER +Tam thymi contained over 30% and significantly more CD4<sup>+</sup> SP cells than control thymi ( $8.0 \times 10^6 \pm 7.9 \times 10^5$ , n=6, p≤0.05) and comparable CD4<sup>+</sup> SP cell numbers to 3-4 month Cre control thymi ( $7.6 \times 10^6 \pm 1.0 \times 10^6$ , n=2, p=0.80) (Figure 5.3c).

The differences in CD8<sup>+</sup> SP cell numbers were less substantial between 6-7 month old control and CAG-Foxn1ER +Tam thymi. Again, CD8<sup>+</sup> SP cell numbers were comparable between 6-7 month old control thymi (Cre control –Tam,  $1.91 \times 10^6 \pm 1.6 \times 10^5$ ; Cre control +Tam,  $1.7 \times 10^6 \pm 1.5 \times 10^5$ ; CAG-Foxn1ER –Tam  $1.93 \times 10^6 \pm 2.0 \times 10^5$ ), and while CAG-Foxn1ER +Tam thymi contained more CD8<sup>+</sup> SP cells, the difference between the controls was only approaching significance ( $2.51 \times 10^6 \pm 2.1 \times 10^5$  cells, n=6, p<0.075) (Figure 5.3c). The number of CD8<sup>+</sup> cells was not significantly different between 6-7 month old CAG-Foxn1ER +Tam thymi and 3-4 month Cre control thymi ( $3.18 \times 10^6 \pm 6.0 \times 10^5$  cells for the latter condition, n=2, p=0.21) (Figure 5.3c). The higher relative number of CD4<sup>+</sup> SP cells compared to CD8<sup>+</sup> SP cells in experimental versus control thymi may reflect the increased expression of MHC Class II which is required for selection of CD4<sup>+</sup> SP cells (discussed later in Section 5.3.3).

Lastly, thymi from 6-7 month old CAG-Foxn1ER +Tam mice contained more CD4<sup>+</sup>CD8<sup>+</sup> DN cells compared to age matched controls (Cre control –Tam,  $4.38 \times 10^6 \pm 9.9 \times 10^5$ ; Cre control +Tam,  $4.5 \times 10^6 \pm 1.0 \times 10^6$ ; CAG-Foxn1ER –Tam  $4.88 \times 10^6 \pm 9.0 \times 10^5$ ; CAG-Foxn1ER +Tam,  $7.14 \times 10^6 \pm 2.6 \times 10^5$ ; n=6; p<0.04) (Figure 5.3c). Moreover, DN cell numbers were not significantly different between 6-7 month CAG-Foxn1ER +Tam and 3-4 month Cre control thymi ( $8.2 \times 10^6 \pm 4.5 \times 10^5$  cells for the later condition; n=2; p=0.09) (Figure 5.3c). These data establish that Foxn1 expression prevents the reduction in size of specific T cell populations associated with age-related thymus involution.



**b** Major T cell subset numbers per thymus

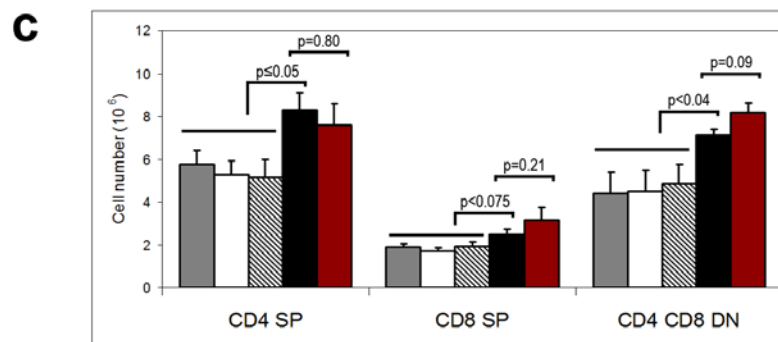
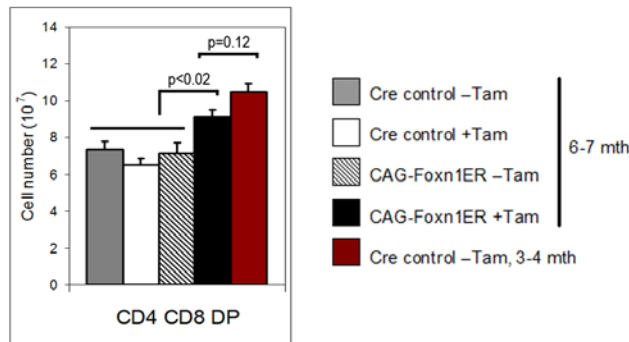


**Figure 5.3 Major T cell subset proportions and numbers following over-expression of Foxn1 in aging thymi.**

T cell subsets (CD4<sup>+</sup>CD8<sup>+</sup> double positive (DP), CD4<sup>+</sup> or CD8<sup>+</sup> single positive (SP) and CD4<sup>-</sup>CD8<sup>-</sup> double negative (DN)) were examined by flow cytometry in experimental and control mice. **(a)** Flow cytometric analysis of CD45<sup>+</sup> gated thymocytes with  $\alpha$ -CD4 and  $\alpha$ -CD8, revealed no difference in the proportions of the populations across all mice. **(b)** However, CAG-Foxn1ER +Tam thymi contained more T cells for each population by absolute number, compared to age-matched controls. CD4<sup>+</sup>CD8<sup>+</sup> DP, CD4<sup>+</sup> SP and CD4<sup>-</sup>CD8<sup>-</sup> DN cell numbers were significantly higher than in controls ( $p < 0.02$ ,  $p \leq 0.05$ ,  $p < 0.04$  respectively,  $n = 6$ ) while CD8<sup>+</sup> SP cell numbers, although higher for CAG-Foxn1ER +Tam, were not significantly different ( $p < 0.075$ ,  $n = 6$ ). Additionally, 6-7 month CAG-Foxn1ER +Tam cell numbers were not significantly different from 3-4 Cre control thymi ( $p > 0.09$ ,  $n = 2$ ) for any population.

In light of the higher CD4<sup>+</sup>CD8<sup>-</sup> DN cell numbers in 6-7 month old CAG-Foxn1ER +Tam thymi compared to controls, the triple negative (TN, CD3<sup>+</sup>CD4<sup>-</sup>CD8<sup>-</sup>) immature intrathymic precursor cell population was analysed. Firstly, the distribution of the TN cell subsets was analysed in experimental and control mice. The proportion of TN1 cells was higher in 6-7 month old Cre control +Tam thymi compared to all other conditions (27%±7.8%, n=4) (Figure 5.4a,b). This appeared to be an effect of Tamoxifen as both Cre control and CAG-Foxn1ER -Tam controls had lower and comparable TN1 proportions (20%±3.1% and 23%±6.6% respectively), although these differences were not significant. In CAG-Foxn1ER +Tam thymi the TN1 proportion was 21%±4.3%, suggesting that if there was a Tamoxifen-induced block in TN1 to TN2 transition (resulting in the higher TN1 proportion) then Foxn1 over-expression overcomes this. Interestingly, a potential Foxn1 target, Delta-like 4 (Dl14) (Bajoghli et al., 2009; Nowell et al., under review) is a crucial mediator of the TN1 to TN2 transition, where it regulates T cell commitment (Koch et al., 2008). Thus, it is tempting to speculate that the apparent effect of Tamoxifen on the TN1 to TN2 transition (whether an effect on Dl14, or otherwise), was corrected by the Foxn1-dependent up-regulation of Dl14.

The proportions of the TN2 and TN3 populations did not show any differences, although -Tam and +Tam conditions were more closely correlated, possibly indicating a mild suppressive effect of Tamoxifen on these populations (Figure 5.4b). However, CAG-Foxn1ER +Tam thymi contained a higher proportion of TN4 precursors (36%±5.4%) compared to all control thymi (although these differences were not significant) (Figure 5.4b). This suggests that mediation of the TN3 to TN4 checkpoint, which is also dependent on Notch, is impaired when Foxn1 is expressed at low levels (Nowell et al., under review; Wolfer et al., 2002)

Next, the absolute TN cell numbers were investigated. 6-7 month old CAG-Foxn1ER +Tam thymi contained significantly more total TN cells than all the control thymi (Cre control -Tam,  $2.84 \times 10^6 \pm 2.0 \times 10^5$ ; Cre control +Tam,  $2.27 \times 10^6 \pm 1.7 \times 10^5$ ; CAG-Foxn1ER -Tam  $2.37 \times 10^6 \pm 5.0 \times 10^5$ ; CAG-Foxn1ER +Tam,  $4.26 \times 10^6 \pm 5.5 \times 10^5$ ; n=4; p<0.05) and a comparable number to 4 month old Cre control ( $4.57 \times 10^6$ , n=1) (Figure 5.4c). The higher number of total TN cells translated into more cells in all four TN sub-populations for the CAG-Foxn1ER +Tam thymi compared to all controls, however these differences were not significant for any of the four TN sub-populations (n=4, p>0.09) (Figure 5.4d). Thus, maintained Foxn1 expression for three months from the onset of involution results in a TN



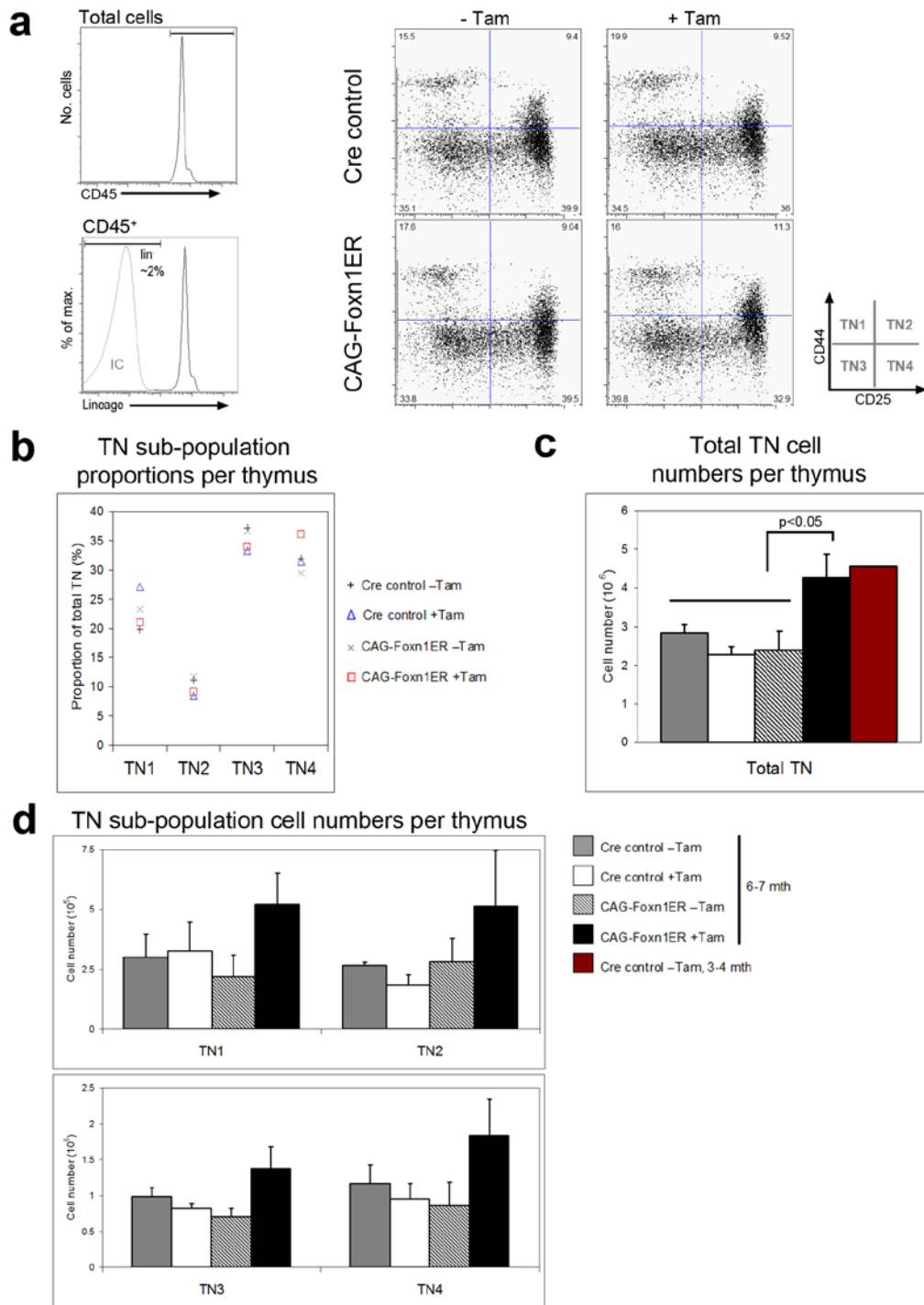


**Figure 5.4 Triple negative (TN) cell proportions and numbers following over-expression of Foxn1 in aging thymi.**

**(a)** Flow cytometric analysis of TN cells ( $CD45^+lin^-$  (lineage = CD3, CD4, CD8, CD11b, CD11c, CD19, NK1.1, Gr-1)) from 6-7 month thymi stained with  $\alpha$ -CD25 and  $\alpha$ -CD44. **(b)** The average TN sub-population proportions per thymus were determined for all experimental conditions ( $n=4$ ). **(c)** The average total TN cell number per thymus was significantly higher in 6-7 month CAG-Foxn1ER +Tam thymi compared to controls ( $n=4$ ,  $p < 0.05$ ) and was comparable to 3-4 month Cre control thymi ( $n=1$ ). **(d)** The average number of cells in each TN subset was higher in CAG-Foxn1ER +Tam thymi compared to controls thymi ( $n=4$ ,  $p > 0.09$ ).

population size that is maintained at the size of to 3-4 month old thymi, and is significantly larger than littermate controls. A note should be made here that within the time frame of this thesis the data presented for the TN population in the 3-4 month Cre control are only minimal and need to be expanded in the future.

### 5.3.3 TEC numbers and phenotype

The outcome of the prevention of involution by over-expression of Foxn1, as described above in relation to T cell numbers and composition, most likely stems from the action of Foxn1 in the thymic epithelium. To investigate this further, TEC numbers and phenotype were analysed.

Firstly, total TEC numbers per thymus were determined; TECs were defined as CD45<sup>-</sup> EpCAM<sup>+</sup>, as previously described in Chapter 1 (Farr et al., 1991) (Figure 5.5a). 6-7 month old CAG-Foxn1ER +Tam thymi contained over 1.5-fold and significantly more TECs per thymus compared to all age-matched control thymi (CAG-Foxn1ER +Tam,  $1.24 \times 10^5 \pm 1.3 \times 10^4$ ; Cre control -Tam,  $7.0 \times 10^4 \pm 6.9 \times 10^3$ ; Cre control +Tam,  $7.7 \times 10^4 \pm 8.9 \times 10^3$ ; CAG-Foxn1ER -Tam,  $6.8 \times 10^4 \pm 1.2 \times 10^4$ ; n=4; p<0.025) (Figure 5.5b). Furthermore, the number of TECs in 6-7month old CAG-Foxn1ER +Tam thymi was comparable to 3-4 month old Cre control thymi ( $1.41 \times 10^5 \pm 2.4 \times 10^4$ , n=4, p=0.55) (Figure 5.5b). Thus, Foxn1 over-expression during the early stages of involution was sufficient to maintain the size of the TEC compartment, which normally decreases as involution progresses.

Next, the phenotypic characteristics of the TECs in the experimental and control mice were investigated. This analysis was performed using two TEC markers, MHC Class II, a functional marker of mature TECs and UEA1, expressed on a subset of mature mTECs. Both markers have been shown to decrease in expression during normal involution and when Foxn1 expression was perturbed postnatally (Chen et al., 2009; Gray et al., 2006; Sun et al., 2010).

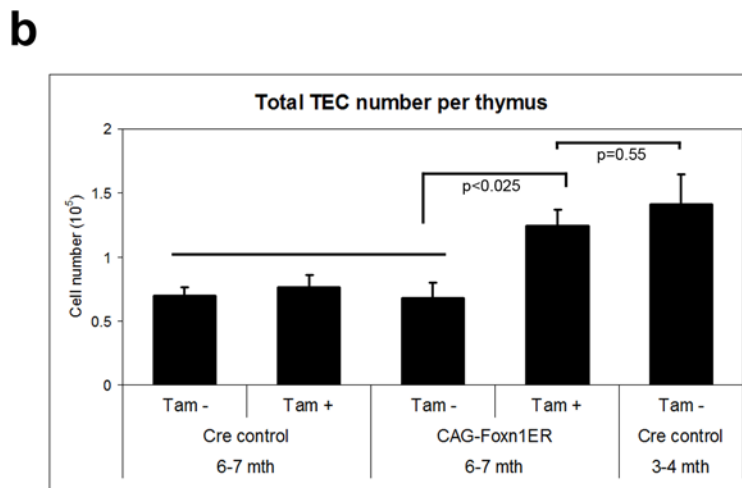
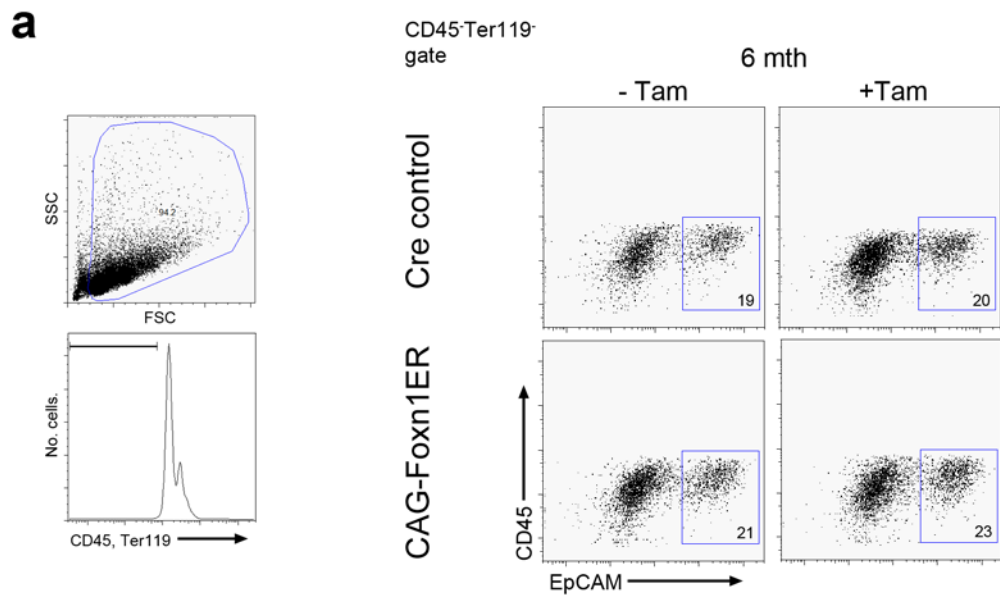


**Figure 5.5 Total TEC numbers are greater when Foxn1 expression is maintained during thymus involution.**

**(a)** Flow cytometric analysis of 6-7 and 3-4 month old thymi. Total TECs were identified using  $\alpha$ -EpCAM after gating on CD45<sup>+</sup>Ter119<sup>-</sup> cells without thymocyte depletion. **(b)** 6-7 month CAG-Foxn1ER +Tam thymi contained significantly more TECs compared to all controls ( $p < 0.025$ ,  $n=4$ ); 6-7 month CAG-Foxn1ER +Tam TEC numbers were comparable to TECs numbers in 3-4 month Cre control thymi ( $p=0.55$ ,  $n=4$ ).

The MHC Class II<sup>hi</sup> proportion of total TECs in CAG-Foxn1ER +Tam thymi was higher than in all controls (Figure 5.6a); a direct comparison of the MHC Class II profiles of total TECs from CAG-Foxn1ER +Tam and Cre control +Tam thymi distinctly illustrates this difference (Figure 5.6b). On average, the MHC Class II<sup>hi</sup> proportion of total TECs was approximately 10% higher in CAG-Foxn1ER +Tam compared to all controls (39.5%±4.3% versus 28.0%±1.4% respectively, n=3) (Figure 5.6c). Additionally, the proportion of MHC Class II<sup>hi</sup> TECs in CAG-Foxn1ER +Tam was comparable to 3-4 month old Cre control TECs (38.0%±1.7%) (Figure 5.6c). The higher proportion of MHC Class II<sup>hi</sup> TECs in CAG-Foxn1ER +Tam thymi compared to age-matched controls might explain the increased number of CD4<sup>+</sup> SP T cells described earlier (Figure 5.3), as MHC Class II plays a critical role in CD4<sup>+</sup> cell development.

Next, UEA1 expression in TECs was investigated. Within the UEA1<sup>+</sup> mTEC population, there are two sub-populations, UEA1<sup>hi</sup> and UEA1<sup>lo</sup>. The proportion of the UEA1<sup>hi</sup> sub-population decreases with age (the proportion at 1 year is less than half that at 1 month) and when Foxn1 expression is down-regulated (Chen et al., 2009). In 6-7 month old CAG-Foxn1ER +Tam mice, the proportion of UEA1<sup>hi</sup> TECs within the UEA1<sup>+</sup> population was 1.4-fold greater for CAG-Foxn1ER +Tam thymi compared to all controls (45%±1.3% versus 32%±1.5% respectively, n=2) (Figure 5.6d,e). Additionally, there was higher proportion of UEA1<sup>hi</sup>MHC Class II<sup>hi</sup> TECs within the UEA1<sup>+</sup> population for CAG-Foxn1ER +Tam compared to all controls (29.2%±0.5% and 22.9%±0.3% respectively, n=2) (Figure 5.6d,e). Unfortunately, due to limited available mice, 3-4 month old Cre control data were not obtained for UEA1 flow cytometric analyses.

Because it was established that CAG-Foxn1ER +Tam thymi contained significantly more TECs than all controls (Figure 5.5b), it can be inferred from the MHC Class II<sup>hi</sup> and UEA1<sup>hi</sup> proportion data presented above, that CAG-Foxn1ER thymi also contain more of these TEC sub-populations by absolute number. Thus, while normal involution results in a decrease in the proportions and number of MHC Class II<sup>hi</sup> and UEA1<sup>hi</sup> TEC sub-populations, maintained expression of Foxn1 prevents these changes from occurring.

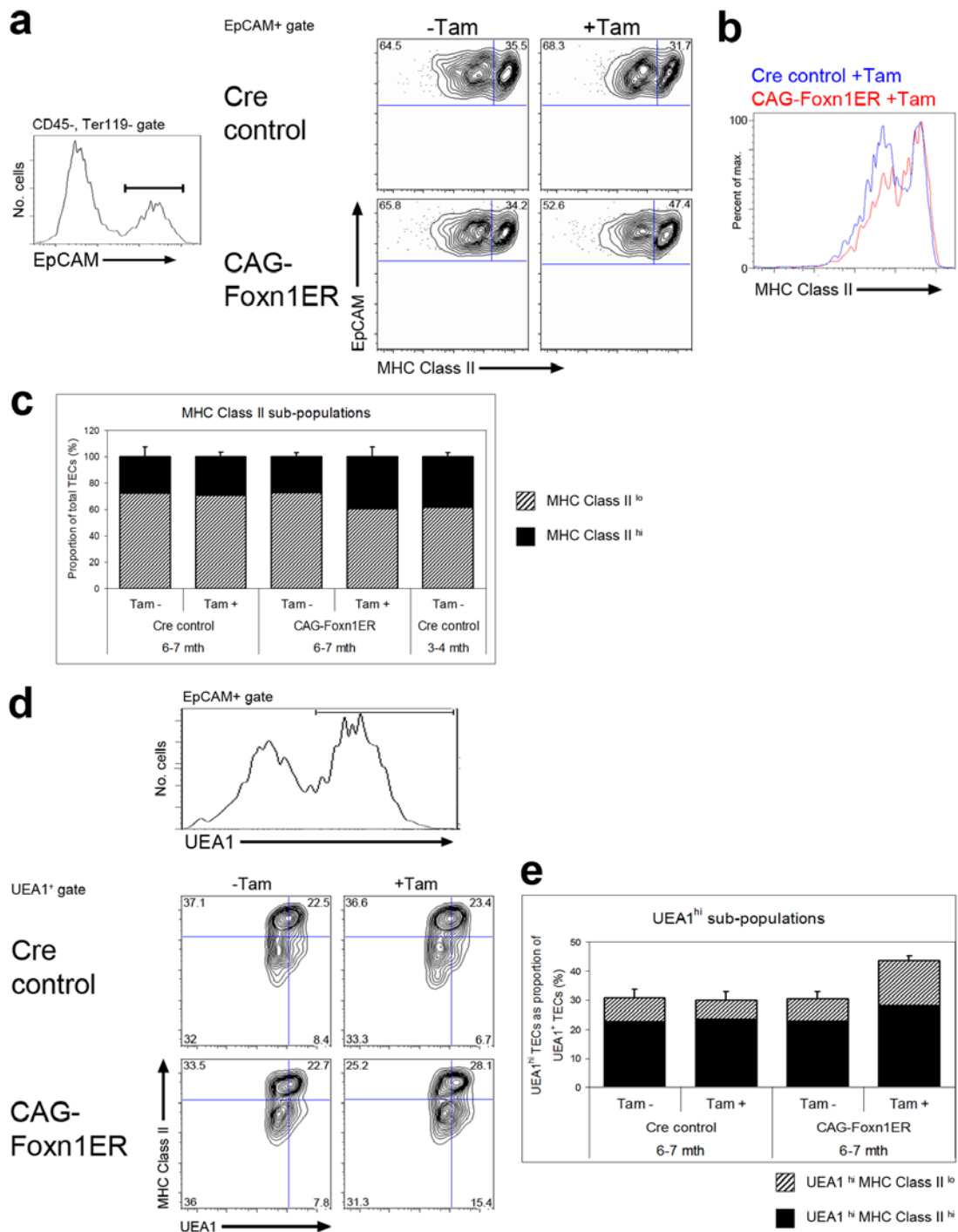


**Figure 5.6 Effect of maintained Foxn1 expression on TEC phenotype.**

(a) Flow cytometric analysis, without thymocyte depletion, was performed on 6-7 month old thymi where total TECs were analysed using EpCAM and MHC Class II, after gating on CD45<sup>-</sup> cells. (b) Histogram representation of contour plot data, shows MHC Class II profile of EpCAM<sup>+</sup> TECs from CAG-Foxn1ER +Tam (red line) and Cre control +Tam thymi (blue line). (c) 6-7 month old CAG-Foxn1ER +Tam thymi contained more MHC Class II<sup>hi</sup> TECs compared to age-matched controls. This proportion was similar to 3-4 month Cre control thymi (n=3). (d) UEA1 versus MHC Class II flow cytometric analysis of EpCAM<sup>+</sup>UEA1<sup>+</sup> TECs from 6-7 month old thymi. Plots are representative of 2 experiments. (e) Proportion and composition of the UEA1<sup>hi</sup> sub-population within the UEA1<sup>+</sup> TEC population (n=2).

### 5.3.4 TEC gene expression and proliferation

To further investigate the characteristics of the TECs in CAG-Foxn1ER +Tam versus control mice, the expression levels of a suite of genes with defined roles in thymus development and/or function were determined. Various TEC genes, including *Pax1*, *Pax9*, *Dll4*, *CCL25*, and *FgfR2IIIb* exhibit expression levels that are responsive to different levels of Foxn1, as shown in a Foxn1 allelic series (Nowell et al., under review). Total EpCAM<sup>+</sup> TECs were isolated from CAG-Foxn1ER +Tam thymi and control thymi (as described in Chapter 1) and assayed for gene expression levels by qRT-PCR. Here, Cre control +/-Tam and CAG-Foxn1ER -Tam TECs were pooled in the control experiment due to limited mouse numbers and on the basis of the comparable data obtained for each condition, as presented above.

First, I determined whether ectopic Foxn1 expression affected expression levels of endogenous Foxn1. This was achieved using a qRT-PCR assay for the 3'UTR of endogenous *Foxn1*, a region which is not present in the transgenic *Foxn1ER* mRNA. The endogenous *Foxn1* level in 6-7 month control TECs was approximately one third of that in 2 month old WT TEC (Figure 5.7a). In contrast, in 6-7 month old CAG-Foxn1ER +Tam TECs, the endogenous *Foxn1* level was more than two-fold higher than in control TECs and at about 70% of the level in 2 month TECs (Figure 5.7a). This suggests that Foxn1 may function in an autoregulatory manner, either directly or indirectly, as Foxn1ER activity resulted in an increase in endogenous *Foxn1* mRNA levels.

Next, a number of Foxn1 dependent TEC genes were analysed. *Pax1*, which is expressed in a subset of cTECs in the postnatal thymus (Wallin et al., 1996) was detected at a higher level in CAG-Foxn1ER +Tam TECs compared to control TECs (over 1.5-fold more) (Figure 5.7a). Surprisingly, the *Pax1* mRNA levels in both 6-7 month samples were higher than in 2 month WT TECs. Very little is known about the postnatal regulation of Pax1, making an explanation difficult; one possibility may be a relative increase in the Pax1-positive cTEC subpopulation with age.

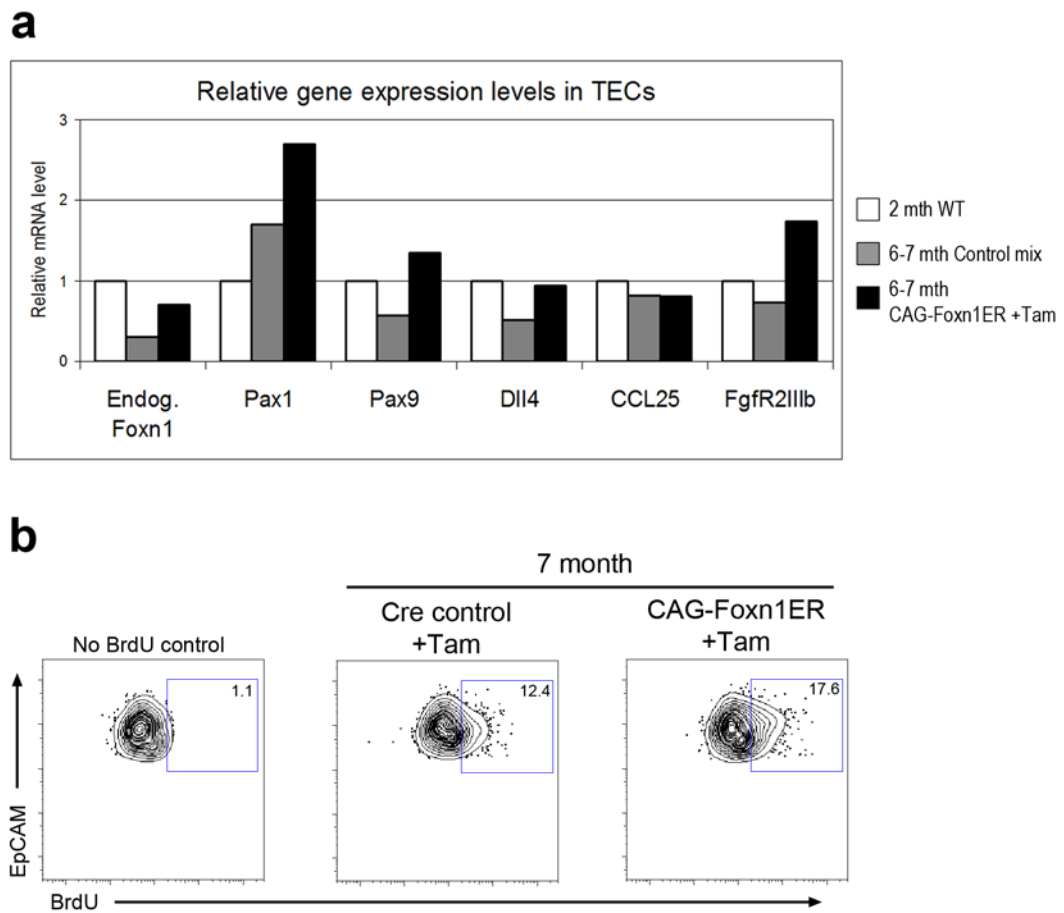


**Figure 5.7 Gene expression and proliferation profile in TECs that over-express Foxn1 during involution.**

**(a)** TEC gene levels were quantified by qRT-PCR for total TECs (EpCAM<sup>+</sup>). TECs were flow cytometrically isolated from three pooled thymi for 2 month WT, 6-7 month CAG-Foxn1ER +Tam and 6-7 month control samples (one mouse from each condition: Cre control+/- tam and CAG-Foxn1ER -Tam were pooled together for the control sample). Endogenous (Endog.) *Foxn1*, *Pax1*, *Pax9*, *Delta-like 4 (Dll4)*, *CCL25* and *FgfR2IIIb* genes were normalised to  $\alpha$ -tubulin. Data represent 6 technical repeats. **(b)** Proliferation analysis of TECs using BrdU. After 3 months of Tamoxifen treatment, 7 month old Cre control and CAG-Foxn1ER were treated with BrdU for 3 days. Two mice per condition were pooled and TECs (EpCAM<sup>+</sup>) were analysed by flow cytometry for BrdU incorporation.

The *Pax9* and *Dll4* mRNA levels in 6-7 month control TECs were approximately half of that in 2 month WT TECs, however over-expression of *Foxn1* resulted in an increase in the mRNA levels for both genes, to levels comparable to 2 month WT (Figure 5.7a). *CCL25* mRNA was expressed at comparable levels across all samples (Figure 5.7a). *CCL25* null thymi are smaller than WT thymi and *CCL25* expression is dosage responsive to *Foxn1* in embryos (Liu et al., 2006; Nowell et al., under review). However, in the adult thymus, where *CCL25* plays a role in the proper recruitment of haematopoietic progenitors, its absence does not affect thymus size or output and its expression does not decrease with age (Gui et al., 2007; Zlotoff et al., 2010). It therefore appears that either, *CCL25* is not required in a *Foxn1*-dosage dependent manner to maintain thymic output, at least in 6-7 month old thymi, or that the *CCL25*-producing TEC population is not affected during the early involution process.

Next, the levels of the TEC-expressed fibroblast growth factor receptor, *FgfR2IIIb*, were analysed. Thymi from transgenic mice that express a dominant negative form of *FgfR2IIIb* in their TE display the hallmarks of thymus involution, including reduced total cellularity, disorganised epithelial architecture and reduction in UEA1 expression (Dooley et al., 2007). *FgfR2IIIb* expression in total TECs decreased by a quarter in 6-7 month old control TECs compared to 2 month old WT TECs. Following maintained over-expression of *Foxn1*, 6-7 month old TECs expressed *FgfR2IIIb* at over 1.5-fold and 2-fold higher levels compared to 2 month WT and 6-7 month control TECs respectively.

Collectively, these gene expression level data demonstrate that over-expression of *Foxn1* in 6-7 month old TEC results in a “younger” gene expression profile which may explain the increase in functional TEC phenotype (MHC Class II<sup>hi</sup>) and resultant increase in thymic output.

Lastly, the cellular mechanism through which *Foxn1* exerts its function in this instance was investigated. In the *Foxn1*<sup>LacZ/LacZ</sup> thymus, where involution occurs prematurely, proliferation was significantly decreased in thymic stromal cells compared to the WT thymus (Chen et al., 2009). Thus, TEC proliferation was investigated here by BrdU analysis. Seven month old Cre control and CAG-*Foxn1*ER mice that had been treated with Tamoxifen for 3 months were treated with BrdU for 3 days and analysed. A higher proportion of total TECs from CAG-*Foxn1*ER thymi incorporated BrdU in this time frame compared to Cre control thymi (17.6% versus 12.4% respectively) (Figure 5.7b). Comparatively, approximately 20% of 4 week old Cre control TECs are proliferating (Chen et al., 2009; Gray et al., 2006). This



suggests that Foxn1 over-expression may promote or maintain proliferation of TECs that would, in contrast, normally decrease with involution. This offers an explanation for the higher number of TECs and thymic output observed in these thymi. This analysis is currently brief and cannot exclude other factors such as apoptosis or preferential changes in proliferation in TEC sub-populations, playing a role and thus further analysis is required.

#### **5.4 Discussion**

The data presented in this Chapter establish that thymic involution can be prevented by forced maintenance of a single transcription factor, Foxn1. Thymi that maintained Foxn1 expression in all TECs were overtly larger and contained significantly more T cells than age-matched controls, and were comparable to thymi at the start of involution, on the basis of the parameters measured herein. 6-7 month old CAG-Foxn1ER +Tam thymi and 3-4 month old Cre control thymi contained a comparable number of T cells in the major populations, CD4<sup>+</sup> SP, CD8<sup>+</sup> SP and CD4<sup>+</sup>CD8<sup>+</sup> DP. Additionally, there were more approximately 1.5-fold more total intrathymic precursor TN cells in 6-7 month old CAG-Foxn1ER +Tam thymi than in age-matched control thymi. The TN population normally decreases with involution – their total number at 9 months is less than half that at 2 months (Heng et al., 2005) – but maintained Foxn1 expression prevented this decrease from occurring.

The higher number of total intrathymic TN cells in CAG-Foxn1ER +Tam mice, compared to all the aged-matched controls, resulted from a higher number of cells across all four TN populations. An increase in all four TN population cell numbers was also observed in a sex steroid ablation model of thymic regeneration (Heng et al., 2005). Importantly, however, further analysis is required with regard to the highly heterogenous TN1 population. For example, c-kit and Flt3 phenotyping will be used to further resolve the TN1 population and investigate whether an increase in ETP cell number is observed following up-regulation of Foxn1 expression (Allman et al., 2003; Godfrey et al., 1992)

The maintained thymic output in 6-7 month old CAG-Foxn1ER +Tam mice compared to age-matched controls is most likely a result of the greater cellularity and functionality of TEC compartment. Over-expression of Foxn1 maintained the size of the TEC compartment at the level observed at the onset of involution, which was approximately 1.5-fold larger than 6-7 month old controls. BrdU analysis demonstrated that there were more proliferating TECs in CAG-Foxn1ER +Tam thymi compared to age-matched controls, although the extent of TEC proliferation was not determined for the 3-4 month old thymus as a comparison.

Furthermore, forced Foxn1 expression maintained the levels of the key functional marker, MHC Class II. Additionally, these TECs expressed a number of genes known to regulate TEC development and function at higher levels than age-matched control TECs.

How does the expression of a single transcription factor prevent thymus involution? It is known that Foxn1 expression decreases with age (see Chapter 3) and that premature reduction or loss of Foxn1 expression in the postnatal thymus results in premature involution (Chen et al., 2009; Cheng et al., 2010; Corbeaux et al., 2010; Sun et al., 2010). This suggests that Foxn1 may be a target, primary or otherwise, of thymic involution. Additionally, it is likely that the age-related decline in Foxn1 expression in the postnatal thymus results in the decrease in the size and functionality of the TEC compartment, which leads to a reduction in T cell development and thymic output. Evidence increasingly suggests that Foxn1 is the master regulator of the TEC programme; as described in a Foxn1 allelic series where Foxn1, almost universally, regulates TEC lineage progression and TEC gene expression during thymus organogenesis (Nowell et al., under review). Thus, Foxn1 is able to prevent thymus involution when its expression is maintained, due to its role in the maintenance of the postnatal thymic microenvironment and its role as the proposed master regulator of the normal TEC programme including modulation of TEC phenotype, function and proliferation.

It is pertinent to make a note of the effect of ER at this point. It was shown that the Foxn1ER fusion protein was transcriptionally comparable to wildtype Foxn1 *in vitro*, and that Foxn1 over-expression resulted in Foxn1 cell-type specific phenotypes in both the thymus and hair (described in this Chapter). However, this does not absolutely exclude the possibility that these phenotypes were caused by the effect of ER on Foxn1 function. To address this, I have generated a R26-CAG-STOP-Foxn1 transgenic mouse line, on which all analyses performed herein will be repeated in the future.

Finally, the data presented show for the first time that thymus involution can be prevented by the maintenance of Foxn1 expression relative to wildtype at the onset of involution. While other reports show, using a number of approaches, that the aged thymus can be regenerated, this is one of the first reports to describe the prevention of thymus involution.

## Chapter 6: Reversal of involution after up-regulation of Foxn1 in the aged thymus

---

### 6.1 Introduction

The previous Chapter described the prevention of thymus involution through the maintenance of Foxn1 expression in the thymic epithelium from the onset of involution constitutes the one of the first report of this nature. In contrast, numerous approaches have been utilized to increase thymic output in compromised or aged thymi, or following HSCTs, in rats, mice and humans. These include IL-7, KGF and IGF-1 treatment protocols and ablation of sex steroid signalling, such as via chemical castration in mice or humans (Goldberg et al., 2007). In most instances, the increase in thymic output was accounted for by an increase in size and organisation of the TEC compartment. Thus, I utilised the CAG-Foxn1ER mice to test the effect of up-regulation of Foxn1 expression on thymus regeneration and output, in aged mice.

### 6.2 Experimental strategy

#### 6.2.1 Experimental mice

All experiments in this Chapter were performed on male mice. Aged  $R26^{CAG-Foxn1ER/+}$ ;  $Foxn1^{Cre/+}$  (CAG-Foxn1ER) mice were treated with Tamoxifen to induce Foxn1 activity and then assayed for thymic output. In the first set of experiments, 12 month old mice were treated with Tamoxifen (+Tam) for two weeks by repeated IP injection every 2 days. This two week period was thought to be sufficient to assay for an effect of Foxn1 as it spanned the estimated turnover time for TECs of 10-14 days in the homeostatic thymus, and, as in thymic rebound experiments, thymus cellularity was restored from 2 weeks following castration (Gray et al., 2006; Sutherland et al., 2005). Additionally, because the TEC compartment and thymic function was restored upon castration of mice as old as 2 years old (Sutherland et al., 2005), a second set of experiments in older mice was performed. A limited number of 18 month old mice were available for analysis within the timeframe of this thesis. These mice were treated with a single dose of Tamoxifen by IP injection and then maintained on Tamoxifen in their drinking water for one month, as a more convenient means of drug administration.

## 6.2.2 Control mice

Littermate control mice for the 12 month experiments were as described in Chapter 5. In brief, there were three control conditions: (1) Cre control mice ( $R26^{+/+};Foxn1^{Cre/+}$ ) treated with carrier only (-Tam), (2) Cre control mice treated with Tamoxifen (+Tam) and, (3) CAG-Foxn1ER mice treated with carrier only – these mice establish the effect of Foxn1ER induction/activity in the absence of Tamoxifen. For experiments in 18 month old mice, the only control condition that was analysed was ‘Cre control +Tam’ due to the limited number of mice at this age.

Tamoxifen or carrier treatments for each age group were the same as described above for the experimental mice: repeat IP injections over two weeks, and a single IP injection followed by drinking water treatment, for 12 and 18 month old mice respectively.

## 6.3 Results

### 6.3.1 Thymus size

As an overt test of the effect of Foxn1 up-regulation in aged mice, I first analysed thymus size. Thymi from 12 month old CAG-Foxn1ER +Tam mice, that had been treated with Tamoxifen for 2 weeks to induce Foxn1ER, were markedly larger than thymi from Cre control +Tam mice that were also treated with Tamoxifen (Figure 6.1a). Furthermore, CAG-Foxn1ER thymi +Tam thymi were larger than CAG-Foxn1ER –Tam, indicating the specific, Tamoxifen-inducible effect of Foxn1ER, and also slightly larger than Cre control –Tam thymi (Figure 6.1a).

Notably, the comparison between Cre control –Tam thymi and Cre control +Tam thymi showed an effect of Tamoxifen on overt thymus size in this experiment; 12 month old Cre control –Tam thymi were markedly larger than 12 month old Cre control +Tam thymi. The effect of Tamoxifen on overt thymus size indicates that the correct comparison to determine the effect of up-regulation of Foxn1 in aged thymi is between CAG-Foxn1ER and Cre control mice treated with Tamoxifen.

The increase in thymus size, under comparable experimental conditions, was also observed in older mice. Thymi from 18 month old CAG-Foxn1ER +Tam mice that had been treated with Tamoxifen for one month, were also markedly overtly larger than Cre control +Tam thymi (Figure 6.1b). Thus, the up-regulation of a single transcription factor, Foxn1, in the

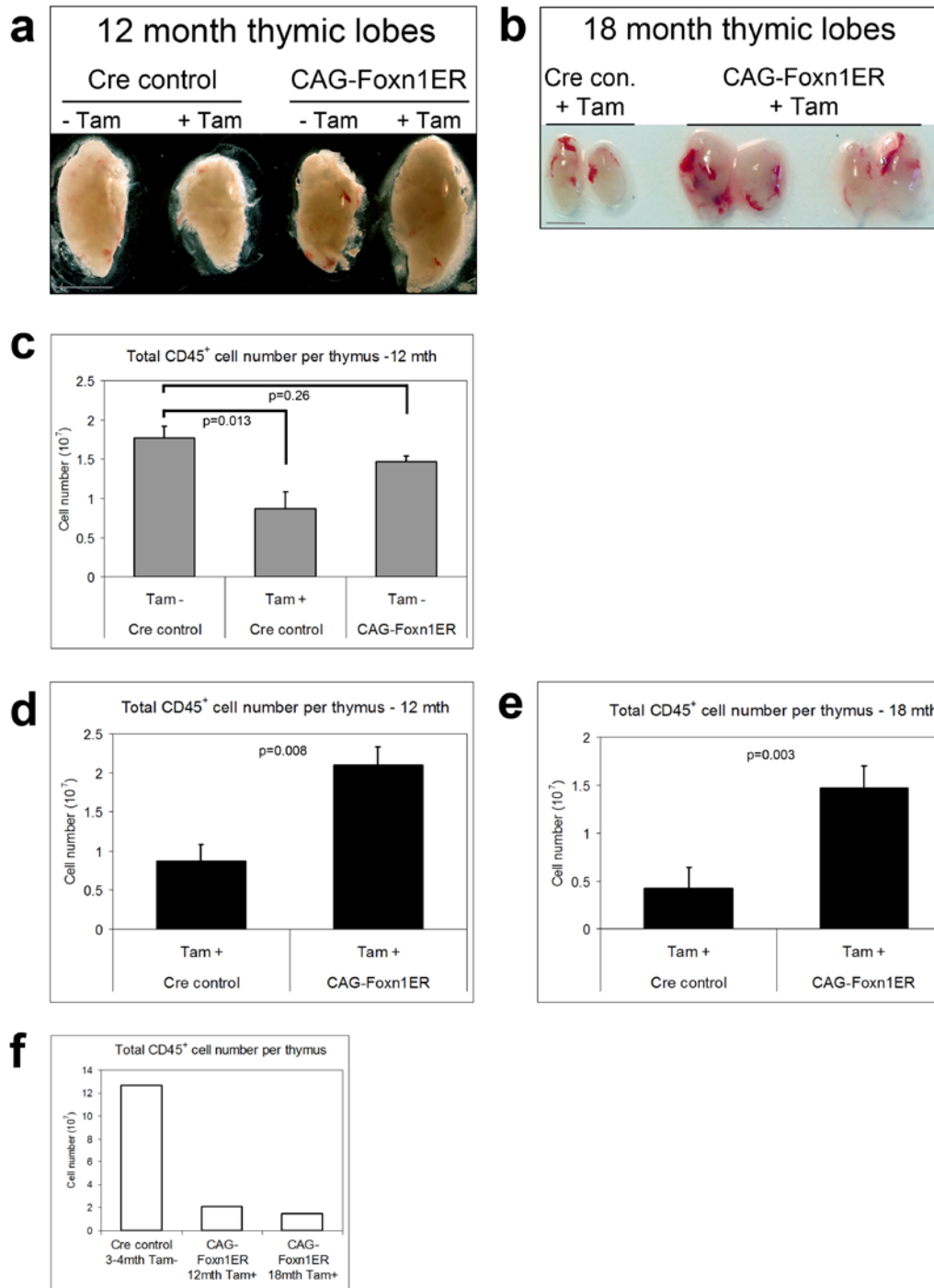


**Figure 6.1** Thymus size and cellularity increase following up-regulation of Foxn1 in aged mice.

**Figure 6.1 Thymus size and cellularity increase following up-regulation of Foxn1 in aged mice.**

**(a, b)** 12 or 18 month thymi that up-regulated Foxn1 (CAG-Foxn1ER +Tam) were overtly larger than littermate control thymi. Image shows single thymus lobes from 12 month old mice and both thymus lobes from 18 month old mice. Images are representative of four and three independent experiments, for 12 and 18 month old mice respectively. Scale bar represent 2.5mm **(c)** Total intrathymic CD45<sup>+</sup> cells numbers for 12 month old control mice. Cre control -Tam thymi contained significantly more CD45<sup>+</sup> cells compared to Cre control +Tam thymi (n=4). Cre control -Tam thymi also contained more CD45<sup>+</sup> cells than CAG-Foxn1ER -Tam, although these differences were not significant (n=2). **(d)** 12 month and **(e)** 18 month old CAG-Foxn1ER +Tam thymi contained significantly more CD45<sup>+</sup> cells compared to Cre control +Tam thymi (n=4 and n=3, respectively). **(f)** Comparison of CD45<sup>+</sup> cellularity between 3-4 month old Cre control mice and 12 and 18 month old CAG-Foxn1ER +Tam thymic involution reversal mice.

---

thymic epithelium of 12 and 18 month old thymi resulted in an increase in overt thymus size, possibly indicating a partial reversal of thymus involution.

### **6.3.2 T cell numbers and composition**

To test whether the observed increase in total thymus size following Foxn1 up-regulation in aged thymi resulted from an increase in thymopoiesis, T cell numbers and composition were analysed.

Firstly, analysis of total intrathymic CD45<sup>+</sup> cell numbers revealed that 12 month old Cre control -Tam thymi contained approximately double the number of cells than Cre control +Tam thymi ( $1.77 \times 10^7 \pm 1.5 \times 10^6$  and  $8.7 \times 10^6 \pm 2.1 \times 10^6$  respectively, n=4, p=0.013) (Figure 6.1c). These data confirm the changes in overt thymus size observed above and show a suppressive effect of Tamoxifen on intrathymic hematopoietic cell number. The effect of Tamoxifen treatment on the wildtype thymus is poorly understood and is most likely the combined effect of a number of different modes of action, including anti-estrogenic, on different cell populations in the thymus. Thymic atrophy and a reduction in T cell number have been reported following Tamoxifen treatment (Luster et al., 1984; Uhmman et al., 2007). Thus, the applicable comparison, to account for the effect of Tamoxifen, is between Cre control +Tam and CAG-Foxn1ER +Tam experimental conditions.

Further analyses of the control mice showed that the number of CD45<sup>+</sup> cells in 12 month old Cre control -Tam and CAG-Foxn1ER -Tam thymi was not significantly different ( $1.77 \times 10^7 \pm 1.5 \times 10^6$  and  $1.47 \times 10^7 \pm 7.0 \times 10^5$ , n=4 and n=2 respectively, p=0.26) (Figure 6.1c). These data show that there is no apparent effect of induction of Foxn1ER on intrathymic CD45<sup>+</sup> cell number in the absence of Tamoxifen.

The comparison of the CD45<sup>+</sup> cell number in thymi from 12 month old CAG-Foxn1ER +Tam and Cre control +Tam mice showed a greater than 2-fold increase following the up-regulation of Foxn1 ( $2.1 \times 10^7 \pm 2.3 \times 10^6$  and  $8.7 \times 10^6 \pm 2.1 \times 10^6$  respectively, n=4, p=0.008) (Figure 6.1d). Similarly, thymi from 18 month old mice that were treated with Tamoxifen for one month contained over 3-fold more CD45<sup>+</sup> cells in CAG-Foxn1ER +Tam compared to Cre control +Tam conditions ( $1.47 \times 10^7 \pm 1.4 \times 10^6$  and  $4.3 \times 10^6 \pm 7.5 \times 10^5$  respectively, n=3, p=0.003) (Figure 6.1e) These data establish that up-regulation of Foxn1 in aged thymi results in an increase in the number of thymocytes compared to the relevant controls.

In these experiments, I have established that age-related thymic involution was partially reversed, as determined by a greater than 2-fold increase in the number of intrathymic hematopoietic cells in CAG-Foxn1ER +Tam compared to Cre control +Tam thymi. Previous studies have shown that thymic involution reversal or rebound varies depending on the approach utilised. For example, in castration models, the thymus cellularity in 2 year old mice was restored to 2 month old levels following castration, while in KGF treatment models, 18 month old mice treated with KGF for two weeks showed a more modest 3-fold increase in thymus cellularity (Alpdogan et al., 2006; Sutherland et al., 2005). The relative increase in thymus cellularity observed following up-regulation of Foxn1 was more in line with KGF treatment recovery levels, as thymus cellularity did not recover to the levels seen in 3-4 month old mice (Figure 6.1f).

### **6.3.2.1 CD4/CD8 T cell analysis**

To test whether the observed increase in thymocyte number reflected a proportional increase in thymocyte subsets, I next analysed CD4/CD8 cell numbers and distribution. The proportions and numbers for the four CD4/CD8 T cell sub-populations (DN, DP and SP) were investigated in 12 month old mice that had been treated with Tamoxifen or carrier for two weeks. The CD4/CD8 subset distribution was comparable within the Tamoxifen treatment conditions but differed between +Tam and -Tam conditions (Figure 6.2a). There was a higher proportion of CD4<sup>+</sup>CD8<sup>-</sup> DN cells (approximately double), and corresponding small decreases in the three other populations, in both CAG-Foxn1ER and Cre control +Tam thymi compared to -Tam conditions.

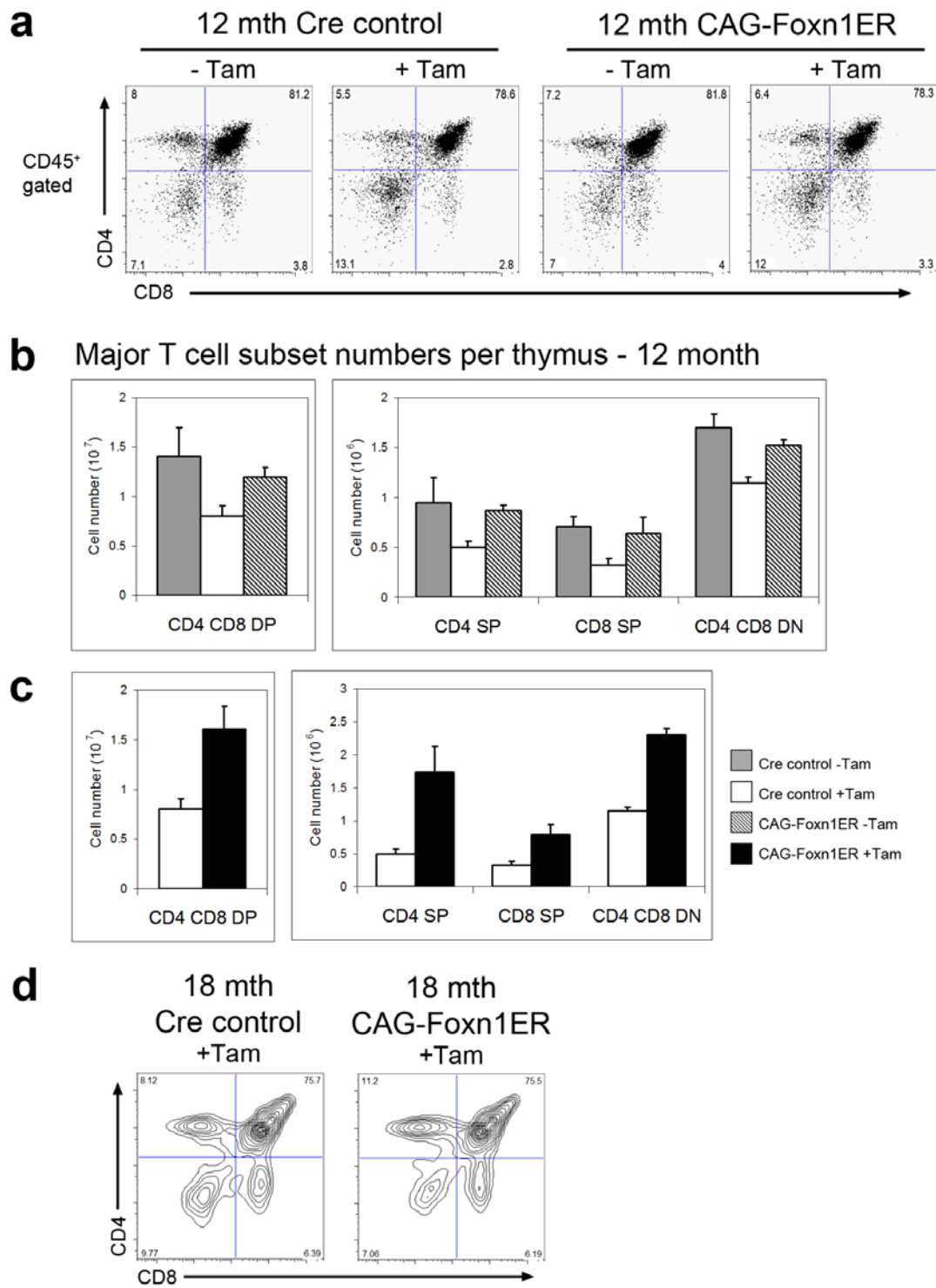


**Figure 6.2 Major T cell subset proportions and numbers following up-regulation of Foxn1 in aged thymi.**

Four major T cell subsets (CD4<sup>+</sup>CD8<sup>+</sup> double positive (DP), CD4<sup>+</sup> or CD8<sup>+</sup> single positive (SP) and CD4<sup>-</sup>CD8<sup>-</sup> double negative (DN)) were examined in 12 and 18 month old thymi following up-regulation of Foxn1 expression compared to controls. **(a, d)** Flow cytometric analysis on CD45<sup>+</sup> gated thymocytes with  $\alpha$ -CD4 and  $\alpha$ -CD8 for 12 and 18 month old thymi. **(b, c)** Absolute cell numbers for the four CD4/CD8 subsets for 12 month old mice (n=2).



The CD4/CD8 subset distributions in thymi from 18 month old CAG-Foxn1ER and Cre control +Tam mice were also investigated. Again, the proportions were comparable with a small increase in CD4<sup>+</sup> SP proportion (approximately 3%) in CAG-Foxn1ER +Tam compared to Cre control +Tam (Figure 6.2d). Unfortunately, a limited number of aged mice meant that this experiment was only performed once, and thus needs to be repeated to verify these differences.

Next, the absolute numbers of DN, DP and SP cells per thymus were determined in 12 month old mice. Because Tamoxifen affected both the total number of CD45<sup>+</sup> cells and the CD4/CD8 subset proportions, the comparison that is relevant here is between CAG-Foxn1ER +Tam and Cre control +Tam thymi (Figure 6.2c); although the cell numbers for all control conditions are shown (Figure 6.2b).

Firstly, CAG-Foxn1ER +Tam thymi contained double the number of CD4<sup>+</sup>CD8<sup>+</sup> DP cells to that found in Cre control +Tam thymi ( $1.6 \times 10^7 \pm 2.3 \times 10^6$  and  $8.0 \times 10^6 \pm 1.0 \times 10^6$  respectively,  $p=0.086$ ,  $n=2$ ) (Figure 6.2c). Also, CAG-Foxn1ER +Tam thymi contained more CD4<sup>+</sup> SP and CD8<sup>+</sup> SP cells than Cre control +Tam thymi, with over 3-fold more CD4<sup>+</sup> SP cells ( $1.73 \times 10^6 \pm 4.0 \times 10^5$  and  $5.0 \times 10^5 \pm 6.4 \times 10^4$  respectively,  $p=0.094$ ,  $n=2$ ) and over 2-fold more CD8<sup>+</sup> SP cells ( $7.9 \times 10^5 \pm 1.5 \times 10^5$  and  $3.2 \times 10^5 \pm 6.3 \times 10^4$  respectively,  $p=0.10$ ,  $n=2$ ) (Figure 6.2c). Lastly, there were significantly more CD4<sup>-</sup>CD8<sup>-</sup> DN cells in CAG-Foxn1ER +Tam thymi compared to Cre control +Tam thymi ( $2.3 \times 10^6 \pm 1.0 \times 10^5$  and  $1.15 \times 10^6 \pm 6.0 \times 10^4$  respectively,  $p=0.01$ ,  $n=2$ ) (Figure 6.2c). Therefore, although the statistical analyses were restricted due to the limited number of aged mice available for biological repeats, these data show that up-regulation of Foxn1 in aged thymi resulted in an increase in the absolute number of all the major T cell subsets per thymus when Tamoxifen treated conditions were compared.

### 6.3.2.2 Triple negative cell analysis

To further investigate the observed increase in the DN T cell numbers, the immature triple negative (TN, CD3<sup>-</sup>CD4<sup>-</sup>CD8<sup>-</sup>) population was examined in 12 month old mice that had been treated with Tamoxifen or carrier for 2 weeks. Firstly, the proportions of the four TN populations were determined. For the control conditions, Cre control -Tam and CAG-Foxn1ER -Tam showed comparable distributions across the four sub-populations (Figure 6.3a,b). Again, an effect of Tamoxifen treatment was observed as Cre control +Tam thymi showed distinct differences compared to the other control thymi. There was a greater than

two-fold increase in the TN1 proportion and a markedly lower TN3 proportion in Cre control +Tam thymi compared to the other control thymi (Figure 6.3a,b). Up-regulation of Foxn1 in CAG-Foxn1ER +Tam thymi restored the aberrant TN1 and TN3 proportions observed following Tamoxifen treatment to near –Tam control levels (Figure 6.3a,b).

Next, the absolute numbers of cells within the TN populations per thymus were determined. CAG-Foxn1ER +Tam thymi contained more total TN cells than control thymi, with over two-fold more cells in CAG-Foxn1ER +Tam thymi compared to Cre control +Tam thymi ( $2.02 \times 10^6 \pm 4.0 \times 10^5$  and  $8.1 \times 10^5 \pm 3.0 \times 10^5$  respectively,  $p=0.073$ ,  $n=3$ ) (Figure 6.3c).

Analyses of the cell numbers within each of the four TN cell subsets in control thymi showed an effect of Tamoxifen; Cre control +Tam thymi contained markedly more TN1 cells and less TN2, TN3 and TN4 cells than Cre control –Tam thymi (Figure 6.3d).

Cre control +Tam thymi contained a high number of TN1 cells and low number of TN2 cells compared to Cre control –Tam thymi. This corroborated the elevated proportion of TN1 cells observed above and was suggestive of a TN1-TN2 block (Figure 6.3d). This block was overcome following up-regulation of Foxn1 in CAG-Foxn1ER +Tam thymi; there was a reduction in the TN1 proportion and significantly more TN2 cells in CAG-Foxn1ER +Tam thymi compared to Cre control +Tam thymi ( $1.42 \times 10^5 \pm 1.0 \times 10^4$  and  $2.6 \times 10^4 \pm 1.0 \times 10^4$  respectively,  $p=0.015$ ,  $n=2$ ) (Figure 6.3e). This TN1-TN2 block was also observed during the experiments described in Chapter 5, although to a lesser degree, and further implicates Foxn1 in the mediation of the TN1-TN2 transition, possibly through regulation of Notch signalling component, Dll4 (Koch et al., 2008; Nowell et al., under review). Additionally, there were greater than two-fold more TN3 and TN4 cells in CAG-Foxn1ER +Tam thymi than in Cre control +Tam (TN3,  $6.34 \times 10^5 \pm 1.9 \times 10^5$  versus  $1.64 \times 10^5 \pm 9.0 \times 10^4$  respectively,  $p=0.15$ ,  $n=2$  and TN4,  $9.73 \times 10^5 \pm 2.7 \times 10^5$  versus  $3.6 \times 10^5 \pm 8.0 \times 10^4$  respectively,  $p=0.16$ ,  $n=2$ ) (Figure 6.3e). These data establish that up-regulation of Foxn1 in aged thymi results in an increase in the size of the TN compartment, which is consistent with a reversal in thymus involution and activity.

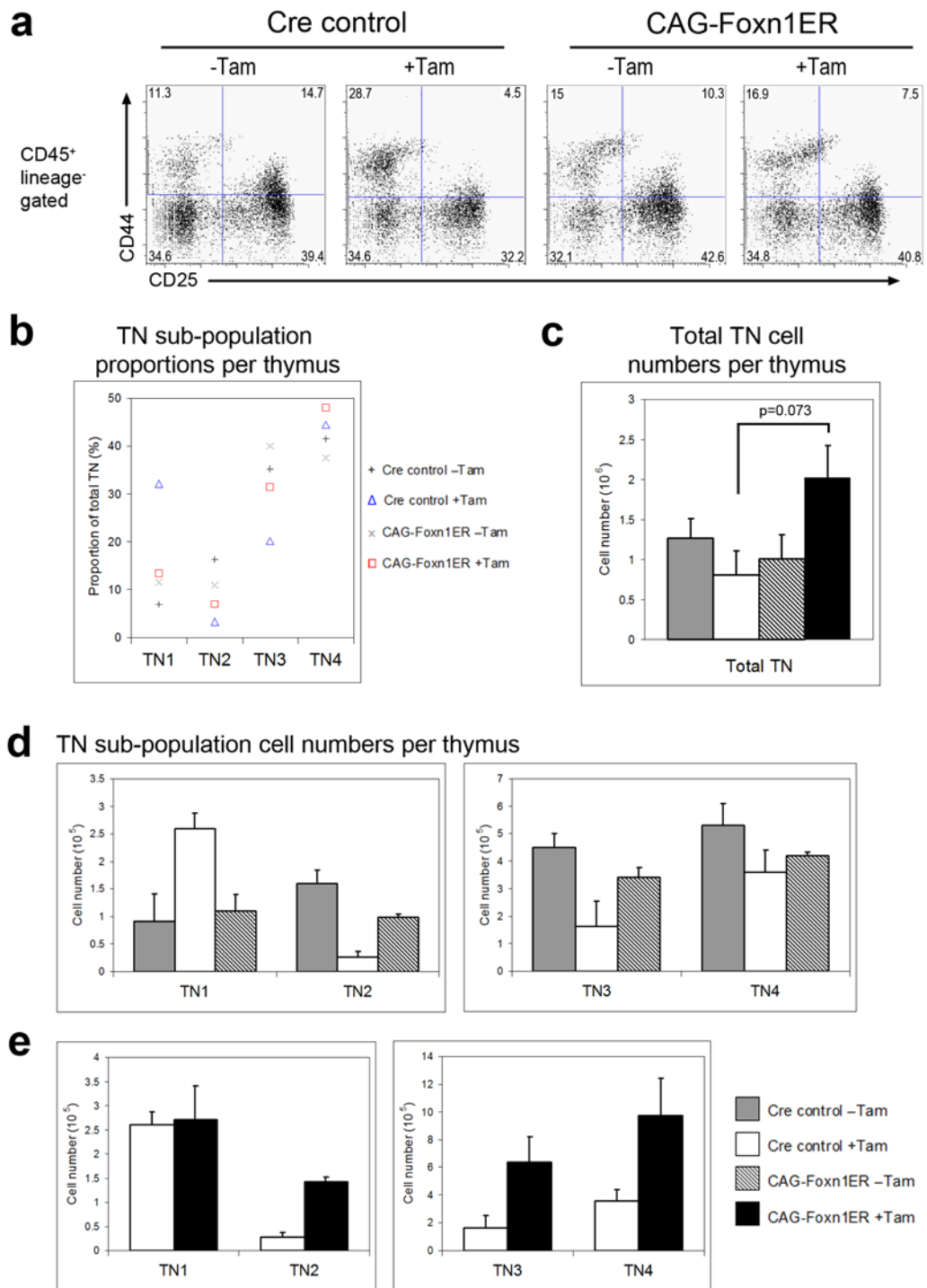


**Figure 6.3 Triple negative (TN) cell proportions and numbers following Foxn1 up-regulation in aged thymi.**

**(a)** Flow cytometric analysis of TN cells ( $CD45^+lin^-$  (lineage = CD3, CD4, CD8, CD11b, CD11c, CD19, NK1.1, Gr-1)) from 12 month thymi with  $\alpha$ -CD25 and  $\alpha$ -CD44. **(b)** The average TN sub-population proportions per thymus were determined for all experimental conditions ( $n=2$ ). **(c)** The average total TN cell numbers per thymus for 12 month old CAG-Foxn1ER compared to control thymi ( $n=3$ ). **(d)** The average TN sub-population cell numbers per thymus for Cre control +/-Tam and CAG-Foxn1ER -Tam control conditions ( $n=2$ ). **(e)** The average TN sub-population cell numbers per thymus for Cre control +Tam and CAG-Foxn1ER +Tam conditions ( $n=2$ ).

### 6.3.3 Total nuclear Foxn1 expression in aged TECs

To confirm that the epithelium in aged CAG-Foxn1ER +Tam thymi expressed higher levels of Foxn1 compared to controls, Foxn1 protein expression was analysed. It was shown that total *Foxn1* mRNA (endogenous plus Foxn1ER) levels were greater than ten-fold higher in postnatal TECs from CAG-Foxn1ER mice compared to Cre control mice, and that Foxn1ER protein was inducible by Tamoxifen treatment (Figures 4.8, 4.9, 5.1). To augment these data, immunohistochemistry for Foxn1, without any signal amplification, was performed to confirm that TECs from 12 month old CAG-Foxn1ER +Tam thymi expressed higher levels of Foxn1 than control thymi. While this analysis cannot differentiate between endogenous Foxn1 and transgenic Foxn1ER, it provides a comparative indication of the level of total nuclear Foxn1 across the experimental conditions. Western blot analysis, which does differentiate between Foxn1 and Foxn1ER by size, was attempted, but was unsuccessful due to the inability in obtaining sufficient TEC samples from aged thymi. Nonetheless, it was evident that Foxn1 was expressed at higher levels in some cells and in a greater number of TECs in 12 month old CAG-Foxn1ER +Tam TECs compared to Cre control TECs (+Tam or -Tam) (Figure 6.4d and 6.4a,b respectively). Furthermore, there was more nuclear Foxn1 expression in TECs in CAG-Foxn1ER +Tam thymi compared to CAG-Foxn1ER -Tam thymi (Figure 6.4d and 6.4c respectively). Thus, Tamoxifen treatment in aged CAG-Foxn1ER +Tam mice resulted in higher total nuclear Foxn1 expression levels in TECs compared to all control conditions.

A technical issue that must be highlighted here is the detection of hrGFP, translated from the transgenic Foxn1ER-IRES-hrGFP bicistronic mRNA. Although hrGFP expression was detected during flow cytometric assays of CAG-Foxn1ER TECs (Figure 4.8), it could not be detected in immunohistochemical assays. The signal shown in the goat isotype control image was from a CAG-Foxn1ER sample, and spanned the detection spectrum for GFP (Figure 6.4). The absence of GFP signal may be as a result of low levels of hrGFP expression that were not detectable by immunohistochemistry, possibly due to the IRES-dependent translation, or because the IHC processing procedures used for the relevant antibodies here were not optimal for hrGFP detection. An  $\alpha$ -hrGFP antibody was used in an attempt to detect hrGFP expression, but this was unsuccessful.

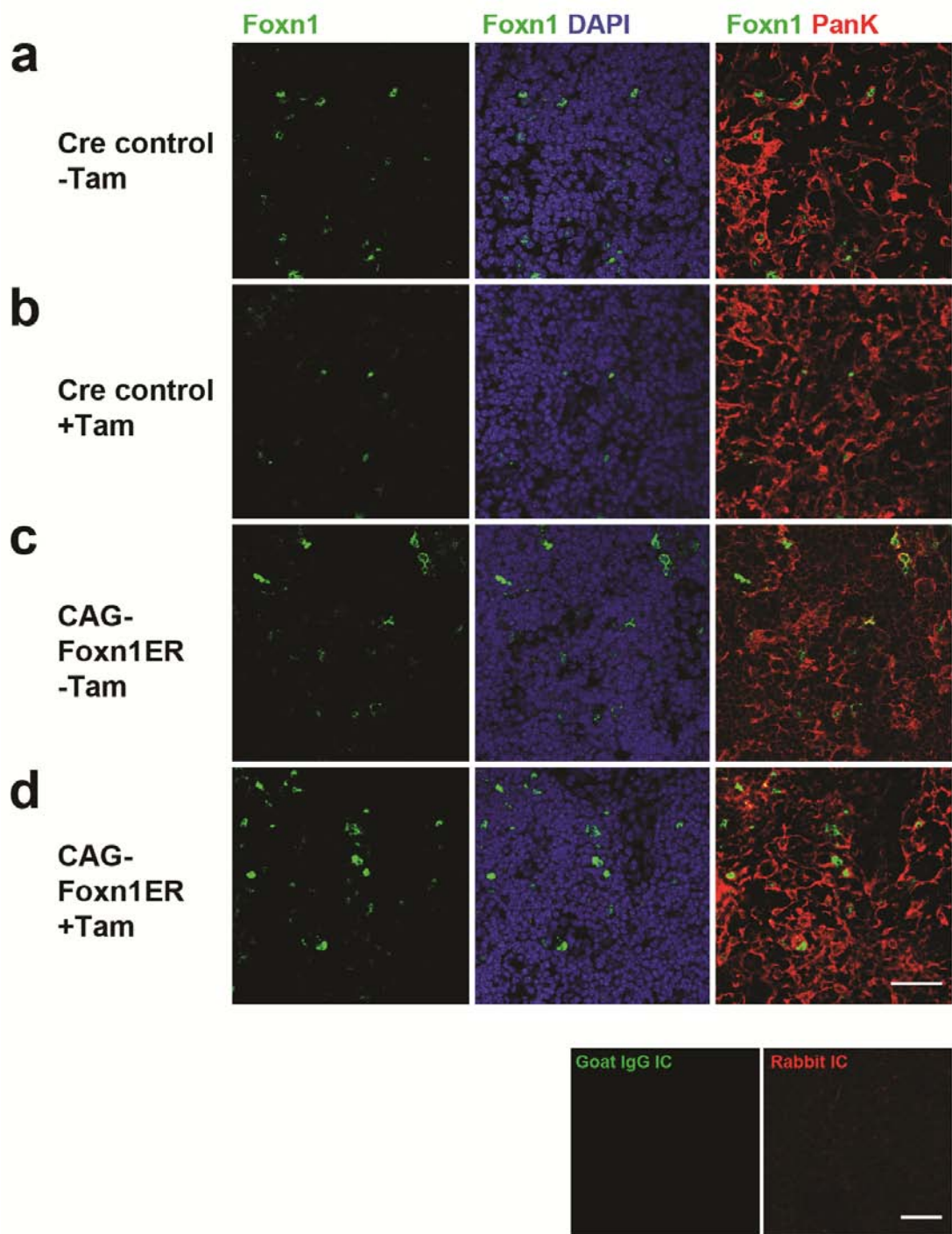


**Figure 6.4 Foxn1 expression in 12 month old CAG-Foxn1ER and control thymi.** Immunohistochemical analysis showing total  $\alpha$ -Foxn1 staining (endogenous and Foxn1ER, green) in TECs (pancytokeratin (PanK) positive, red) in 12 month old thymic sections. **(a, b)** Foxn1 expression in Cre control thymi with and without Tamoxifen treatment. **(c)** Some Foxn1, presumably Foxn1ER, was present in the cytoplasm in CAG-Foxn1ER -Tam TECs. **(d)** Foxn1 is expressed in more TECs in CAG-Foxn1ER thymi TECs compared to controls. Scale bars represent 50 $\mu$ m.

#### **6.3.4 TEC architecture and phenotype**

The structure of the TEC compartment in the thymus deteriorates with age, including the disruption of the cortical and medullary junction (CMJ) and in some areas the loss of clearly demarcated cortical and medullary regions. To determine whether up-regulation of Foxn1 in aged thymi restored the thymic architecture to a “younger” status, immunohistochemical assays using antibodies that broadly demarcate the cortical and medullary compartments, were performed. CDR1 and Keratin 5 (K5) antibodies that broadly identify cTECs and mTECs respectively were used here.

In a younger Cre control –Tam thymus (6 months old) the cortical and medullary regions were well defined and generally did not overlap (Figure 6.5e). As expected, the TEC compartment in a 12 month old Cre control –Tam thymus was generally more disorganised. This included co-expression of K5 and CDR1, especially at the CMJ, larger areas of K5<sup>+</sup> TECs in the cortical regions (indicated with asterisks in Figure 6.5) and the loss of the extended epithelial network in some regions (Figure 6.5a). CAG-Foxn1ER –Tam thymi and Cre control +Tam thymi exhibited a similar phenotype, with a further decrease in medullary areas observed in the latter condition (Figure 6.5b,c). In contrast, following up-regulation of Foxn1 for 2 weeks in 12 month old thymi, the TEC architecture was restored and resembled the structure of a younger thymus with broadly well defined cortical and medullary compartments (Figure 6.5d).

Thymic epithelial architecture was also investigated in 18 month old mice. In Cre control +Tam thymi, the TEC compartment was more drastically disorganised with complete destruction of the CMJ in some regions and overlapping CDR1 and K5 expression (Figure 6.5f). Following Foxn1 up-regulation in CAG-Foxn1ER +Tam thymi, the TEC structure was restored with well defined cortex and medullary regions and a clearly demarcated CMJ (Figure 6.5g). These data establish that up-regulation of Foxn1 is able to restore the disorganised architecture of the TEC compartment in aged thymi. This is consistent with other models of reversal or rebound of thymus involution, such as castration, that also report restoration of TEC architecture (Sutherland et al., 2005).

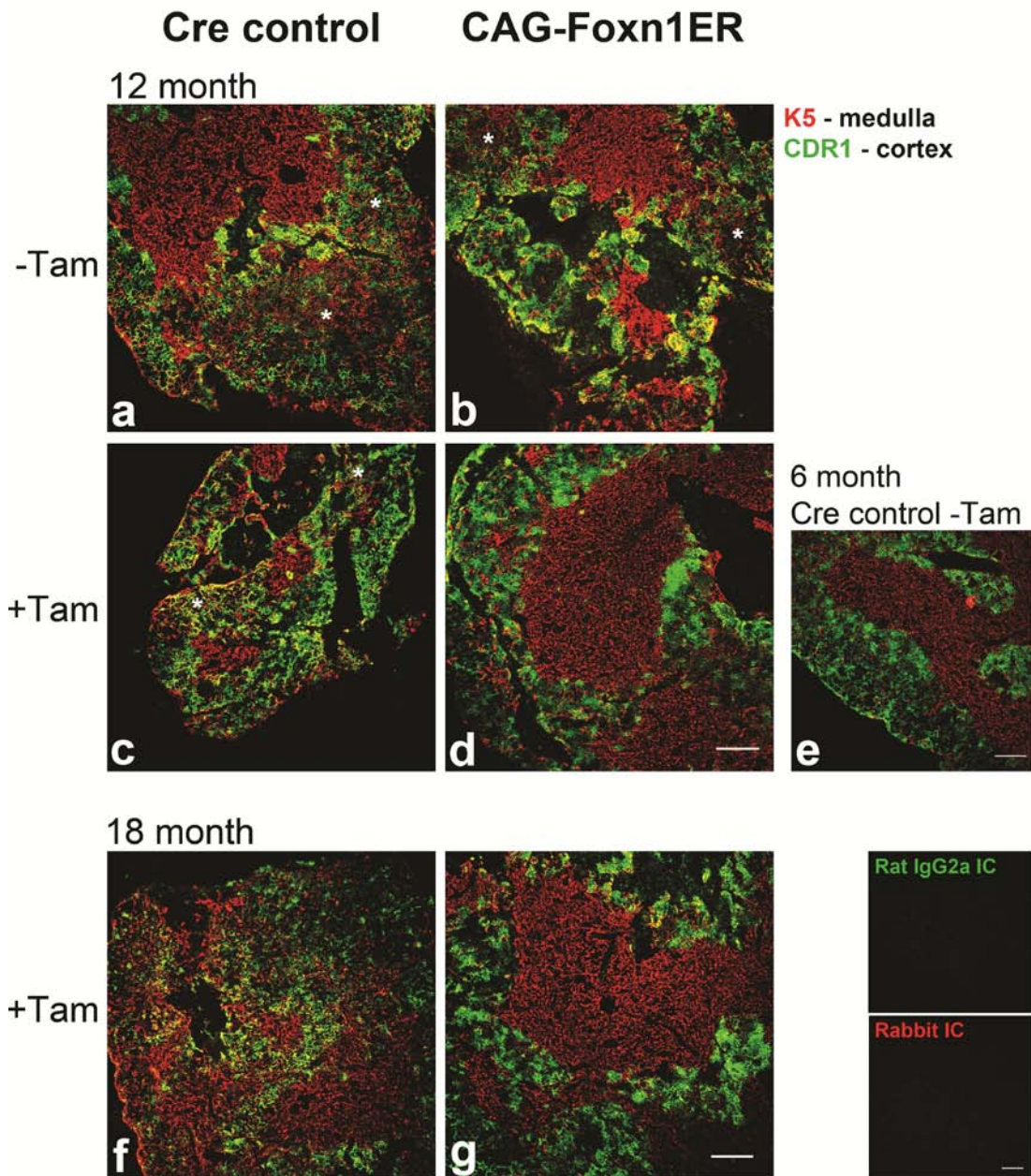


**Figure 6.5 Thymic epithelium architecture was restored following up-regulation of Foxn1 in aged thymi.**

Immunohistochemical analysis using  $\alpha$ -Keratin 5 (medulla, red) and  $\alpha$ -CDR1 (cortex, green) broadly show the architecture of the thymic epithelium. **(a, b, c)** 12 month old Cre control +/- Tam and CAG-Foxn1ER -Tam thymi had more disorganised epithelial architecture than CAG-Foxn1ER +Tam and 6 month old Cre control thymi **(d, e)**. Asterisks indicate regions of expanded K5 expression in the cortex. **(f)** The thymic epithelium in 18 month old Cre control +Tam thymi was more disorganised than in CAG-Foxn1ER +Tam thymi **(g)**. Scale bars represent 200 $\mu$ m.

Next, the observed changes in the TEC compartment of aged thymi following Foxn1 up-regulation were quantified by flow cytometry. Twelve month old CAG-Foxn1ER +Tam thymi contained more EpCAM<sup>+</sup> TECs compared to all controls ( $4.1 \times 10^4$  cells versus the control average of  $1.9 \times 10^4$ , n=2) (Figure 6.6a). Furthermore, within the expanded TEC compartment in 12 month old CAG-Foxn1ER +Tam thymi there was a higher proportion of UEA1<sup>+</sup> TECs compared to all controls (UEA1<sup>+</sup> proportions: Cre control –Tam, 31.1%; Cre control +Tam 12.5%; CAG-Foxn1ER –Tam, 31.2%; CAG-Foxn1ER +Tam, 52.8%; n=1) (Figure 6.6b). Cre control +Tam thymi contained a lower proportion of UEA1<sup>+</sup> TECs compared to Cre control –Tam and CAG-Foxn1ER –Tam thymi, possibly indicative of an effect of Tamoxifen on TECs (Figure 6.6b). Notably, CAG-Foxn1ER +Tam thymi contained a 4-fold higher proportion of UEA1<sup>+</sup> TECs than Cre control +Tam thymi. The flow cytometric data for UEA1 showed close correspondence to immunohistochemical analysis. Again, CAG-Foxn1ER +Tam thymi contained more UEA1<sup>+</sup> cells in the medulla with bright UEA1 clusters observed in the medulla that were drastically reduced in all control thymi (Figure 6.7a).

Similarly, in 18 month old CAG-Foxn1ER +Tam thymi, up-regulation of Foxn1 resulted in an increase in the proportion of UEA1<sup>+</sup> TECs compared to Cre control +Tam thymi (40.2% and 16.8% of total TECs respectively, n=1) (Figure 6.6c). Immunohistochemical analysis showed more bright UEA1<sup>+</sup> clusters in the medulla of CAG-Foxn1ER +Tam thymi compared to Cre control +Tam thymi (Figure 6.7b).

Lastly, the functional TEC cell marker, MHC Class II, was examined in 18 month old mice. CAG-Foxn1ER +Tam thymi contained a higher proportion of MHC Class II<sup>hi</sup> TECs than Cre control +Tam thymi indicating that up-regulation of Foxn1 resulted in a larger functional TEC compartment (36.5% and 22.3% of total TECs respectively, n=1) (Figure 6.6d).

Collectively, these data show that up-regulation of Foxn1 in aged thymi resulted in an increase in the proportions of UEA1<sup>+</sup> and MHC Class II<sup>hi</sup> TEC populations among all TECs. These changes in TEC phenotype may explain, at least in part, the increase in thymic output observed and further contribute to the set of data that establish Foxn1 up-regulation as a means of reversing thymus involution.



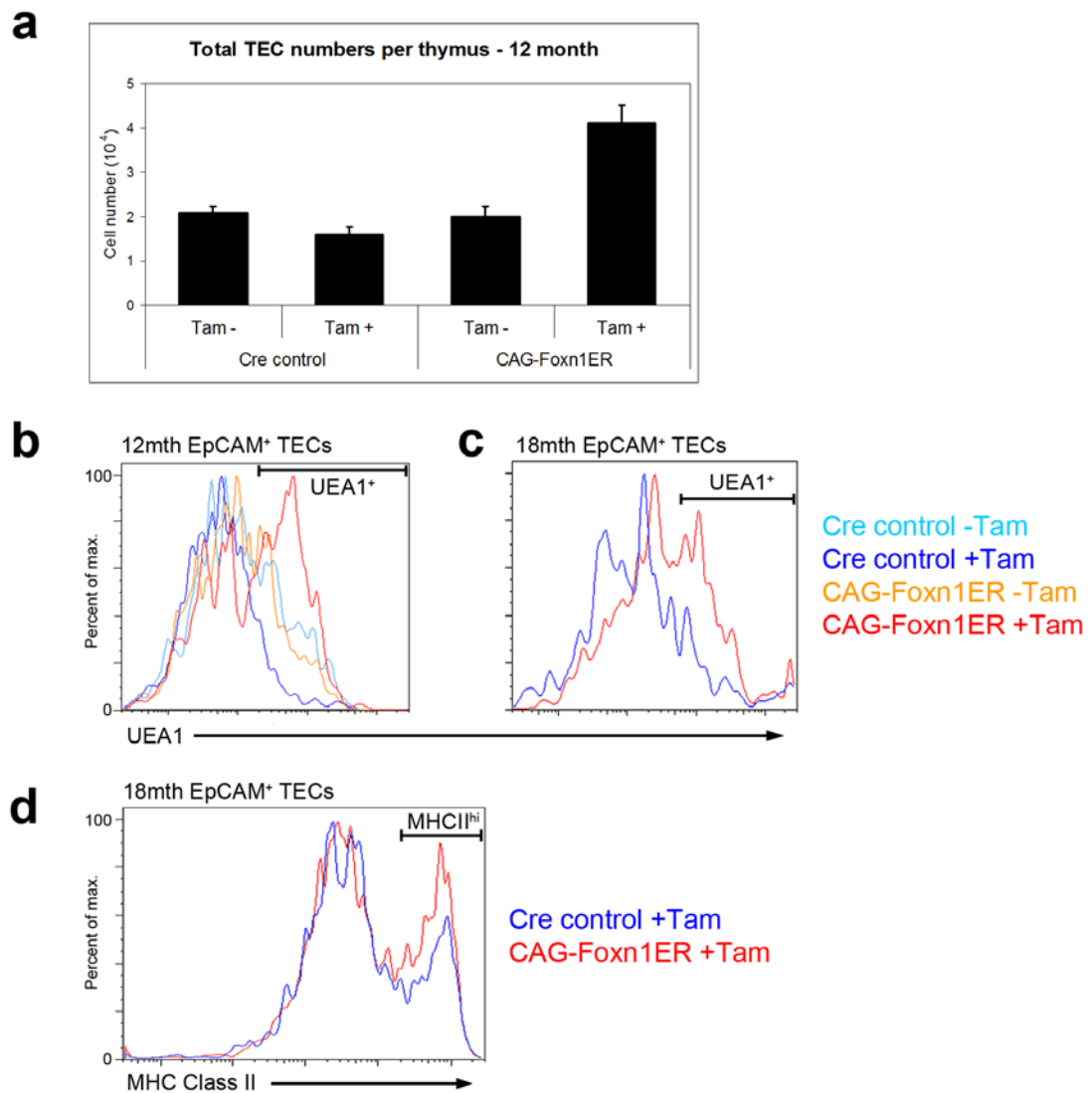


**Figure 6.6** Foxn1 up-regulation results in a larger and phenotypically “younger” TEC compartment in aged thymi.

(a) 12 month old CAG-Foxn1ER +Tam thymi contained more TECs than Cre control +/- and CAG-Foxn1ER -Tam (n=2). (b, c) Flow cytometric analysis, without thymocyte depletion, was performed on 12 and 18 month old thymi where total TECs were analysed using  $\alpha$ -EpCAM, after gating on CD45<sup>-</sup> and Ter119<sup>-</sup> cells. Histograms show UEA1 profiles; CAG-Foxn1ER +Tam thymi contained a higher proportion of UEA1<sup>+</sup> cells in the TEC compartment compared to controls. UEA1<sup>+</sup> gates were determined from FMO controls. (d) Histogram shows MHC Class II profiles for 18 month old Cre control and CAG-Foxn1ER +Tam TECs.

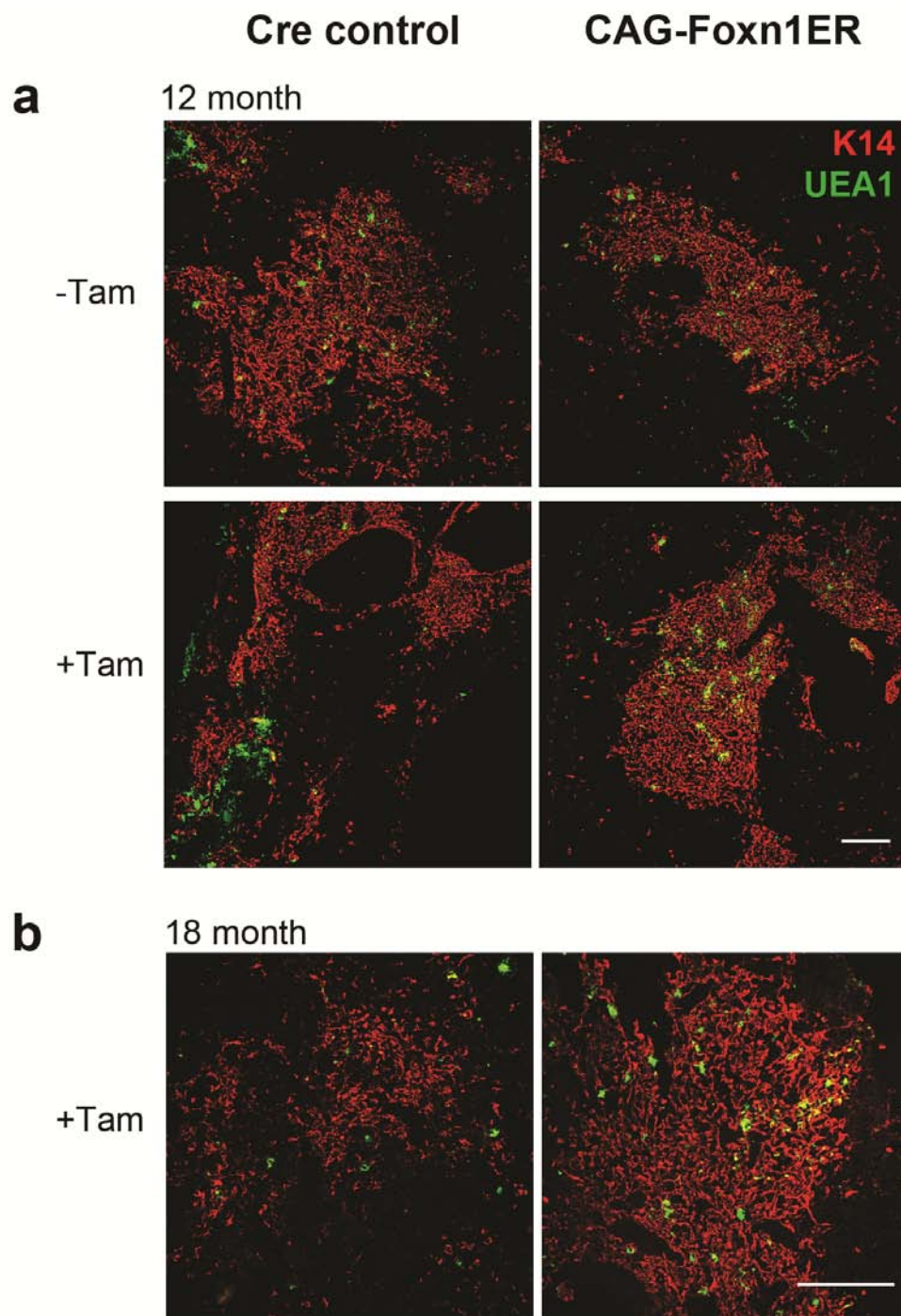


**Figure 6.7 Foxn1 up-regulation increased UEA1 expression in aged thymi.**  
**(a, b)** Immunohistochemical analysis showing staining for the lectin *Ulex europaeus* agglutinin I (UEA1) in the medulla ( $K14^+$  TECs) of 12 month and 18 month old thymi. CAG-Foxn1ER +Tam thymi contained more UEA1<sup>+</sup> TECs compared to all controls. Scale bars represent 200 $\mu$ m. The relevant isotype control for K14 (Rabbit IC) is shown in Figure 6.5.

The larger and architecturally restored TEC compartment observed following Foxn1 up-regulation in aged thymi could result from an effect of Foxn1 on proliferation, or from an effect on TEC maintenance or apoptosis, or a combination of these cellular processes. That the TEC compartment was double the size in CAG-Foxn1ER +Tam thymi compared to all control thymi, suggests that TEC proliferation may play a role, at least in part. It was previously shown that reduced or maintained Foxn1 expression during thymus involution resulted in a decrease or increase in TEC proliferation, respectively (Chen et al., 2009; Chapter 5). Therefore, proliferation was investigated in TECs in aged thymi by examining the TEC-specific proliferative potential marker, p63 (Senoo et al., 2007). The limited number of aged mice did not allow for additional proliferation analyses, for example with BrdU, to be performed.

Firstly, immunohistochemical analysis using an antibody that recognised all protein isoforms of p63 was performed. Twelve month old CAG-Foxn1ER +Tam thymi contained more TECs that expressed p63 compared to Cre control +Tam thymi, indicating that the TEC compartment was more actively proliferative following Foxn1 up-regulation (Figure 6.8a). The p63 expression was nuclear and confined to TECs (Figure 6.8a). The isoform of p63 that specifically marks proliferative potential in TECs is  $\Delta Np63$ , with its expression also shown to decrease following Wnt inhibition-mediated degeneration of the thymus (Osada et al., 2010; Senoo et al., 2007). CAG-Foxn1ER thymi contained more TECs that expressed  $\Delta Np63$  than Cre control +Tam thymi (Figure 6.8b). These  $\Delta Np63^+$  TECs were primarily in the medulla of the thymus (in agreement a previous report - Senoo et al., 2007) and, interestingly, most also co-expressed Keratin 8 (K8). K8, a pan-cortical marker, also marks a small population of mTECs that have a globular phenotype and express high levels of MHC Class II (Gray et al., 2006). Thus, as determined by the read-out of p63 expression, Foxn1 up-regulation resulted in an increase in proliferating TECs and/or TECs with proliferative potential in aged thymi, providing an explanation, at least in part, for the Foxn1-driven process of involution reversal.

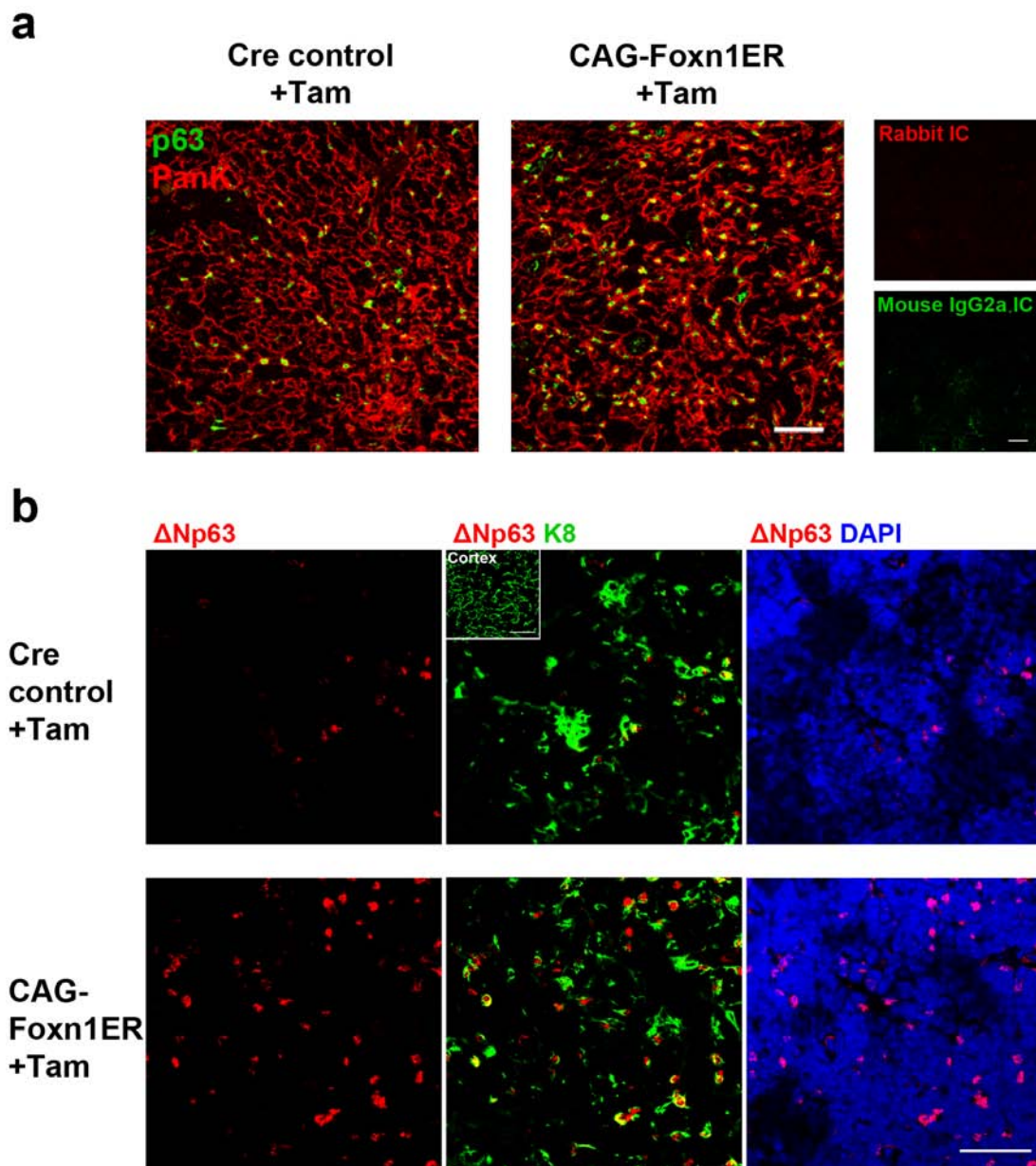


**Figure 6.8 p63 expression in aged thymi following up-regulation of Foxn1.** Immunohistochemical analysis of the TEC-specific proliferative potential marker, p63, in 12 month old thymi. **(a)** Images show representative sections for co-staining of  $\alpha$ -p63, which marks all isoforms of p63, and  $\alpha$ -pancytokeration (PanK), which marks the epithelium. **(b)** Images show representative sections for  $\alpha$ - $\Delta$ Np63 (that specifically marks proliferative potential in TECs), Keratin 8 (K8) and nuclei (DAPI) stains. Images show medullary areas, characterised by the globular epithelial K8 staining pattern – insert shows comparative K8 staining in the cortex. Right panels show co-stains of left panels. Scale bars represent 50 $\mu$ m. The relevant isotype control images for  $\Delta$ Np63 (rabbit IC) and K8 (rat IgG2a) are shown in Figure 6.5.

### 6.3.5 TEC gene expression

To further investigate the characteristics of the TECs in the larger, architecturally restored epithelial compartment that resulted from the up-regulation of Foxn1 in aged thymi, the expression levels of a panel of genes with known roles in thymus development and function were determined. The expression of various genes expressed in TECs, including *Pax1*, *Pax9*, *Dll4*, *CCL25* and *FgfR2IIIb*, was shown to be responsive to different levels of Foxn1 by analysis of a Foxn1 allelic series (Nowell et al., under review). Thus, in the analysis here, total EpCAM<sup>+</sup> TECs were isolated from 18 month old CAG-Foxn1ER +Tam thymi and control thymi and assayed for gene expression levels by qRT-PCR (as described in Chapter 1). Here, Cre control +Tam and CAG-Foxn1ER –Tam TECs were pooled in the control experiment due to limited mouse numbers.

Firstly, due to the potential autoregulatory mechanism of Foxn1, illustrated by the up-regulation of the endogenous transcript in the experiments performed in Chapter 5, endogenous *Foxn1* levels were investigated in aged TECs. In contrast to the experiments where Foxn1 up-regulation from 3 months of age resulted in an increase in endogenous *Foxn1*, endogenous *Foxn1* was not expressed at up-regulated levels following activation of Foxn1ER in 18 month CAG-Foxn1ER +Tam TECs, compared to the control. This suggests that the endogenous Foxn1 locus is no longer accessible to Foxn1ER, possibly due to age-related chromatin modifications.

*Pax1* mRNA expression was 1.5-fold higher in 18 month old CAG-Foxn1ER +Tam TECs compared to control TECs; while *Pax9* expression showed a more dramatic increase with an over 6-fold up-relative increase in CAG-Foxn1ER +Tam TECs compared to control TECs (Figure 6.9). Additionally, the mRNA expression level of the TEC-expressed fibroblast growth factor receptor, *FgfR2IIIb*, increased 3-fold following up-regulation of Foxn1 (Figure 6.9). Lastly, the Foxn1-responsive regulators of hematopoietic cell colonisation and commitment, *CCL25* and *Dll4*, were over 1.5-fold and 2-fold increased, respectively, following up-regulation of Foxn1 in aged TECs. The increased *Dll4* expression in CAG-Foxn1ER +Tam TECs compared to control TECs offers a potential explanation for the release of the TN-1TN2 block during TN cell development observed in Figure 6.3.

Thus, the increased expression levels for these genes following up-regulation of Foxn1 substantiate the restoration of the TEC compartment and increase in thymic output that was previously described in this Chapter.

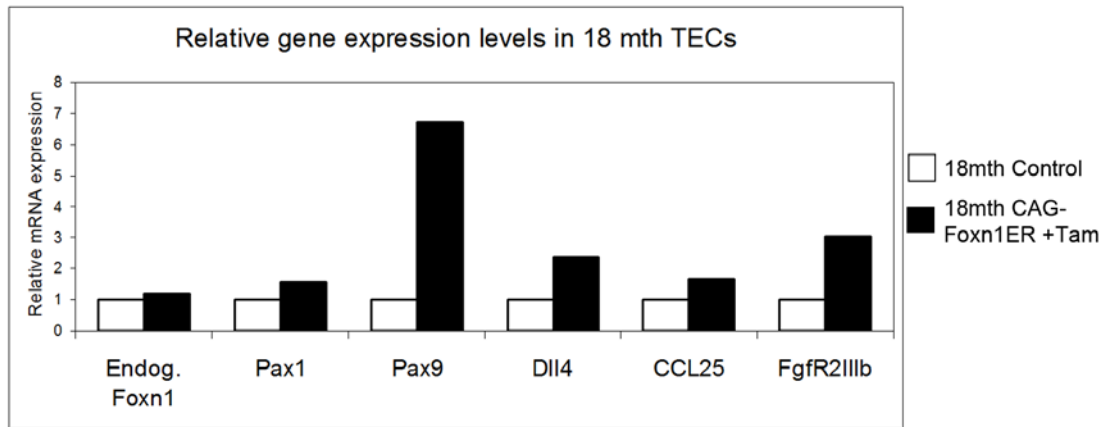


**Figure 6.9 Gene expression profile for aged TECs following Foxn1 up-regulation.** TEC gene levels were quantified by qRT-PCR for total TECs (EpCAM<sup>+</sup>). TECs were isolated by flow cytometry from thymi from three pooled mice for 18 month CAG-Foxn1ER +Tam and 18 month control samples (two Cre control +Tam mice and one CAG-Foxn1ER -Tam mice were pooled together). Endogenous (Endog.) *Foxn1*, *Pax1*, *Pax9*, *Delta-like 4 (Dll4)*, *CCL25* and *FgfR2IIIb* genes were normalised to  $\alpha$ -tubulin. Data represent 3 technical repeats.

## 6.4 Discussion

The previous Chapter described how maintenance of Foxn1 expression prevented involution in the postnatal thymus. This Chapter details the partial reversal of thymus involution through up-regulation of Foxn1 in aged thymi, as defined by the parameters measured herein. When Foxn1 was up-regulated by Tamoxifen treatment of 12 or 18 month old CAG-Foxn1ER mice, there was an increase in thymus cellularity, with a greater than two-fold increase in the total number of intrathymic haematopoietic cells compared to Tamoxifen treated control mice. This represented an increase in cell number per thymus for all the major T cell and TN cell subsets analysed here, indicating an increase in thymic activity. The driving force behind this increase in thymic activity was most likely a more structured, proliferative and functional TEC compartment that up-regulated various genes important for thymus development and function.

A few strategies currently exist that promote immune reconstitution in aged mouse models through the targeted increase of thymus activity, including sex steroid modulation and KGF treatment protocols. The increases in thymus cellularity and function in these approaches varies from several-fold (KGF) to complete recovery (castration) (Alpdogan et al., 2006; Sutherland et al., 2005). Foxn1 up-regulation in 12 month and 18 month old thymi resulted in a greater than two-fold and three-fold increase in thymus cellularity, respectively (which probably represents the different Tamoxifen treatment periods) falling in line with results observed in KGF treatment protocols.

Of note here is the effect of Tamoxifen on the thymus. Tamoxifen appeared to affect T cell cellularity, some TN population proportions and UEA1 expression on TECs. The most prominent effect of Tamoxifen may be on the viability of mature T cells, as the sizes of the TEC compartment and TN population were comparable between all controls and lower than CAG-Foxn1ER +Tam condition. In contrast, these effects of Tamoxifen were not observed in the experiments in Chapter 5 where all control conditions generated similar results, although there were 10% less CD45<sup>+</sup> cells in Cre control +Tam compared to Cre control – Tam thymi. This may be due differences in the Tamoxifen treatment: high dose administered by IP injection for two weeks in the aged mice and a lower dose administered through the drinking water for 3-4 month old mice. Nonetheless, the up-regulation of Foxn1 in aged thymi resulted in the partial reversal of thymus involution with an increase in cellularity and restoration of the TEC compartment, despite the requirement for Tamoxifen administration to maintain Foxn1 over-expression.

The effect of Tamoxifen on the thymus is poorly characterised although thymic atrophy and reduction in thymocytes has been reported (Luster et al., 1984; Uhmman et al., 2007). Additionally, thymus cellularity was reduced in estrogen receptor knock-out mice, which is a phenotype that could be recapitulated to some degree due to the anti-estrogenic effects of Tamoxifen (Staples et al., 1999). Indeed, future experiments will be aimed at ascertaining the effect of the Tamoxifen treatment regime used here on the cellular composition of bone marrow – the source of the thymic seeding cells. Furthermore, as discussed in the previous Chapter, further phenotypic resolution within the TN1 population (e.g. analysis of c-kit expression) is required to investigate (1) the effect Tamoxifen on this population and (2) the effect up-regulation of Foxn1 on this population, especially with regards to the ETP population. These analyses are important given the significant effect of Tamoxifen on the proportion of TN1 cells and the apparent ability of Foxn1 to restore the TN1 proportion to normal levels (Figure 6.3b).

The issue of the effect of Tamoxifen will be addressed in the future using another transgenic mouse line transgenic mouse line that I have generated, R26-CAG-STOP-Foxn1. These mice will be crossed with a *Foxn1*<sup>CreERt2</sup> transgenic mouse line that has recently been generated in the Blackburn lab. This should render a single dose of Tamoxifen sufficient to induce transgenic Foxn1 expression via CreER-mediated excision of the stop cassette.

To my knowledge, this represents the first report of the regeneration of the aged thymus, or any organ, through the up-regulation of a single transcription factor. While other instances exist where transcription factors, including forkhead factors, are required or promote organ or tissue regeneration, this is first instance where a transcription factor is the primary instigator of regeneration. The notion that Foxn1 is the master regulator of the thymic epithelial programme, with a host of TEC genes responsive to Foxn1 dosage, lends to the scenario here where Foxn1 alone is able to provoke thymus regeneration. The data presented here describe a novel method of thymus regeneration through modulation of Foxn1 and thus a new approach to immune reconstitution in aged organisms.



## Chapter 7: Concluding remarks

---

### 7.1 Foxn1 in the postnatal thymus

This thesis examined the expression of Foxn1 in the postnatal thymus and the effect of up-regulation of Foxn1 on thymus involution. The data presented showed that Foxn1 is expressed at different levels in the major TEC compartments, and in mature and immature TEC sub-populations, and that Foxn1 expression decreases with age. Furthermore, using a newly generated, regulatable Foxn1 mouse model, I showed that forced over-expression of Foxn1 was able to prevent thymus involution, and that up-regulation of Foxn1 in aged thymi was able to partially reverse thymus involution.

This is the first study to accurately quantify *Foxn1* mRNA expression in aging TECs. While a previous study reported that *Foxn1* mRNA expression was reduced by 16-fold in 12 month old mice compared to 1 month old mice, this analysis was not performed on defined TEC populations (Ortman et al., 2002). The data presented in this thesis show that the decrease in *Foxn1* expression with age is less profound, with an approximate 10-fold reduction in *Foxn1* mRNA expression in TECs in 12 month old mice compared to 1 month old mice.

A further point of interest, with regards to previously published data and data presented herein, is the proportion of Foxn1 negative TECs in the postnatal thymus. Corbeaux et al. (2010) showed, using a Foxn1:eGFP reporter, in which a ~30kb fragment upstream of Foxn1 exon 2 was used to drive GFP expression, that only ~70% of TECs are Foxn1<sup>+</sup> at 10-15 weeks of age. The data presented in Chapter 3 show, using a Foxn1<sup>GFP</sup> reporter model in which GFP is knocked into the Foxn1 locus, that probably all TECs express Foxn1 at 12 weeks of age. While the exact Foxn1 expression state of the Foxn1<sup>neg/lo</sup> population observed (10% of total TECs) needs to be determined, the data presented show that Foxn1<sup>+</sup> TECs constitute a significantly larger proportion of postnatal TECs than previously reported (90% or 100% versus 70% respectively). It is important to know the extent of Foxn1 expression in the postnatal thymus, especially in regard to its proposed role as a primary target of involution, and the data presented suggest that the entire postnatal TEC lineage expresses Foxn1.

A number of recent studies have shown the requirement for Foxn1 in the maintenance of the postnatal thymic microenvironment, suggesting that Foxn1 may be a primary target of

involution (Chen et al., 2009; Cheng et al., 2010; Corbeaux et al., 2010; Sun et al., 2010). Thus, I asked whether maintained over-expression of Foxn1 from the onset of involution was able to prevent or delay thymic involution. Using the regulatable Foxn1 mouse model generated during this study, I showed that Foxn1 over-expression was sufficient to prevent thymus involution, at least within the parameters measured herein, providing further evidence that Foxn1 is a primary target of thymus involution. To my knowledge, this is the first report that demonstrates, through regulation of Foxn1 expression, that thymus involution can be prevented.

Next, I asked whether up-regulation of Foxn1 was able to reverse thymus involution in aged mice. Compared to the relevant controls, Foxn1 up-regulation resulted in a greater than 2-fold increase in total thymus cellularity with a proportional increase in the major T cell populations observed. While a host of strategies currently exist to promote thymus function in aged mice, this is the first report, to my knowledge, that demonstrates an increase in thymus cellularity through the controlled up-regulation of a transcription factor in thymic epithelial cells.

How does the up-regulation of Foxn1 in aged thymi result in the regeneration of the thymic epithelium and subsequent increase in T cell production? It was shown in Chapter 3 that Foxn1 expression decreases with age in TECs, with approximately double the proportion of Foxn1<sup>lo/neg</sup> TECs at 12 months compared to at 3 months (Figure 3.3). Although these aged TECs down-regulated Foxn1, they maintained an epithelial identity (EpCAM<sup>+</sup>), although it has been shown that a small proportion of historically Foxn1<sup>+</sup> TECs undergo an epithelial to mesenchymal transition (Youm et al., 2009). Also, it was shown that approximately 90% of TECs in aged CAG-Foxn1ER thymi expressed Foxn1ER (as determined by GFP expression from the Foxn1ER-GFP bicistronic mRNA, Figure 4.8). Thus, the regeneration of the epithelium and increased thymic productivity observed, following up-regulation of Foxn1 in TECs that have age-dependently down-regulated Foxn1, may stem from the restoration of functionality in most, if not all, TECs.

At the molecular level, the observed up-regulation of key TEC genes, through the proposed master-regulatory action of Foxn1, may explain the regeneration of the thymic epithelium and improved T cell production. *CCL25* (up-regulated 1.5-fold) plays a role in recruitment of hematopoietic precursor cells to the thymus (Zlotoff et al., 2010), while *Dll4* (up-regulated 2-fold) is critical for commitment to the T cell lineage (Koch et al., 2008). Furthermore, the

increased TEC compartment size observed, following up-regulation of Foxn1, may result from an improved responsiveness to mitogenic Fgf signalling due to the up-regulation of FgfR2IIIb (up-regulated 3-fold) (Dooley et al., 2007). Additionally, the apparent increase in the number of  $\Delta$ Np63 positive TECs following Foxn1 up-regulation indicates a greater proliferative potential in the TEC compartment (Senoo et al., 2007). Interestingly, *Pax6* – the master regulator of eye development – controls proliferation of cells during eye lens regeneration (Madhavan et al., 2006). Thus, Foxn1, through its role as a proposed master regulator of TEC development, is able to provoke thymic epithelial regeneration by enhancing function and proliferation of aged TECs.

## **7.2 Experimental considerations: present and future**

An important aspect of the Tamoxifen-inducible system that was not addressed during this study was the precise quantity of Foxn1 protein present in the nuclei of TECs, following Tamoxifen-induced nuclear translocation of the Foxn1ER protein. It was shown that total *Foxn1* mRNA levels increased, and that more TECs expressed nuclear Foxn1 in CAG-Foxn1ER thymi treated with Tamoxifen, compared to the relevant controls. However, future experiments will be aimed at quantifying the amount of total nuclear Foxn1 protein in postnatal CAG-Foxn1ER TECs, following Tamoxifen induction. This analysis is severely hindered by the difficulty in obtaining sufficient nuclear protein fractions from postnatal TECs for protein analysis protocols; an approach that could be utilised in this case is capillary electrophoresis.

A further issue to consider is the general effect of Tamoxifen on thymic output parameters investigated in this thesis. High doses of Tamoxifen affected thymus cellularity and T cell populations in aged mice. While the proper controls were performed and shown (i.e. Cre control mice treated with Tamoxifen), this makes it more challenging to delineate Foxn1's function in reversing thymus involution, and in reversing thymus involution and the compounding effects of Tamoxifen on the thymus. This will be addressed in the future using newly generated mouse models, Foxn1<sup>CreER</sup> and R26-CAG-STOP-Foxn1 (which I have recently generated), such that a single dose of Tamoxifen will be sufficient to induce Cre-mediated excision of the STOP cassette, and thus Foxn1 over-expression.

Further future experiments will also be performed to show that the increase in thymus cellularity and T cell populations, following up-regulation of Foxn1, translates into improved immune system functionality, especially in the context of the involution reversal

experiments. This will be addressed by investigating peripheral T cell characteristics (e.g. functionality and composition) in aged mice that have up-regulated Foxn1.

One approach that could be used to investigate peripheral T cell functionality of the mouse model described in this thesis, would be to test the ability to respond to and overcome an immune system challenge, for example following pathogen infection. This thesis has established that Foxn1 up-regulation in the aged thymic epithelium resulted in an increase in the number of major intrathymic T cell subsets. An infectious challenge experiment would determine whether this translated into an increase in peripheral T cell functionality and an improved immune system. Aged mice that up-regulate Foxn1 may be expected to have an increased capacity to overcome a pathogen infection compared to age-matched controls.

One of the potential negative side effects that should be considered, in the context of an increase in the intrathymic T cells in aged mice, is autoimmunity. It would be pertinent to investigate whether the deletion of autoreactive T cell clones proceeded effectively following the increase in intrathymic CD4<sup>+</sup> and CD8<sup>+</sup> SP T cells observed in CAG-Foxn1ER mice. This is especially relevant given that instances of autoimmune disorders are more prevalent in the aged, suggesting that mechanisms in place to prevent autoimmunity become dysregulated with age (Larbi et al., 2008). However, evidence suggests that Foxn1 plays a role in the differentiation of the AIRE<sup>+</sup> mTEC lineage, which has a critical role in negative selection (Nowell et al., under review). Thus, an up-regulation of Foxn1 in aged thymus may not only result in an increase in intrathymic T cells, but also an increase in the size and functionality of the TEC lineage that mediates negative selection.

It will also be interesting to investigate synergistic approaches to thymus regeneration in aged mice, for example simultaneous KGF treatment and Foxn1 up-regulation. This is particularly relevant given that up-regulation of Foxn1 resulted in an increase in the expression of the KGF receptor, FgfR2IIIb, in TECs. Additionally, it will be interesting to establish whether Foxn1 over-expression is able to rescue the thymic defects observed in *FgfR2IIIb* mutants. These analyses may provide insight into the relationship between Foxn1 and KGF signalling pathways in the thymus.

Furthermore, it will be interesting to determine the transiency of thymus regeneration following Foxn1 up-regulation. Most approaches used to increase thymic output are transient in nature, including sex steroid ablation and KGF treatment. Thus two questions could be

addressed. Firstly, whether transient up-regulation of Foxn1 is sufficient to permanently prevent or reverse thymus involution, and secondly, whether thymus involution can be permanently prevented or reversed by maintained over-expression of Foxn1.

The data presented in this thesis describe for the first time that up-regulation of Foxn1 is able to prevent and reverse thymus involution in mice. Firstly, this contributes to the recently described notion that Foxn1 is a primary target for thymus involution, and secondly, represents a novel method to reverse thymus involution. This offers the tantalising possibility that manipulation of Foxn1 expression could be used in the future as a clinical approach to immune reconstitution.

## References

- Abdul-Hai, A., Or, R., Slavin, S., Friedman, G., Weiss, L., Matsa, D. and Ben-Yehuda, A.** (1996). Stimulation of immune reconstitution by interleukin-7 after syngeneic bone marrow transplantation in mice. *Exp Hematol* **24**, 1416-22.
- Abu-Issa, R., Smyth, G., Smoak, I., Yamamura, K. and Meyers, E. N.** (2002). Fgf8 is required for pharyngeal arch and cardiovascular development in the mouse. *Development* **129**, 4613-25.
- Adkins, B., Tidmarsh, G. F. and Weissman, I. L.** (1988). Normal thymic cortical epithelial cells developmentally regulate the expression of a B-lineage transformation-associated antigen. *Immunogenetics* **27**, 180-6.
- Aifantis, I., Buer, J., von Boehmer, H. and Azogui, O.** (1997). Essential role of the pre-T cell receptor in allelic exclusion of the T cell receptor beta locus. *Immunity* **7**, 601-7.
- Allman, D., Sambandam, A., Kim, S., Miller, J. P., Pagan, A., Well, D., Meraz, A. and Bhandoola, A.** (2003). Thymopoiesis independent of common lymphoid progenitors. *Nat Immunol* **4**, 168-74.
- Alpdogan, O., Hubbard, V. M., Smith, O. M., Patel, N., Lu, S., Goldberg, G. L., Gray, D. H., Feinman, J., Kochman, A. A., Eng, J. M., Suh, D., Muriglan, S. J., Boyd, R. L. and van den Brink, M. R.** (2006). Keratinocyte growth factor (KGF) is required for postnatal thymic regeneration. *Blood* **107**, 2453-60.
- Alpdogan, O., Muriglan, S. J., Eng, J. M., Willis, L. M., Greenberg, A. S., Kappel, B. J. and van den Brink, M. R.** (2003a). IL-7 enhances peripheral T cell reconstitution after allogeneic hematopoietic stem cell transplantation. *J Clin Invest* **112**, 1095-107.
- Alpdogan, O., Muriglan, S. J., Kappel, B. J., Doubrovina, E., Schmaltz, C., Schiro, R., Eng, J. M., Greenberg, A. S., Willis, L. M., Rotolo, J. A., O'Reilly, R. J. and van den Brink, M. R.** (2003b). Insulin-like growth factor-I enhances lymphoid and myeloid reconstitution after allogeneic bone marrow transplantation. *Transplantation* **75**, 1977-83.
- Alpdogan, O. and van den Brink, M. R.** (2005). IL-7 and IL-15: therapeutic cytokines for immunodeficiency. *Trends Immunol* **26**, 56-64.
- Anderson, G., Jenkinson, E. J., Moore, N. C. and Owen, J. J.** (1993). MHC class II-positive epithelium and mesenchyme cells are both required for T-cell development in the thymus. *Nature* **362**, 70-3.
- Anderson, M. S., Venanzi, E. S., Klein, L., Chen, Z., Berzins, S. P., Turley, S. J., von Boehmer, H., Bronson, R., Dierich, A., Benoist, C. and Mathis, D.** (2002). Projection of an immunological self shadow within the thymus by the aire protein. *Science* **298**, 1395-401.
- Andrew, D. and Aspinall, R.** (2001). Il-7 and not stem cell factor reverses both the increase in apoptosis and the decline in thymopoiesis seen in aged mice. *J Immunol* **166**, 1524-30.
- Ardavin, C.** (1997). Thymic dendritic cells. *Immunol Today* **18**, 350-61.
- Ardavin, C., Wu, L., Li, C. L. and Shortman, K.** (1993). Thymic dendritic cells and T cells develop simultaneously in the thymus from a common precursor population. *Nature* **362**, 761-3.
- Arstila, T. P., Casrouge, A., Baron, V., Even, J., Kanellopoulos, J. and Kourilsky, P.** (1999). A direct estimate of the human alphabeta T cell receptor diversity. *Science* **286**, 958-61.

- Ashfield, R., Patel, A. J., Bossone, S. A., Brown, H., Campbell, R. D., Marcu, K. B. and Proudfoot, N. J.** (1994). MAZ-dependent termination between closely spaced human complement genes. *Embo J* **13**, 5656-67.
- Auerbach, R.** (1960). Morphogenetic interactions in the development of the mouse thymus gland. *Dev Biol* **2**, 271-84.
- Awong, G., Herer, E., Surh, C. D., Dick, J. E., La Motte-Mohs, R. N. and Zuniga-Pflucker, J. C.** (2009). Characterization in vitro and engraftment potential in vivo of human progenitor T cells generated from hematopoietic stem cells. *Blood* **114**, 972-82.
- Bajoghli, B., Aghaallaei, N., Hess, I., Rode, I., Netuschil, N., Tay, B. H., Venkatesh, B., Yu, J. K., Kaltenebach, S. L., Holland, N. D., Diekhoff, D., Happe, C., Schorpp, M. and Boehm, T.** (2009). Evolution of genetic networks underlying the emergence of thymopoiesis in vertebrates. *Cell* **138**, 186-97.
- Bajoghli, B., Guo, P., Aghaallaei, N., Hirano, M., Strohmeier, C., McCurley, N., Bockman, D. E., Schorpp, M., Cooper, M. D. and Boehm, T.** (2010). A thymus candidate in lampreys. *Nature* **470**, 90-4.
- Balciunaite, G., Keller, M. P., Balciunaite, E., Piali, L., Zuklys, S., Mathieu, Y. D., Gill, J., Boyd, R., Sussman, D. J. and Hollander, G. A.** (2002). Wnt glycoproteins regulate the expression of FoxN1, the gene defective in nude mice. *Nat Immunol* **3**, 1102-8.
- Bell, J. J. and Bhandoola, A.** (2008). The earliest thymic progenitors for T cells possess myeloid lineage potential. *Nature* **452**, 764-7.
- Benoist, C. and Mathis, D.** (1989). Positive selection of the T cell repertoire: where and when does it occur? *Cell* **58**, 1027-33.
- Benz, C., Heinzl, K. and Bleul, C. C.** (2004). Homing of immature thymocytes to the subcapsular microenvironment within the thymus is not an absolute requirement for T cell development. *Eur J Immunol* **34**, 3652-63.
- Blackburn, C. C., Augustine, C. L., Li, R., Harvey, R. P., Malin, M. A., Boyd, R. L., Miller, J. F. and Morahan, G.** (1996). The nu gene acts cell-autonomously and is required for differentiation of thymic epithelial progenitors. *Proc Natl Acad Sci U S A* **93**, 5742-6.
- Blackburn, C. C. and Manley, N. R.** (2004). Developing a new paradigm for thymus organogenesis. *Nat Rev Immunol* **4**, 278-89.
- Bleul, C. C., Corbeaux, T., Reuter, A., Fisch, P., Monting, J. S. and Boehm, T.** (2006). Formation of a functional thymus initiated by a postnatal epithelial progenitor cell. *Nature* **441**, 992-6.
- Bluestone, J. A., Pardoll, D., Sharrow, S. O. and Fowlkes, B. J.** (1987). Characterization of murine thymocytes with CD3-associated T-cell receptor structures. *Nature* **326**, 82-4.
- Blyth, K., Stewart, M., Bell, M., James, C., Evan, G., Neil, J. C. and Cameron, E. R.** (2000). Sensitivity to myc-induced apoptosis is retained in spontaneous and transplanted lymphomas of CD2-mycER mice. *Oncogene* **19**, 773-82.
- Boehm, T., Scheu, S., Pfeffer, K. and Bleul, C. C.** (2003). Thymic medullary epithelial cell differentiation, thymocyte emigration, and the control of autoimmunity require lympho-epithelial cross talk via LTbetaR. *J Exp Med* **198**, 757-69.
- Bolotin, E., Smogorzewska, M., Smith, S., Widmer, M. and Weinberg, K.** (1996). Enhancement of thymopoiesis after bone marrow transplant by in vivo interleukin-7. *Blood* **88**, 1887-94.

- Boyd, R. L., Tucek, C. L., Godfrey, D. I., Izon, D. J., Wilson, T. J., Davidson, N. J., Bean, A. G., Ladyman, H. M., Ritter, M. A. and Hugo, P.** (1993). The thymic microenvironment. *Immunol Today* **14**, 445-59.
- Brandle, D., Muller, C., Rulicke, T., Hengartner, H. and Pircher, H.** (1992). Engagement of the T-cell receptor during positive selection in the thymus down-regulates RAG-1 expression. *Proc Natl Acad Sci U S A* **89**, 9529-33.
- Brugnera, E., Bhandoola, A., Cibotti, R., Yu, Q., Guinter, T. I., Yamashita, Y., Sharrow, S. O. and Singer, A.** (2000). Coreceptor reversal in the thymus: signaled CD4+8+ thymocytes initially terminate CD8 transcription even when differentiating into CD8+ T cells. *Immunity* **13**, 59-71.
- Capone, M., Hockett, R. D., Jr. and Zlotnik, A.** (1998). Kinetics of T cell receptor beta, gamma, and delta rearrangements during adult thymic development: T cell receptor rearrangements are present in CD44(+)CD25(+) Pro-T thymocytes. *Proc Natl Acad Sci U S A* **95**, 12522-7.
- Chen, B. J., Cui, X., Sempowski, G. D. and Chao, N. J.** (2003). Growth hormone accelerates immune recovery following allogeneic T-cell-depleted bone marrow transplantation in mice. *Exp Hematol* **31**, 953-8.
- Chen, L., Xiao, S. and Manley, N. R.** (2009). Foxn1 is required to maintain the postnatal thymic microenvironment in a dosage-sensitive manner. *Blood* **113**, 567-74.
- Cheng, L., Guo, J., Sun, L., Fu, J., Barnes, P. F., Metzger, D., Chambon, P., Oshima, R. G., Amagai, T. and Su, D. M.** (2010). Postnatal tissue-specific disruption of transcription factor FoxN1 triggers acute thymic atrophy. *J Biol Chem* **285**, 5836-47.
- Chilosi, M., Zamo, A., Brighenti, A., Malpeli, G., Montagna, L., Piccoli, P., Pedron, S., Lestani, M., Inghirami, G., Scarpa, A., Doglioni, C. and Menestrina, F.** (2003). Constitutive expression of DeltaN-p63alpha isoform in human thymus and thymic epithelial tumours. *Virchows Arch* **443**, 175-83.
- Chu, Y. W., Schmitz, S., Choudhury, B., Telford, W., Kapoor, V., Garfield, S., Howe, D. and Gress, R. E.** (2008). Exogenous insulin-like growth factor 1 enhances thymopoiesis predominantly through thymic epithelial cell expansion. *Blood* **112**, 2836-46.
- Clark, K. L., Halay, E. D., Lai, E. and Burley, S. K.** (1993). Co-crystal structure of the HNF-3/fork head DNA-recognition motif resembles histone H5. *Nature* **364**, 412-20.
- Corbeaux, T., Hess, I., Swann, J. B., Kanzler, B., Haas-Assenbaum, A. and Boehm, T.** (2010). Thymopoiesis in mice depends on a Foxn1-positive thymic epithelial cell lineage. *Proc Natl Acad Sci U S A*.
- Dean, A. G. and Sullivan, K. M.** (2010). OpenEpi: Open Source Epidemiologic Statistics for Public Health, Version 2.3.1, (ed. A. G. Dean K. M. Sullivan M. M. Soe and R. A. Mir).
- Depreter, M. G., Blair, N. F., Gaskell, T. L., Nowell, C. S., Davern, K., Pagliocca, A., Stenhouse, F. H., Farley, A. M., Fraser, A., Vrana, J., Robertson, K., Morahan, G., Tomlinson, S. R. and Blackburn, C. C.** (2008). Identification of Plet-1 as a specific marker of early thymic epithelial progenitor cells. *Proc Natl Acad Sci U S A* **105**, 961-6.
- Derbinski, J., Pinto, S., Rosch, S., Hexel, K. and Kyewski, B.** (2008). Promiscuous gene expression patterns in single medullary thymic epithelial cells argue for a stochastic mechanism. *Proc Natl Acad Sci U S A* **105**, 657-62.
- Dixit, V. D.** (2010). Thymic fatness and approaches to enhance thymopoietic fitness in aging. *Curr Opin Immunol* **22**, 521-8.



- Donskoy, E. and Goldschneider, I.** (2003). Two developmentally distinct populations of dendritic cells inhabit the adult mouse thymus: demonstration by differential importation of hematogenous precursors under steady state conditions. *J Immunol* **170**, 3514-21.
- Dooley, J., Erickson, M., Larochelle, W. J., Gillard, G. O. and Farr, A. G.** (2007). FGFR2IIIb signaling regulates thymic epithelial differentiation. *Dev Dyn* **236**, 3459-71.
- Dowling, M. R. and Hodgkin, P. D.** (2009). Why does the thymus involute? A selection-based hypothesis. *Trends Immunol* **30**, 295-300.
- Duijvestijn, A. M. and Hoefsmit, E. C.** (1981). Ultrastructure of the rat thymus: the micro-environment of T-lymphocyte maturation. *Cell Tissue Res* **218**, 279-92.
- Ehrlich, L. I., Serwold, T. and Weissman, I. L.** (2011). In vitro assays misrepresent in vivo lineage potentials of murine lymphoid progenitors. *Blood* **117**.
- Farr, A., Nelson, A., Truex, J. and Hosier, S.** (1991). Epithelial heterogeneity in the murine thymus: a cell surface glycoprotein expressed by subcapsular and medullary epithelium. *J Histochem Cytochem* **39**, 645-53.
- Feil, R., Wagner, J., Metzger, D. and Chambon, P.** (1997). Regulation of Cre recombinase activity by mutated estrogen receptor ligand-binding domains. *Biochem Biophys Res Commun* **237**, 752-7.
- Finch, P. W. and Rubin, J. S.** (2004). Keratinocyte growth factor/fibroblast growth factor 7, a homeostatic factor with therapeutic potential for epithelial protection and repair. *Adv Cancer Res* **91**, 69-136.
- Fitzpatrick, F. T., Kendall, M. D., Wheeler, M. J., Adcock, I. M. and Greenstein, B. D.** (1985). Reappearance of thymus of ageing rats after orchidectomy. *J Endocrinol* **106**, R17-9.
- Flanagan, S. P.** (1966). 'Nude', a new hairless gene with pleiotropic effects in the mouse. *Genet Res* **8**, 295-309.
- Flomerfelt, F. A., El Kassar, N., Gurunathan, C., Chua, K. S., League, S. C., Schmitz, S., Gershon, T. R., Kapoor, V., Yan, X. Y., Schwartz, R. H. and Gress, R. E.** (2010). Tbeta modulates thymic stromal cell proliferation and thymus function. *J Exp Med* **207**, 2521-32.
- Flores, K. G., Li, J., Sempowski, G. D., Haynes, B. F. and Hale, L. P.** (1999). Analysis of the human thymic perivascular space during aging. *J Clin Invest* **104**, 1031-9.
- Fontenot, J. D., Rasmussen, J. P., Williams, L. M., Dooley, J. L., Farr, A. G. and Rudensky, A. Y.** (2005). Regulatory T cell lineage specification by the forkhead transcription factor foxp3. *Immunity* **22**, 329-41.
- Foss, D. L., Donskoy, E. and Goldschneider, I.** (2001). The importation of hematogenous precursors by the thymus is a gated phenomenon in normal adult mice. *J Exp Med* **193**, 365-74.
- Foster, K., Sheridan, J., Veiga-Fernandes, H., Roderick, K., Pachnis, V., Adams, R., Blackburn, C., Kioussis, D. and Coles, M.** (2008). Contribution of neural crest-derived cells in the embryonic and adult thymus. *J Immunol* **180**, 3183-9.
- Fowlkes, B. J., Edison, L., Mathieson, B. J. and Chused, T. M.** (1985). Early T lymphocytes. Differentiation in vivo of adult intrathymic precursor cells. *J Exp Med* **162**, 802-22.
- Frank, J., Pignata, C., Panteleyev, A. A., Prowse, D. M., Baden, H., Weiner, L., Gaetaniello, L., Ahmad, W., Pozzi, N., Cserhalmi-Friedman, P. B., Aita, V. M., Uyttendaele, H., Gordon, D., Ott,**

- J., Brissette, J. L. and Christiano, A. M.** (1999). Exposing the human nude phenotype. *Nature* **398**, 473-4.
- Friedrich, G. and Soriano, P.** (1991). Promoter traps in embryonic stem cells: a genetic screen to identify and mutate developmental genes in mice. *Genes Dev* **5**, 1513-23.
- George, A. J. and Ritter, M. A.** (1996). Thymic involution with ageing: obsolescence or good housekeeping? *Immunol Today* **17**, 267-72.
- Germain, R. N.** (2002). T-cell development and the CD4-CD8 lineage decision. *Nat Rev Immunol* **2**, 309-22.
- Godfrey, D. I., Izon, D. J., Tucek, C. L., Wilson, T. J. and Boyd, R. L.** (1990). The phenotypic heterogeneity of mouse thymic stromal cells. *Immunology* **70**, 66-74.
- Godfrey, D. I., Kennedy, J., Suda, T. and Zlotnik, A.** (1993). A developmental pathway involving four phenotypically and functionally distinct subsets of CD3-CD4-CD8- triple-negative adult mouse thymocytes defined by CD44 and CD25 expression. *J Immunol* **150**, 4244-52.
- Godfrey, D. I., Zlotnik, A. and Suda, T.** (1992). Phenotypic and functional characterization of c-kit expression during intrathymic T cell development. *J Immunol* **149**, 2281-5.
- Goldberg, G. L., Zakrzewski, J. L., Perales, M. A. and van den Brink, M. R.** (2007). Clinical strategies to enhance T cell reconstitution. *Semin Immunol* **19**, 289-96.
- Gordon, J., Bennett, A. R., Blackburn, C. C. and Manley, N. R.** (2001). Gcm2 and Foxn1 mark early parathyroid- and thymus-specific domains in the developing third pharyngeal pouch. *Mech Dev* **103**, 141-3.
- Gordon, J., Wilson, V. A., Blair, N. F., Sheridan, J., Farley, A., Wilson, L., Manley, N. R. and Blackburn, C. C.** (2004). Functional evidence for a single endodermal origin for the thymic epithelium. *Nat Immunol* **5**, 546-53.
- Gordon, J., Xiao, S., Hughes, B., 3rd, Su, D. M., Navarre, S. P., Condie, B. G. and Manley, N. R.** (2007). Specific expression of lacZ and cre recombinase in fetal thymic epithelial cells by multiplex gene targeting at the Foxn1 locus. *BMC Dev Biol* **7**, 69.
- Goronzy, J. J. and Weyand, C. M.** (2005). T cell development and receptor diversity during aging. *Curr Opin Immunol* **17**, 468-75.
- Gossen, M., Freundlieb, S., Bender, G., Muller, G., Hillen, W. and Bujard, H.** (1995). Transcriptional activation by tetracyclines in mammalian cells. *Science* **268**, 1766-9.
- Gray, D. H., Chidgey, A. P. and Boyd, R. L.** (2002). Analysis of thymic stromal cell populations using flow cytometry. *J Immunol Methods* **260**, 15-28.
- Gray, D. H., Fletcher, A. L., Hammett, M., Seach, N., Ueno, T., Young, L. F., Barbuto, J., Boyd, R. L. and Chidgey, A. P.** (2008). Unbiased analysis, enrichment and purification of thymic stromal cells. *J Immunol Methods* **329**, 56-66.
- Gray, D. H., Seach, N., Ueno, T., Milton, M. K., Liston, A., Lew, A. M., Goodnow, C. C. and Boyd, R. L.** (2006). Developmental kinetics, turnover, and stimulatory capacity of thymic epithelial cells. *Blood* **108**, 3777-85.
- Gray, D. H., Tull, D., Ueno, T., Seach, N., Classon, B. J., Chidgey, A., McConville, M. J. and Boyd, R. L.** (2007). A unique thymic fibroblast population revealed by the monoclonal antibody MTS-15. *J Immunol* **178**, 4956-65.

- Greenstein, B. D., Fitzpatrick, F. T., Kendall, M. D. and Wheeler, M. J.** (1987). Regeneration of the thymus in old male rats treated with a stable analogue of LHRH. *J Endocrinol* **112**, 345-50.
- Gruver, A. L., Hudson, L. L. and Sempowski, G. D.** (2007). Immunosenescence of ageing. *J Pathol* **211**, 144-56.
- Gui, J., Zhu, X., Dohkan, J., Cheng, L., Barnes, P. F. and Su, D. M.** (2007). The aged thymus shows normal recruitment of lymphohematopoietic progenitors but has defects in thymic epithelial cells. *Int Immunol* **19**, 1201-11.
- Hakim, F. T., Memon, S. A., Cepeda, R., Jones, E. C., Chow, C. K., Kasten-Sportes, C., Odom, J., Vance, B. A., Christensen, B. L., Mackall, C. L. and Gress, R. E.** (2005). Age-dependent incidence, time course, and consequences of thymic renewal in adults. *J Clin Invest* **115**, 930-9.
- Hamazaki, Y., Fujita, H., Kobayashi, T., Choi, Y., Scott, H. S., Matsumoto, M. and Minato, N.** (2007). Medullary thymic epithelial cells expressing Aire represent a unique lineage derived from cells expressing claudin. *Nat Immunol* **8**, 304-11.
- Hannenhalli, S. and Kaestner, K. H.** (2009). The evolution of Fox genes and their role in development and disease. *Nat Rev Genet* **10**, 233-40.
- Hare, K. J., Jenkinson, E. J. and Anderson, G.** (2000). An essential role for the IL-7 receptor during intrathymic expansion of the positively selected neonatal T cell repertoire. *J Immunol* **165**, 2410-4.
- Hassall, A. H.** (1849). The microscopic anatomy of the human body in health and disease. London.
- Hayashi, S. and McMahon, A. P.** (2002). Efficient recombination in diverse tissues by a tamoxifen-inducible form of Cre: a tool for temporally regulated gene activation/inactivation in the mouse. *Dev Biol* **244**, 305-18.
- He, X., Dave, V. P., Zhang, Y., Hua, X., Nicolas, E., Xu, W., Roe, B. A. and Kappes, D. J.** (2005). The zinc finger transcription factor Th-POK regulates CD4 versus CD8 T-cell lineage commitment. *Nature* **433**, 826-33.
- Henderson, J.** (1904). On the relationship of the thymus to the sexual organs: I. The influence of castration on the thymus. *J Physiol* **31**, 222-9.
- Heng, T. S., Goldberg, G. L., Gray, D. H., Sutherland, J. S., Chidgey, A. P. and Boyd, R. L.** (2005). Effects of castration on thymocyte development in two different models of thymic involution. *J Immunol* **175**, 2982-93.
- Hetzer-Egger, C., Schorpp, M., Haas-Assenbaum, A., Balling, R., Peters, H. and Boehm, T.** (2002). Thymopoiesis requires Pax9 function in thymic epithelial cells. *Eur J Immunol* **32**, 1175-81.
- Higashi, A. Y., Ikawa, T., Muramatsu, M., Economides, A. N., Niwa, A., Okuda, T., Murphy, A. J., Rojas, J., Heike, T., Nakahata, T., Kawamoto, H., Kita, T. and Yanagita, M.** (2009). Direct hematological toxicity and illegitimate chromosomal recombination caused by the systemic activation of CreERT2. *J Immunol* **182**, 5633-40.
- Hince, M., Sakkal, S., Vlahos, K., Dudakov, J., Boyd, R. and Chidgey, A.** (2008). The role of sex steroids and gonadectomy in the control of thymic involution. *Cell Immunol* **252**, 122-38.
- Hochedlinger, K., Yamada, Y., Beard, C. and Jaenisch, R.** (2005). Ectopic expression of Oct-4 blocks progenitor-cell differentiation and causes dysplasia in epithelial tissues. *Cell* **121**, 465-77.

- Itoi, M., Kawamoto, H., Katsura, Y. and Amagai, T.** (2001). Two distinct steps of immigration of hematopoietic progenitors into the early thymus anlage. *Int Immunol* **13**, 1203-11.
- Itoi, M., Tsukamoto, N. and Amagai, T.** (2007). Expression of Dll4 and CCL25 in Foxn1-negative epithelial cells in the post-natal thymus. *Int Immunol* **19**, 127-32.
- Janas, M. L. and Turner, M.** (2010). Stromal cell-derived factor 1alpha and CXCR4: newly defined requirements for efficient thymic beta-selection. *Trends Immunol* **31**, 370-6.
- Janes, S. M., Ofstad, T. A., Campbell, D. H., Watt, F. M. and Prowse, D. M.** (2004). Transient activation of FOXP1 in keratinocytes induces a transcriptional programme that promotes terminal differentiation: contrasting roles of FOXP1 and Akt. *J Cell Sci* **117**, 4157-68.
- Jerome, L. A. and Papaioannou, V. E.** (2001). DiGeorge syndrome phenotype in mice mutant for the T-box gene, Tbx1. *Nat Genet* **27**, 286-91.
- Josefowicz, S. Z. and Rudensky, A.** (2009). Control of regulatory T cell lineage commitment and maintenance. *Immunity* **30**, 616-25.
- Kampinga, J., Berges, S., Boyd, R. L., Brekelmans, P., Colic, M., van Ewijk, W., Kendall, M. D., Ladyman, H., Nieuwenhuis, P., Ritter, M. A. and et al.** (1989). Thymic epithelial antibodies: immunohistological analysis and introduction of nomenclature. *Thymus* **13**, 165-73.
- Kato, S. and Schoefl, G. I.** (1989). Microvasculature of normal and involuted mouse thymus. Light- and electron-microscopic study. *Acta Anat (Basel)* **135**, 1-11.
- Kaye, J., Hsu, M. L., Sauron, M. E., Jameson, S. C., Gascoigne, N. R. and Hedrick, S. M.** (1989). Selective development of CD4+ T cells in transgenic mice expressing a class II MHC-restricted antigen receptor. *Nature* **341**, 746-9.
- Keefe, R., Dave, V., Allman, D., Wiest, D. and Kappes, D. J.** (1999). Regulation of lineage commitment distinct from positive selection. *Science* **286**, 1149-53.
- Kendall, M. D.** (1991). Functional anatomy of the thymic microenvironment. *J Anat* **177**, 1-29.
- Kirkpatrick, J. A., Jr. and DiGeorge, A. M.** (1968). Congenital absence of the thymus. *Am J Roentgenol Radium Ther Nucl Med* **103**, 32-7.
- Koch, U., Fiorini, E., Benedito, R., Besseyrias, V., Schuster-Gossler, K., Pierres, M., Manley, N. R., Duarte, A., Macdonald, H. R. and Radtke, F.** (2008). Delta-like 4 is the essential, nonredundant ligand for Notch1 during thymic T cell lineage commitment. *J Exp Med* **205**, 2515-23.
- Kvell, K., Varcza, Z., Bartis, D., Hesse, S., Parnell, S., Anderson, G., Jenkinson, E. J. and Pongracz, J. E.** (2010). Wnt4 and LAP2alpha as pacemakers of thymic epithelial senescence. *PLoS One* **5**, e10701.
- Kyewski, B. and Derbinski, J.** (2004). Self-representation in the thymus: an extended view. *Nat Rev Immunol* **4**, 688-98.
- Kyewski, B. A.** (1987). Seeding of thymic microenvironments defined by distinct thymocyte-stromal cell interactions is developmentally controlled. *J Exp Med* **166**, 520-38.
- Kyewski, B. A., Fathman, C. G. and Rouse, R. V.** (1986). Intrathymic presentation of circulating non-MHC antigens by medullary dendritic cells. An antigen-dependent microenvironment for T cell differentiation. *J Exp Med* **163**, 231-46.

- La Motte-Mohs, R. N., Herer, E. and Zuniga-Pflucker, J. C.** (2005). Induction of T-cell development from human cord blood hematopoietic stem cells by Delta-like 1 in vitro. *Blood* **105**, 1431-9.
- Larbi, A., Fulop, T. and Pawelec, G.** (2008). Immune receptor signaling, aging and autoimmunity. *Adv Exp Med Biol* **640**, 312-24.
- Le Douarin, N. M. and Jotereau, F. V.** (1975). Tracing of cells of the avian thymus through embryonic life in interspecific chimeras. *J Exp Med* **142**, 17-40.
- Lee, D., Prowse, D. M. and Brissette, J. L.** (1999). Association between mouse nude gene expression and the initiation of epithelial terminal differentiation. *Dev Biol* **208**, 362-74.
- Lind, E. F., Prockop, S. E., Porritt, H. E. and Petrie, H. T.** (2001). Mapping precursor movement through the postnatal thymus reveals specific microenvironments supporting defined stages of early lymphoid development. *J Exp Med* **194**, 127-34.
- Linette, G. P., Grusby, M. J., Hedrick, S. M., Hansen, T. H., Glimcher, L. H. and Korsmeyer, S. J.** (1994). Bcl-2 is upregulated at the CD4<sup>+</sup> CD8<sup>+</sup> stage during positive selection and promotes thymocyte differentiation at several control points. *Immunity* **1**, 197-205.
- Liu, C., Saito, F., Liu, Z., Lei, Y., Uehara, S., Love, P., Lipp, M., Kondo, S., Manley, N. and Takahama, Y.** (2006). Coordination between CCR7- and CCR9-mediated chemokine signals in prevascular fetal thymus colonization. *Blood* **108**, 2531-9.
- Lucas, K., Vremec, D., Wu, L. and Shortman, K.** (1998). A linkage between dendritic cell and T-cell development in the mouse thymus: the capacity of sequential T-cell precursors to form dendritic cells in culture. *Dev Comp Immunol* **22**, 339-49.
- Luster, M. I., Hayes, H. T., Korach, K., Tucker, A. N., Dean, J. H., Greenlee, W. F. and Boorman, G. A.** (1984). Estrogen immunosuppression is regulated through estrogenic responses in the thymus. *J Immunol* **133**, 110-6.
- Mackall, C. L., Fry, T. J., Bare, C., Morgan, P., Galbraith, A. and Gress, R. E.** (2001). IL-7 increases both thymic-dependent and thymic-independent T-cell regeneration after bone marrow transplantation. *Blood* **97**, 1491-7.
- Mackall, C. L., Punt, J. A., Morgan, P., Farr, A. G. and Gress, R. E.** (1998). Thymic function in young/old chimeras: substantial thymic T cell regenerative capacity despite irreversible age-associated thymic involution. *Eur J Immunol* **28**, 1886-93.
- Madhavan, M., Haynes, T. L., Frisch, N. C., Call, M. K., Minich, C. M., Tsonis, P. A. and Del Rio-Tsonis, K.** (2006). The role of Pax-6 in lens regeneration. *Proc Natl Acad Sci U S A* **103**, 14848-53.
- Maki, K., Sunaga, S., Komagata, Y., Kodaira, Y., Mabuchi, A., Karasuyama, H., Yokomuro, K., Miyazaki, J. I. and Ikuta, K.** (1996). Interleukin 7 receptor-deficient mice lack gammadelta T cells. *Proc Natl Acad Sci U S A* **93**, 7172-7.
- Manley, N. R. and Capecchi, M. R.** (1995). The role of Hoxa-3 in mouse thymus and thyroid development. *Development* **121**, 1989-2003.
- Manley, N. R., Richie, E. R., Blackburn, C. C., Condie, B. G. and Sage, J.** (2010). Structure and function of the thymic microenvironment. *Frontiers in Bioscience* **in press**.
- Markert, M. L., Devlin, B. H., Alexieff, M. J., Li, J., McCarthy, E. A., Gupton, S. E., Chinn, I. K., Hale, L. P., Kepler, T. B., He, M., Sarzotti, M., Skinner, M. A., Rice, H. E. and Hoehner, J.**

- C. (2007). Review of 54 patients with complete DiGeorge anomaly enrolled in protocols for thymus transplantation: outcome of 44 consecutive transplants. *Blood* **109**, 4539-47.
- Markert, M. L., Devlin, B. H. and McCarthy, E. A.** (2010). Thymus transplantation. *Clin Immunol* **135**, 236-46.
- Miller, J. F.** (1961). Immunological function of the thymus. *Lancet* **2**, 748-9.
- Min, D., Panoskaltsis-Mortari, A., Kuro, O. M., Hollander, G. A., Blazar, B. R. and Weinberg, K. I.** (2007). Sustained thymopoiesis and improvement in functional immunity induced by exogenous KGF administration in murine models of aging. *Blood* **109**, 2529-37.
- Min, H., Montecino-Rodriguez, E. and Dorshkind, K.** (2004). Reduction in the developmental potential of intrathymic T cell progenitors with age. *J Immunol* **173**, 245-50.
- Min, H., Montecino-Rodriguez, E. and Dorshkind, K.** (2006). Reassessing the role of growth hormone and sex steroids in thymic involution. *Clin Immunol* **118**, 117-23.
- Mombaerts, P., Clarke, A. R., Rudnicki, M. A., Iacomini, J., Itoharu, S., Lafaille, J. J., Wang, L., Ichikawa, Y., Jaenisch, R., Hooper, M. L. and et al.** (1992a). Mutations in T-cell antigen receptor genes alpha and beta block thymocyte development at different stages. *Nature* **360**, 225-31.
- Mombaerts, P., Iacomini, J., Johnson, R. S., Herrup, K., Tonegawa, S. and Papaioannou, V. E.** (1992b). RAG-1-deficient mice have no mature B and T lymphocytes. *Cell* **68**, 869-77.
- Montecino-Rodriguez, E., Min, H. and Dorshkind, K.** (2005). Reevaluating current models of thymic involution. *Semin Immunol* **17**, 356-61.
- Moore, T. A. and Zlotnik, A.** (1995). T-cell lineage commitment and cytokine responses of thymic progenitors. *Blood* **86**, 1850-60.
- Moore-Scott, B. A. and Manley, N. R.** (2005). Differential expression of Sonic hedgehog along the anterior-posterior axis regulates patterning of pharyngeal pouch endoderm and pharyngeal endoderm-derived organs. *Dev Biol* **278**, 323-35.
- Morris, L., Gordon, J. and Blackburn, C. C.** (2006). Identification of a tandem duplicated array in the RhoX alpha locus on mouse chromosome X. *Mamm Genome* **17**, 178-87.
- Morrissey, P. J., McKenna, H., Widmer, M. B., Braddy, S., Voice, R., Charrier, K., Williams, D. E. and Watson, J. D.** (1994). Steel factor (c-kit ligand) stimulates the in vitro growth of immature CD3-/CD4-/CD8- thymocytes: synergy with IL-7. *Cell Immunol* **157**, 118-31.
- Muller, S. M., Stolt, C. C., Terszowski, G., Blum, C., Amagai, T., Kessaris, N., Iannarelli, P., Richardson, W. D., Wegner, M. and Rodewald, H. R.** (2008). Neural crest origin of perivascular mesenchyme in the adult thymus. *J Immunol* **180**, 5344-51.
- Napolitano, L. A., Schmidt, D., Gotway, M. B., Ameli, N., Filbert, E. L., Ng, M. M., Clor, J. L., Epling, L., Sinclair, E., Baum, P. D., Li, K., Killian, M. L., Bacchetti, P. and McCune, J. M.** (2008). Growth hormone enhances thymic function in HIV-1-infected adults. *J Clin Invest* **118**, 1085-98.
- Nehls, M., Kyewski, B., Messerle, M., Waldschutz, R., Schuddekopf, K., Smith, A. J. and Boehm, T.** (1996). Two genetically separable steps in the differentiation of thymic epithelium. *Science* **272**, 886-9.
- Nehls, M., Pfeifer, D., Schorpp, M., Hedrich, H. and Boehm, T.** (1994). New member of the winged-helix protein family disrupted in mouse and rat nude mutations. *Nature* **372**, 103-7.

- Nicolas, J. F., Savino, W., Reano, A., Viac, J., Brochier, J. and Dardenne, M.** (1985). Heterogeneity of thymic epithelial cell (TEC) keratins--immunohistochemical and biochemical evidence for a subset of highly differentiated TEC in the mouse. *J Histochem Cytochem* **33**, 687-94.
- Nowell, C. S., Tetélin, S., Bredekamp, N., Tischner, C., Sheridan, J. M., Stenhouse, F., Heussen, R., Jin, X., Sinclair, A., Smith, A. J. H. and Blackburn, C. C.** (under review). Foxn1 regulates lineage progression but not fate choice in cortical and medullary thymic epithelial cells.
- Olsen, N. J., Olson, G., Viselli, S. M., Gu, X. and Kovacs, W. J.** (2001). Androgen receptors in thymic epithelium modulate thymus size and thymocyte development. *Endocrinology* **142**, 1278-83.
- Ortman, C. L., Dittmar, K. A., Witte, P. L. and Le, P. T.** (2002). Molecular characterization of the mouse involuted thymus: aberrations in expression of transcription regulators in thymocyte and epithelial compartments. *Int Immunol* **14**, 813-22.
- Osada, M., Jardine, L., Misir, R., Andl, T., Millar, S. E. and Pezzano, M.** (2010). DKK1 mediated inhibition of Wnt signaling in postnatal mice leads to loss of TEC progenitors and thymic degeneration. *PLoS One* **5**, e9062.
- Peschon, J. J., Morrissey, P. J., Grabstein, K. H., Ramsdell, F. J., Maraskovsky, E., Gliniak, B. C., Park, L. S., Ziegler, S. F., Williams, D. E., Ware, C. B., Meyer, J. D. and Davison, B. L.** (1994). Early lymphocyte expansion is severely impaired in interleukin 7 receptor-deficient mice. *J Exp Med* **180**, 1955-60.
- Peters, H., Neubuser, A., Kratochwil, K. and Balling, R.** (1998). Pax9-deficient mice lack pharyngeal pouch derivatives and teeth and exhibit craniofacial and limb abnormalities. *Genes Dev* **12**, 2735-47.
- Petrie, H. T. and Kincade, P. W.** (2005). Many roads, one destination for T cell progenitors. *J Exp Med* **202**, 11-3.
- Petrie, H. T., Pearse, M., Scollay, R. and Shortman, K.** (1990). Development of immature thymocytes: initiation of CD3, CD4, and CD8 acquisition parallels down-regulation of the interleukin 2 receptor alpha chain. *Eur J Immunol* **20**, 2813-5.
- Petrie, H. T. and Zuniga-Pflucker, J. C.** (2007). Zoned out: functional mapping of stromal signaling microenvironments in the thymus. *Annu Rev Immunol* **25**, 649-79.
- Pido-Lopez, J., Imami, N., Andrew, D. and Aspinall, R.** (2002). Molecular quantitation of thymic output in mice and the effect of IL-7. *Eur J Immunol* **32**, 2827-36.
- Porritt, H. E., Rumfelt, L. L., Tabrizifard, S., Schmitt, T. M., Zuniga-Pflucker, J. C. and Petrie, H. T.** (2004). Heterogeneity among DN1 prothymocytes reveals multiple progenitors with different capacities to generate T cell and non-T cell lineages. *Immunity* **20**, 735-45.
- Radtke, M. L. and Kolesar, J. M.** (2005). Palifermin (Kepivance) for the treatment of oral mucositis in patients with hematologic malignancies requiring hematopoietic stem cell support. *J Oncol Pharm Pract* **11**, 121-5.
- Revest, J. M., Suniara, R. K., Kerr, K., Owen, J. J. and Dickson, C.** (2001). Development of the thymus requires signaling through the fibroblast growth factor receptor R2-IIIb. *J Immunol* **167**, 1954-61.
- Robles, A. I., Larcher, F., Whalin, R. B., Murillas, R., Richie, E., Gimenez-Conti, I. B., Jorcano, J. L. and Conti, C. J.** (1996). Expression of cyclin D1 in epithelial tissues of transgenic mice results in epidermal hyperproliferation and severe thymic hyperplasia. *Proc Natl Acad Sci U S A* **93**, 7634-8.

- Rossi, S., Blazar, B. R., Farrell, C. L., Danilenko, D. M., Lacey, D. L., Weinberg, K. I., Krenger, W. and Hollander, G. A.** (2002). Keratinocyte growth factor preserves normal thymopoiesis and thymic microenvironment during experimental graft-versus-host disease. *Blood* **100**, 682-91.
- Rossi, S. W., Jeker, L. T., Ueno, T., Kuse, S., Keller, M. P., Zuklys, S., Gudkov, A. V., Takahama, Y., Krenger, W., Blazar, B. R. and Hollander, G. A.** (2007). Keratinocyte growth factor (KGF) enhances postnatal T-cell development via enhancements in proliferation and function of thymic epithelial cells. *Blood* **109**, 3803-11.
- Rouse, R. V., Bolin, L. M., Bender, J. R. and Kyewski, B. A.** (1988). Monoclonal antibodies reactive with subsets of mouse and human thymic epithelial cells. *J Histochem Cytochem* **36**, 1511-7.
- Sakata, T., Iwagami, S., Tsuruta, Y., Teraoka, H., Tatsumi, Y., Kita, Y., Nishikawa, S., Takai, Y. and Fujiwara, H.** (1990). Constitutive expression of interleukin-7 mRNA and production of IL-7 by a cloned murine thymic stromal cell line. *J Leukoc Biol* **48**, 205-12.
- Sambrook, J. and Russell, D. W.** (2001). Molecular cloning : a laboratory manual. Cold Spring Harbor, NY: Cold Spring Harbor Laboratory Press.
- Sano, S., Takahama, Y., Sugawara, T., Kosaka, H., Itami, S., Yoshikawa, K., Miyazaki, J., van Ewijk, W. and Takeda, J.** (2001). Stat3 in thymic epithelial cells is essential for postnatal maintenance of thymic architecture and thymocyte survival. *Immunity* **15**, 261-73.
- Savino, W., Villa-Verde, D. M. and Lannes-Vieira, J.** (1993). Extracellular matrix proteins in intrathymic T-cell migration and differentiation? *Immunol Today* **14**, 158-61.
- Schlake, T., Schorpp, M., Nehls, M. and Boehm, T.** (1997). The nude gene encodes a sequence-specific DNA binding protein with homologs in organisms that lack an anticipatory immune system. *Proc Natl Acad Sci U S A* **94**, 3842-7.
- Schmitt, T. M., Ciofani, M., Petrie, H. T. and Zuniga-Pflucker, J. C.** (2004a). Maintenance of T cell specification and differentiation requires recurrent notch receptor-ligand interactions. *J Exp Med* **200**, 469-79.
- Schmitt, T. M., de Pooter, R. F., Gronski, M. A., Cho, S. K., Ohashi, P. S. and Zuniga-Pflucker, J. C.** (2004b). Induction of T cell development and establishment of T cell competence from embryonic stem cells differentiated in vitro. *Nat Immunol* **5**, 410-7.
- Schmitt, T. M. and Zuniga-Pflucker, J. C.** (2002). Induction of T cell development from hematopoietic progenitor cells by delta-like-1 in vitro. *Immunity* **17**, 749-56.
- Schuddekopf, K., Schorpp, M. and Boehm, T.** (1996). The whn transcription factor encoded by the nude locus contains an evolutionarily conserved and functionally indispensable activation domain. *Proc Natl Acad Sci U S A* **93**, 9661-4.
- Schwab, R., Szabo, P., Manavalan, J. S., Weksler, M. E., Posnett, D. N., Pannetier, C., Kourilsky, P. and Even, J.** (1997). Expanded CD4+ and CD8+ T cell clones in elderly humans. *J Immunol* **158**, 4493-9.
- Sempowski, G. D., Gooding, M. E., Liao, H. X., Le, P. T. and Haynes, B. F.** (2002). T cell receptor excision circle assessment of thymopoiesis in aging mice. *Mol Immunol* **38**, 841-8.
- Senoo, M., Pinto, F., Crum, C. P. and McKeon, F.** (2007). p63 Is essential for the proliferative potential of stem cells in stratified epithelia. *Cell* **129**, 523-36.
- Shakib, S., Desanti, G. E., Jenkinson, W. E., Parnell, S. M., Jenkinson, E. J. and Anderson, G.** (2009). Checkpoints in the development of thymic cortical epithelial cells. *J Immunol* **182**, 130-7.



- Sheridan, J. M.** (2007). Generation of a compartmentalised thymus organoid in vitro using fetal thymic epithelial progenitor cells. *PhD thesis, University of Edinburgh*.
- Shortman, K., Egerton, M., Spangrude, G. J. and Scollay, R.** (1990). The generation and fate of thymocytes. *Semin Immunol* **2**, 3-12.
- Sinha, M. L., Fry, T. J., Fowler, D. H., Miller, G. and Mackall, C. L.** (2002). Interleukin 7 worsens graft-versus-host disease. *Blood* **100**, 2642-9.
- Soriano, P.** (1999). Generalized lacZ expression with the ROSA26 Cre reporter strain. *Nat Genet* **21**, 70-1.
- Sprent, J., Gao, E. K. and Webb, S. R.** (1990). T cell reactivity to MHC molecules: immunity versus tolerance. *Science* **248**, 1357-63.
- Staples, J. E., Gasiewicz, T. A., Fiore, N. C., Lubahn, D. B., Korach, K. S. and Silverstone, A. E.** (1999). Estrogen receptor alpha is necessary in thymic development and estradiol-induced thymic alterations. *J Immunol* **163**, 4168-74.
- Steinmann, G. G., Klaus, B. and Muller-Hermelink, H. K.** (1985). The involution of the ageing human thymic epithelium is independent of puberty. A morphometric study. *Scand J Immunol* **22**, 563-75.
- Strathdee, D., Whitelaw, C. B. and Clark, A. J.** (2008). Distal transgene insertion affects CpG island maintenance during differentiation. *J Biol Chem* **283**, 11509-15.
- Sun, L., Guo, J., Brown, R., Amagai, T., Zhao, Y. and Su, D. M.** (2010). Declining expression of a single epithelial cell-autonomous gene accelerates age-related thymic involution. *Aging Cell* **9**, 347-57.
- Suniara, R. K., Jenkinson, E. J. and Owen, J. J.** (2000). An essential role for thymic mesenchyme in early T cell development. *J Exp Med* **191**, 1051-6.
- Surh, C. D., Gao, E. K., Kosaka, H., Lo, D., Ahn, C., Murphy, D. B., Karlsson, L., Peterson, P. and Sprent, J.** (1992). Two subsets of epithelial cells in the thymic medulla. *J Exp Med* **176**, 495-505.
- Sutherland, J. S., Goldberg, G. L., Hammett, M. V., Uldrich, A. P., Berzins, S. P., Heng, T. S., Blazar, B. R., Millar, J. L., Malin, M. A., Chidgey, A. P. and Boyd, R. L.** (2005). Activation of thymic regeneration in mice and humans following androgen blockade. *J Immunol* **175**, 2741-53.
- Sutherland, J. S., Spyroglou, L., Muirhead, J. L., Heng, T. S., Prieto-Hinojosa, A., Prince, H. M., Chidgey, A. P., Schwarzer, A. P. and Boyd, R. L.** (2008). Enhanced immune system regeneration in humans following allogeneic or autologous hemopoietic stem cell transplantation by temporary sex steroid blockade. *Clin Cancer Res* **14**, 1138-49.
- Takahama, Y.** (2006). Journey through the thymus: stromal guides for T-cell development and selection. *Nat Rev Immunol* **6**, 127-35.
- Tanchot, C., Fernandes, H. V. and Rocha, B.** (2000). The organization of mature T-cell pools. *Philos Trans R Soc Lond B Biol Sci* **355**, 323-8.
- Teh, H. S., Kisielow, P., Scott, B., Kishi, H., Uematsu, Y., Bluthmann, H. and von Boehmer, H.** (1988). Thymic major histocompatibility complex antigens and the alpha beta T-cell receptor determine the CD4/CD8 phenotype of T cells. *Nature* **335**, 229-33.

**Timsit, J., Savino, W., Safieh, B., Chanson, P., Gagnerault, M. C., Bach, J. F. and Dardenne, M.** (1992). Growth hormone and insulin-like growth factor-I stimulate hormonal function and proliferation of thymic epithelial cells. *J Clin Endocrinol Metab* **75**, 183-8.

**Trigueros, C., Hozumi, K., Silva-Santos, B., Bruno, L., Hayday, A. C., Owen, M. J. and Pennington, D. J.** (2003). Pre-TCR signaling regulates IL-7 receptor alpha expression promoting thymocyte survival at the transition from the double-negative to double-positive stage. *Eur J Immunol* **33**, 1968-77.

**Trop, S., Rhodes, M., Wiest, D. L., Hugo, P. and Zuniga-Pflucker, J. C.** (2000). Competitive displacement of pT alpha by TCR-alpha during TCR assembly prevents surface coexpression of pre-TCR and alpha beta TCR. *J Immunol* **165**, 5566-72.

**Uehara, S., Hayes, S. M., Li, L., El-Khoury, D., Canelles, M., Fowlkes, B. J. and Love, P. E.** (2006). Premature expression of chemokine receptor CCR9 impairs T cell development. *J Immunol* **176**, 75-84.

**Ueno, T., Saito, F., Gray, D. H., Kuse, S., Hieshima, K., Nakano, H., Kakiuchi, T., Lipp, M., Boyd, R. L. and Takahama, Y.** (2004). CCR7 signals are essential for cortex-medulla migration of developing thymocytes. *J Exp Med* **200**, 493-505.

**Uhmann, A., Dittmann, K., Nitzki, F., Dressel, R., Koleva, M., Frommhold, A., Zibat, A., Binder, C., Adham, I., Nitsche, M., Heller, T., Armstrong, V., Schulz-Schaeffer, W., Wienands, J. and Hahn, H.** (2007). The Hedgehog receptor Patched controls lymphoid lineage commitment. *Blood* **110**, 1814-23.

**Ushiki, T.** (1986). A scanning electron-microscopic study of the rat thymus with special reference to cell types and migration of lymphocytes into the general circulation. *Cell Tissue Res* **244**, 285-98.

**van de Wijngaert, F. P., Kendall, M. D., Schuurman, H. J., Rademakers, L. H. and Kater, L.** (1984). Heterogeneity of epithelial cells in the human thymus. An ultrastructural study. *Cell Tissue Res* **237**, 227-37.

**van Ewijk, W., Wang, B., Hollander, G., Kawamoto, H., Spanopoulou, E., Itoi, M., Amagai, T., Jiang, Y. F., Germeraad, W. T., Chen, W. F. and Katsura, Y.** (1999). Thymic microenvironments, 3-D versus 2-D? *Semin Immunol* **11**, 57-64.

**Van Vliet, E., Jenkinson, E. J., Kingston, R., Owen, J. J. and Van Ewijk, W.** (1985). Stromal cell types in the developing thymus of the normal and nude mouse embryo. *Eur J Immunol* **15**, 675-81.

**von Freeden-Jeffry, U., Vieira, P., Lucian, L. A., McNeil, T., Burdach, S. E. and Murray, R.** (1995). Lymphopenia in interleukin (IL)-7 gene-deleted mice identifies IL-7 as a nonredundant cytokine. *J Exp Med* **181**, 1519-26.

**Wada, H., Masuda, K., Satoh, R., Kakugawa, K., Ikawa, T., Katsura, Y. and Kawamoto, H.** (2008). Adult T-cell progenitors retain myeloid potential. *Nature* **452**, 768-72.

**Wallace, H. A., Marques-Kranc, F., Richardson, M., Luna-Crespo, F., Sharpe, J. A., Hughes, J., Wood, W. G., Higgs, D. R. and Smith, A. J.** (2007). Manipulating the mouse genome to engineer precise functional syntenic replacements with human sequence. *Cell* **128**, 197-209.

**Wallin, J., Eibel, H., Neubuser, A., Wilting, J., Koseki, H. and Balling, R.** (1996). Pax1 is expressed during development of the thymus epithelium and is required for normal T-cell maturation. *Development* **122**, 23-30.

- Weigel, D., Jurgens, G., Kuttner, F., Seifert, E. and Jackle, H.** (1989). The homeotic gene fork head encodes a nuclear protein and is expressed in the terminal regions of the Drosophila embryo. *Cell* **57**, 645-58.
- Weiner, L., Han, R., Scicchitano, B. M., Li, J., Hasegawa, K., Grossi, M., Lee, D. and Brissette, J. L.** (2007). Dedicated epithelial recipient cells determine pigmentation patterns. *Cell* **130**, 932-42.
- Welniak, L. A., Sun, R. and Murphy, W. J.** (2002). The role of growth hormone in T-cell development and reconstitution. *J Leukoc Biol* **71**, 381-7.
- Wilson, A., Held, W. and MacDonald, H. R.** (1994). Two waves of recombinase gene expression in developing thymocytes. *J Exp Med* **179**, 1355-60.
- Wolfer, A., Wilson, A., Nemir, M., MacDonald, H. R. and Radtke, F.** (2002). Inactivation of Notch1 impairs VDJbeta rearrangement and allows pre-TCR-independent survival of early alpha beta Lineage Thymocytes. *Immunity* **16**, 869-79.
- Wu, L., Antica, M., Johnson, G. R., Scollay, R. and Shortman, K.** (1991). Developmental potential of the earliest precursor cells from the adult mouse thymus. *J Exp Med* **174**, 1617-27.
- Xu, P. X., Zheng, W., Laclef, C., Maire, P., Maas, R. L., Peters, H. and Xu, X.** (2002). Eya1 is required for the morphogenesis of mammalian thymus, parathyroid and thyroid. *Development* **129**, 3033-44.
- Youm, Y. H., Yang, H., Sun, Y., Smith, R. G., Manley, N. R., Vandanmagsar, B. and Dixit, V. D.** (2009). Deficient ghrelin receptor-mediated signaling compromises thymic stromal cell microenvironment by accelerating thymic adiposity. *J Biol Chem* **284**, 7068-77.
- Zamisch, M., Moore-Scott, B., Su, D. M., Lucas, P. J., Manley, N. and Richie, E. R.** (2005). Ontogeny and regulation of IL-7-expressing thymic epithelial cells. *J Immunol* **174**, 60-7.
- Zeisig, B. B., Milne, T., Garcia-Cuellar, M. P., Schreiner, S., Martin, M. E., Fuchs, U., Borkhardt, A., Chanda, S. K., Walker, J., Soden, R., Hess, J. L. and Slany, R. K.** (2004). Hoxa9 and Meis1 are key targets for MLL-ENL-mediated cellular immortalization. *Mol Cell Biol* **24**, 617-28.
- Zhu, X., Gui, J., Dohkan, J., Cheng, L., Barnes, P. F. and Su, D. M.** (2007). Lymphohematopoietic progenitors do not have a synchronized defect with age-related thymic involution. *Aging Cell* **6**, 663-72.
- Zlotoff, D. A., Sambandam, A., Logan, T. D., Bell, J. J., Schwarz, B. A. and Bhandoola, A.** (2010). CCR7 and CCR9 together recruit hematopoietic progenitors to the adult thymus. *Blood* **115**, 1897-905.
- Zou, D., Silvius, D., Davenport, J., Grifone, R., Maire, P. and Xu, P. X.** (2006). Patterning of the third pharyngeal pouch into thymus/parathyroid by Six and Eya1. *Dev Biol* **293**, 499-512.